



PROCEEDINGS OF INTERNATIONAL CONFERENCE ON ISTANBUL AND EARTHQUAKE 2022

Organized by IAU Disaster Training Application and Research Center (AFAM)

İSTANBUL AYDIN
ÜNİVERSİTESİ
AFAM
AFET EĞİTİM, UYGULAMA
VE ARAŞTIRMA MERKEZİ





Proceedings of International Conference on Istanbul and Earthquake 2022

Organized by IAU Disaster Training Application and Research Center (AFAM)

İSTANBUL-202

İSTANBUL AYDIN ÜNİVERSİTESİ YAYINLARI
İSTANBUL AYDIN UNIVERSITY PUBLICATIONS

**PROCEEDINGS OF INTERNATIONAL CONFERENCE
ON ISTANBUL AND EARTHQUAKE 2022**

Organized by IAU Disaster Training Application and Research Center (AFAM)

İmtiyaz Sahibi: / President of The Board of Publication

Dr. Mustafa Aydın

Genel Yayın Yönetmeni / Editor in Chief

Prof. Dr. Mehmet Fatih ALTAN

Yardımcı Editörler / Associate Editors

Assist. Prof. Dr. Ouiame CHAKKOR

Res. Assist. Abdullah NİGDELİOĞLU

Res. Assist. Abdullah Zubeyr HAYVALI

Sayfa Tasarım / Layout Design

İstanbul Aydın Üniversitesi Görsel Tasarım Birimi

Basım Yeri: / Printing Place

Armoni Nüans Görsel Sanatlar ve İletişim Hizmeti San. ve Tic. A.Ş.

Yukarıdudullu, Bostancı Yolu Cad. Keyap Çarşısı B- 1 Blk. N.24

Ümraniye / İSTANBUL

ISBN: 978 625 7783 48 4

Copyright © İstanbul Aydın Üniversitesi / İstanbul Aydın University

Bu kitabın tüm hakları İstanbul Aydın Üniversitesi'ne aittir.

All rights of this books belong to Istanbul Aydın University.

Bu yapıtın tüm hakları saklıdır. Yazılar ve görsel malzeme izin almadan tümüyle veya kısmen yayımlanamaz.

This book is a gift of Istanbul Aydın University, it cannot be sold.

PREFACE

Dear Participants,

Istanbul, one of the most important cities in the world, is in a geography where major earthquakes have occurred throughout history. Istanbul has been exposed to earthquakes many times. These earthquakes caused great damage to the city. This region, where earthquakes have occurred, but which cannot be abandoned, has been a residential area many times. Since it is not abandoned, it is necessary to look for ways to prevent earthquakes from being a disaster by taking precautions. The studies are carried on by considering them from multiple perspectives. It can be grouped under two main headings as structural and non-structural measures. In this conference, valuable participants presented their papers on structural measures. The only address for structural measures against earthquakes; building security. After the structures are strong, earthquakes will remain a natural phenomenon. In this conference, where different studies were presented, different analyzes from a wide variety of countries were discussed. When these international studies are combined, it will lead to better results. It is one of our greatest wishes that the "Istanbul and Earthquake" conferences will contribute to the world city of Istanbul. Thank you for giving us strength with your participation. We look forward to the conferences planned to be held in the coming years. I wish you success in your work.

Prof. Dr. Mehmet Fatih Altan

Editor

ORGANIZATION

Scientific Committee

Scientific Committee Chairman

- Prof. Dr. Alper ILKI- Istanbul Technical University (Turkey)

Scientific Committee Members

- Prof. Dr. Mehmet Fatih ALTAN- Istanbul Aydin University (Turkey)
- Prof. Dr. Benchaa BENABED- Algeria University of Laghouat (Algeria)
- Prof. Dr. Mahmut BILGEHAN- Kastamonu University (Turkey)
- Prof. Dr. Ramazan DEMIRBOGA- Alfaisal University (Saudi Arabia)
- Prof. Dr. Sukru ERSOY- Yildiz Technical University (Turkey)
- Prof. Dr. Zeki GUNDUZ- Istanbul Aydin University (Turkey)
- Prof. Dr. Nemet HASSAINI- Shadid Beheshti University (Iran)
- Prof. Dr. Mahmood HOSSEINI- Eastern Mediterranean University (North Cyprus)
- Prof. Dr. Murat Emre KARTAL- Izmir Demokrasi University (Turkey)
- Prof. Dr. Arkadiusz KWIECIEN- Cracow University of Technology (Poland)
- Prof. Dr. Sevket OZDEN- Istanbul Okan University (Turkey)
- Assoc. Prof. Dr. Savas ERDEM- Istanbul University (Turkey)
- Assoc. Prof. Dr. Mehrdad HEJAZI- University of Isfahan (Iran)
- Assoc. Prof. Dr. Ahmet Emin KURTOGLU- Iğdır University (Turkey)
- Assoc. Prof. Dr. Roman RABENSEIFER- Slovak University of Technology in Bratislava (Slovakia)
- Assoc. Prof. Dr. Hosseim Tajmir RIAHI- University of Isfahan (Iran)

- Assoc. Prof. Dr. Messaoud SAIDANI- Coventry University (U.K)
- Assoc. Prof. Dr. Safiullah OMARY- INSA de Strasbourg (France)
- Assoc. Prof. Dr. Ismail Cengiz YILMAZ-Istanbul Arel University (Turkey)
- Assist. Prof. Dr. Ouiame CHAKKOR- Istanbul Aydin University (Turkey)
- Assist. Prof. Dr. Hafez KEYPOUR- Istanbul Aydin University (Turkey)
- Assist. Prof. Dr. Zeyneb KILIC- Istanbul Aydin University (Turkey)
- Assist. Prof. Dr. Hakan KOMAN- Istanbul Aydin University (Turkey)
- Assist. Prof. Dr. Saed MOGHIMI- Istanbul Aydin University (Turkey)
- Assist. Prof. Dr. Halil NOHUTCU- Celal Bayar University (Turkey)

Organizing Committee

Organizing Committee Chairman

- Prof. Dr. Mehmet Fatih ALTAN – Istanbul Aydin University/ Disaster Training Application and Research Center

Organizing Committee Members

- Serhat YILMAZ- Istanbul Aydin University/ Disaster Training Application and Research Center
- Assoc. Prof. Dr. Mehmet SOYLEMEZ- Adiyaman University
- Assist. Prof. Dr. Ouiame CHAKKOR- Istanbul Aydin University/ Disaster Training Application and Research Center
- Assist. Prof. Dr. Hakan KOMAN- Istanbul Aydin University/ Disaster Training Application and Research Center
- Res. Assist. Abdullah NIGDELIOGLU- Istanbul Aydin University/ Disaster Training Application and Research Center
- Res. Assist. Abdullah Zubeyr HAYVALI- Istanbul Aydin University/ Disaster Training Application and Research Center
- Res. Assist. Yasmina ED DARIY- Mohamed V University

TABLE OF CONTENTS

Analysis of selected aspects of the life cycle for flexible joints between reinforced concrete frame and masonry infills	11-29
<i>Krzysztof Zima, Damian Wieczorek, Arkadiusz Kwiecie</i>	
Seismic performance of the polymer flexible joints in rc frames with various infill wall aspect ratios	31-46
<i>A. Tugrul Akyildiz, Arkadiusz Kwiecie</i>	
Earthquake protection of rc frames with infills joined by pufj and frpu systems	47-68
<i>Arkadiusz Kwiecie</i>	
Seismic retrofit of low- and mid-rise rc buildings by encasement technique	69-90
<i>Mahmood Hosseini, Almotasim Billah Alabeidy, Mehmet Cemal Genes</i>	
Fatigue behaviour of ultra-high performance concrete under cyclic stress reversal loading	91-103
<i>Birol Fitik</i>	
Anti-earthquake measures for the historical building of ali qapu.....	105-125
<i>Mehrdad Hejazi</i>	
Response control on seismic retrofit for low-rise rc building in Thailand using elastoplastic dampers	127-139
<i>Panumas Saingam</i>	
Urban transformation applications in low-rise reinforced concrete buildings.....	141-150
<i>Abdullah Niğdelioğlu, Ouiame Chakkor, Mehmet Fatih Altan</i>	
Investigation of the effect of material models on behavior of reinforced concrete columns by analytical models	151-161
<i>Selim Aykutlu, Sinan Cansız</i>	

- A study on beam discontinuity and recessed balcony **63-177**
Halil Nohutcu, Adem Solak, Taner Kılıc
- Investigation of social awareness and awaress regarding the concept of risky building in the context of the potential Istanbul earthquake..... **179-194**
Yunus Orhan, İsmail Cengiz Yılmaz
- The effect of labor characteristics on worker training in the construction sector **95-203**
Melek Ceylan, Sinan Cansiz
- The effect of vocational qualification certificate on occupational accidents occuring in the consruction sector **205-213**
Melek Ceylan, Sinan Cansız
- Earthquake reinforcement of historical masonary buildings of Topkapı Palace Incılı Mansion **215**
Hafez Keypour, Ali Tarmigh, Cevdet Senturk, Zeyneb Kılıc
- Behaviour of highly ductile pvc-confined tubular stub columns..... **216**
Ahmet Emin Kurtoğlu
- Probabilistic assessment of the ground vibration induced by rock explosion..... **217**
Mahdi Shadabfar, Nemat Hassani, Hadi Kordestani
- The application of normalized distributed energy directly calculated from structural acceleration response as a sensitive damage index for structural damage identification **218**
Hadi Kordestani, Zhang Chunwei, Mahdi Shadabfar
- Simplified seismic retrofit countermeasures for urban gas risers..... **219**
Nemat Hassani, Saeed Behesht, Mohammad Safishiro, Takada Yasuo Ogawa, Junichi Ueno, Hossein Mohammadsaleh, Kaveh Zanganehand Masoud Samadian

ANALYSIS OF SELECTED ASPECTS OF THE LIFE CYCLE FOR FLEXIBLE JOINTS BETWEEN REINFORCED CONCRETE FRAMES AND MASONRY INFILLS

Krzysztof Zima¹, Damian Wieczorek², Arkadiusz Kwiecień³

¹Cracow University of Technology, 31-155 Cracow Warszawska 24, krzysztof.zima@pk.edu.pl

²Cracow University of Technology, 31-155 Cracow Warszawska 24, damian.wieczorek@pk.edu.pl

³Cracow University of Technology, 31-155 Cracow Warszawska 24, akwiecie@pk.edu.pl

*Responsible author: akwiecie@pk.edu.pl

ABSTRACT

The study presents innovative anti-seismic protection systems using PolyUrethane Flexible Joints (PUFJ) at the frame-infill interface and bonding of glass fiber meshes to the weak masonry substrate to form Fiber Reinforced PU (FRPU) as an emergency repair intervention. Due to the possibility of using the systems in existing and newly built structures in areas of increased risk of seismic excitations, the authors made an attempt to define the life cycle scenarios of these systems in terms of the possibility of extending the service life of these structures. The definition of the construction life cycle scenarios and the estimation of the corresponding investment costs and costs related to the operation and decommissioning of a given system were based on the approach presented in the ISO 15686 standard package “Buildings and constructed assets”, part 2 – Service life prediction procedures and part 5 – Life cycle costing. The simulations covered a total of five variants of the systems application: (i) prefabricated PUFJ at 4 interfaces (in newly constructed buildings), (ii) injected PUFJ at 3 interfaces (improvement of existing buildings) and application of FRPU as a quick emergency or strengthening system (for buildings damaged by earthquakes) in variants (iii) at infill diagonals, (iv) at infill edges, and (v) as combination of the systems presented above (according to requirements). The cost analysis also took into account the potential impact of changes in the value of money over time and an increase in the production costs of building materials.

KEYWORDS: repair costs, earthquakes, LCC, PolyUrethane Flexible Joints (PUFJ), Fiber Reinforced PolyUrethane (FRPU)

1. EARTHQUAKES AND REPAIR COSTS OF BUILDING ELEMENTS

Earthquakes are very serious threats in many regions of the world. Very important preventive elements are methods of preventing building cracks and collapsing, which causes both financial losses and often a threat to the life of people staying in the buildings. Securing buildings is of course associated with a large financial outlay, but when considering the protection of life and the costs of securing buildings and reconstruction costs, the former should be considered more often. Generally to start a discussion of life protection opportunities and security costs, the cost of security throughout the life cycle of buildings should be considered. Life cycle costs also have their normative approach in the form of ISO 15686-5:2017. “Buildings and constructed assets – Service-life planning – Part 5: Life-cycle costing” (ISO, 2017). The ISO standard includes, among others life cycle definitions and the so-called “whole life cycle”. The life cycle cost analysis may be performed with the use of simple or complex methods. Simple methods are applied only in cases of uncomplicated comparisons. Their basic limitation is to involve calculations but excluding the effect of changes in the time value of money and changes in energy prices. On the other hand, complex methods are based on mathematical economic models, which consider changes in the time value of money (discounting) – Wieczorek et al. (2019). In the article, the authors used complex methods to evaluate the effectiveness of the application of selected methods.

Makra et al (2021) described the M7.0 earthquake that occurred on October 30, 2020 in the Aegean Sea near the island of Samos (Greece) and the west coast of Turkey, which had a major impact on the city of Izmir, approximately 70 km from the epicenter earthquake. The greatest damage caused by the Samos (Aegean Sea) earthquake was observed in the Bayarkli (a metropolitan district of Izmir) area, with 7-10-story reinforced concrete buildings with solid masonry walls, erected between 1990 and 2000. Combined with the fact that the long-term (0.5-1.5 s) recorded spectral accelerations in the sediments were noticeably high due to the pool effects in terms of the maximum ground acceleration (~ 0.1 g), the authors of the study note that the observed long-term movement triggered, and due to double resonance, major damage and collapse of many buildings occurred. The preliminary assessment of the seismic risk with the use of recorded ground movements showed that despite the fact that the observed damage was to be expected, the relationship between spectral accelerations and design loads does not justify such an intensity of damage. According to the authors, other additional parameters, such as compliance with regulations, construction quality and modification of the structural system, have an impact on the size of the observed damage.

According Atmaca et al. (2020) it is observed in Turkey that a large part of the housing stock consist of RC and masonry structural system in urban and rural areas, respectively. The authors analyzed the technical condition and damage to reinforced concrete and brick buildings during six major earthquakes that took place in 1992-2020 in various regions of Turkey. The conclusions presented in the article emphasize, inter alia, that reinforced concrete buildings were designed and constructed without meeting the requirements of earthquake regulations and insufficient control mechanism, errors were made in both design and workmanship. In addition, a large number of brick buildings are made by local craftsmen without any engineering knowledge (mainly in rural areas), which often does not cause damage under vertical loads, but generates serious damage to buildings caused by horizontal loads during earthquakes. An analysis of earthquakes and their effects led the authors to conclude that poor construction quality, inadequate material properties, heavy earth roofs and weak gable walls are the general causes of insufficient dynamic performance of masonry buildings.

In turn, the authors in (Günaydin et al, 2020) analyzed a major earthquake of moment magnitude $M_w = 6.8$, which took place on January 24, 2020, that struck the Sivrice district of Elazığ, located in the southwest of the Eastern Anatolia region of Turkey. Many brick buildings were then seriously damaged or completely collapsed, especially in the rural areas of cities Elazığ and Malatya. The authors concluded that the main causes of damage or collapse of brick buildings were poor quality of workmanship and structure, inadequate material properties of masonry walls, weak load-bearing walls, heavy earth roofs and free or high gable walls. The damage or collapse mechanisms appeared in the form of diagonal or incline tension cracks, outward bulking of walls, out-of-plane failure of walls and separation cracks between the perpendicular walls or masonry units (Günaydin et al, 2020). It should be added that many brick buildings were partially damaged or completely collapsed, which highlighted the problem that brick buildings built in rural Turkey are very susceptible to even relatively small earthquakes.

In the article, (Yon et al, 2020) listed the main significant reasons of damages and collapse of structural stock for masonry dwellings such: heavy earthen roofs, insufficient corner connection, and therefore propagation of out-of-plane mechanism, weak in-plane bearing capacity, soil–structure interaction, minor local damages. The causes of the non-planar failure mechanism can be found in such reasons as: incorrect connections between two perpendicular elements, large unsupported wall lengths and the absence of tied beams. This type of failure mechanism occurs when all or a significant part of the wall collapses during an

earthquake. This problem can be eliminated for existing masonry walls enclosed with a girder by corner-to-corner polymer tapes reinforcement. Moreover, decreasing the useless dimensions of openings or closing the extra openings by bonding is another alternative solution to increase in-plane bearing capacity and prevent out-of-plane failure (Yon et al, 2020).

Next research (Ramirez et al, 2012) shows the expected cost of repairing earthquake damage in a set of 30 archetype reinforced concrete moment frame buildings with varying in height from 1 to 20 stories and special RC moment frames, designed according to modern seismic codes. As part of the research, the authors found that in the case of the basic set of projects compliant with the loss standards Design Basis Earthquake, intensity constitute a significant percentage of the value, ranging from 16% to 50%. The corresponding annual losses range from 0.5% to about 1.3% of the reconstruction value of the facility. Present value of annual losses in the assumed 50-year time horizon, with a 3% discount rate, ranged from approximately 12% to 34% of the facility replacement cost.

In the article (Bostenaru Dan, 2018) an analysis of costs of preventive retrofit and costs of repair after earthquake hazards was made. A comparison of preventive upgrades and post-earthquake repairs shows the importance of planning measures to prevent the effects of an earthquake. If the retrofit measure is applied at the right time between successive earthquakes, or before the first earthquake, and in the right proportions, substantial savings are to be expected in repair costs (Bostenaru Dan, 2018). In addition, one should remember about the great benefits for building users, i.e. significantly less damage caused by the earthquake, and thus subsequent remedial actions. It also seems important to protect the national heritage, protected by controlled conservation measures, compared to the repair of the most important elements that may be damaged in an earthquake. In this case, also the cash outlays do not seem to be the most important. In line with the latest trends in disaster management, cost-benefit analyzes include, among others, social sciences and humanities, cultural heritage, economics and sociology of architecture. So there are hard-to-measure benefits that determine what modernization system and strategy should be applied and balanced with costs, based on multi-criteria analyzes. As research has shown, the total costs of repair and retrofit are about 30% of the potential cost of rebuilding and the cost for repair, in contrast, vary from between 3 to 8 times more than the preventive retrofit.

De Martino et al (2017) discusses data related to the 2009 L'Aquila earthquake in the Abruzzi region of central Italy, focusing on empirical damage and the real cost

of repairing damaged residential buildings. The collected data concerns 2,500 residential buildings of both reinforced concrete and masonry structures. The repair intervention consists of: repair of damaged non-structural parts and relevant finishing works; local repair of damaged structural components; demolition and reconstruction of fully damaged or unsafe non-structural or secondary structural elements (i.e. interior or exterior infills, outdoor curtain wall, heavy plasters, fireplaces and chimneypots, porches, eaves, repair of damaged facilities, etc.). Repair costs in the present case include, among others costs related to demolition and debris removal (including costs of transport and storage in landfills), costs of repairs and additions, costs of repair and finishing works related to reinforcement (only for buildings with severe structural damage), testing of facilities, technical work to improve health and safety, design and support fees; moving furniture. For both types of buildings: reinforced concrete and masonry buildings the most populated class of cost was that between 100 and 200 EUR/m², but sometimes even more than 700 EUR/m².

2. INNOVATIVE ANTI-SEISMIC PROTECTION SYSTEMS VARIANTS

In this chapter, the use of innovative material solutions of anti-seismic protection systems is presented such as PoliUrethane Flexible Joints – PUFJ, that is deformable structural connectors transferring high loads and high deformations and Fiber Reinforced PoliUrethanes – FRPU, deformable adhesives and composite matrices, which have the ability of dissipating energy.

Five variants of innovative anti-seismic protection systems application were chosen for life cycle costs analysis (LCCA) – Figure 1:

- (i) prefabricated PUFJ at 4 interfaces – variant V1,
- (ii) injected PUFJ at 3 interfaces without application of FRPU – V2,
- (iii) injected PUFJ at 3 interfaces and application of FRPU only at infill diagonals – V3,
- (iv) injected PUFJ at 3 interfaces and application of FRPU only at infill edges – V4,
- (v) injected PUFJ at 3 interfaces and application of FRPU as a combination of the systems V3 and V4 – V5.

The conducted research shows that the behavior of reinforced concrete (RC) frames with infills made of masonry walls is significantly influenced by the difference in stiffness and strength between the frame and the infill. This can result in relatively early damage formation to infills or even concrete columns.

The use of innovative technologies can protect buildings against such situations. In the presented variants, a system of elastic protection was used, using PolyUrethane Flexible Joints (PUFJ) made of polyurethane Sika PM, used at the frame-filling interface (Rousakis et al, 2020). As shown in Figure 1, two solutions were applied using PUFJ on 3 or 4 wall-column and wall-ceiling contacts. The V3, V4 and V5 variants differ in the way of using FRPU – in the case of V3, a diagonal wall reinforcement was used, in V4, the reinforcement was applied along the perimeter of the wall along the joints of the wall with columns and ceilings, and in the case of V5, both diagonal and perimeter reinforcements were used. Polyurethane adhesive (Sika PS) was used in the variants V3, V4 and V5 to bond glass fiber meshes to a weak masonry substrate to produce Fiber Reinforced PolyUrethanes (FRPU). This allows for the use of a specific emergency repair intervention on seriously damaged infills. The test results presented in (Rousakis et al, 2020) showed an improvement in in-plane and out-of-plane filling performance under the influence of seismic excitations. The results confirmed the remarkable delay of significant damage to the filling with very high inter-story RC frame drifts due to the use of PUFJ.

Therefore, attention should be paid to the durability of such innovative solutions, assuming their long-term use, both in newly constructed and existing buildings. The tests of accelerated aging and thermal stability showed the mechanical stability of PS-polyurethane at temperatures up to 200 °C and small degradation of the surface under the influence of UV radiation. The paper (Kwiecień et al, 2020) presents the results of PS polyurethane tensile tests, which show low sensitivity of PS polyurethane to atmospheric conditions with exposure to UV radiation, certain reactivity to water environments of various chemical nature and resistance to soil and freezing in both air and water. Thus, the research results show that the presented solutions can be used quite commonly in practice.

All variants are shown in Figure 1.

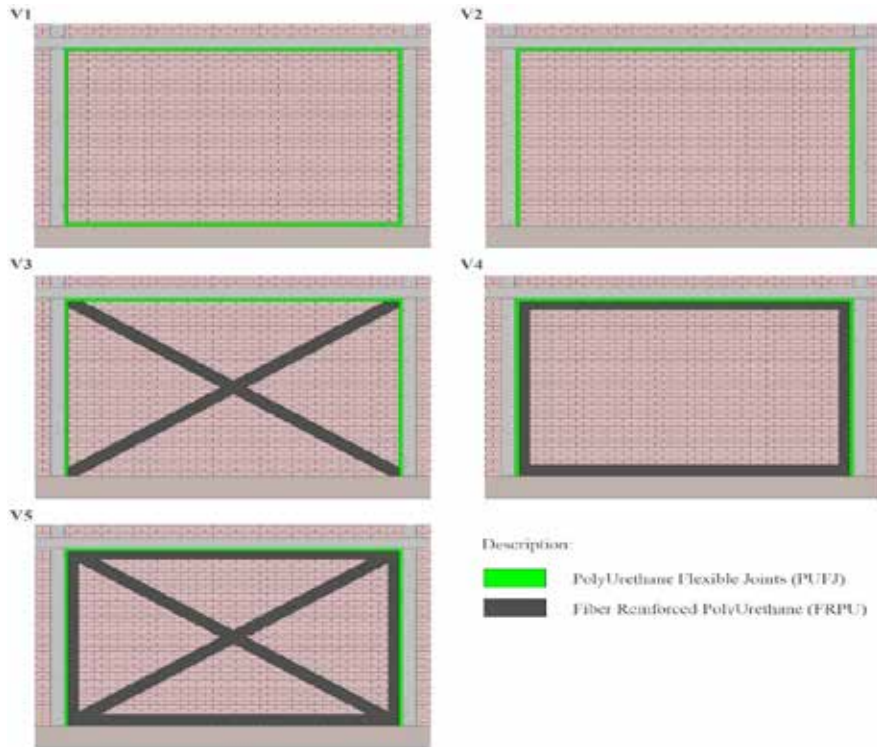


Figure 1. Innovative anti-seismic protection systems: V1 – prefabricated PUFJ at 4 interfaces; V2 – injected PUFJ at 3 interfaces without application of FRPU; V3 – injected PUFJ at 3 interfaces and application of FRPU at infill diagonals; V4 – injected PUFJ at 3 interfaces and application of FRPU at infill edges; V5 – injected PUFJ at 3 interfaces and application of FRPU at infill diagonals and edges both.

In the next chapter, calculations on the cost-effectiveness of such solutions will be presented, taking into account possible scenarios of the life cycle of buildings.

3. DEFINITION OF LIFE CYCLE SCENARIOS FOR INNOVATIVE ANTI-SEISMIC PROTECTION SYSTEMS

A life cycle scenario is a set of defined functions and processes that are arranged in a certain logical sequence, and the effects of which lead to the achievement of the goal of a given project, defined in the adopted product management strategy during its life cycle (Plebankiewicz et al, 2018). The ISO 15686-5:2017 (ISO, 2017)

identifies the concept of life cycle scenario with maintenance activities. The following three types of maintenance activities are distinguished in the ISO standard:

- (i) preventive in intention – including condition-based or predictive and scheduled,
- (ii) corrective in intention – including allowances for emergency and unforeseen events or reactive corrections to failures,
- (iii) deferred – a decision about timing and urgency, which can have cost consequences.

For the purposes of the definition of life cycle scenarios, for all variants of the innovative anti-seismic protection systems application, it was assumed that all maintenance activities would be planned for the location of a building in the most seismically exposed area, composed of reinforced concrete frames with masonry infills. The estimated service life of a building value is at least 50 years of use, in accordance with the Eurocode standards approach. It was also found that in the most disadvantaged situation, the frequency of earthquakes causing significant material and social losses can be as high as 9 to 12 years. Therefore, 10 years was assumed as the average time of necessity to carry out activities and bear repair costs.

All life cycle scenarios have been defined for three sets (states) of works that can be done on a wall filled with brick material. In “set A” it was assumed that in the initial time a masonry wall with a thickness of 10 cm, a height of 3.2 m and a length of 4.8 m will be made as infill of reinforced concrete frames. In addition, internal and external cladding on the wall as respectively cement-lime and cement plasters with a layer thickness of up to 1.5 cm was considered. In “set B” the elements of electric and central heating installation were added to the set of works analogous to those in “set A”. It was assumed that the cables of both types of installation would be laid on the analyzed wall, with two electrical sockets and one heater mounted thereon. The “set C” also takes into account the necessity to repair the concrete edges, which may break in the area of the cover at the corner reinforcement bars in the edge zone. Thus, “set C” consists of the common elements of the works of “set A” and “set B”.

As for the characteristics of the individual life cycle scenarios to the successive variants presented in Figure 1 and for the reference scenario, the following assumptions have been made:

- in the reference scenario (variant V0), a maintenance corrective activities in intention strategy was adopted, according to which, earthquake may occur

after every 10 years of use, in extreme cases causing up to 100% damage to the masonry wall; therefore in this variant, it is also necessary to take into account up to 100% of the cost of removal of debris after each damage to the wall and up to 100% of the cost of rebuilding the installation and making up to 100% of the scope of concrete edge repair; variant V0 does not assume the use of any anti-seismic protection system and the building's lifetime is forecasted at 50 years,

- variant V1 assumes the simultaneous execution of the prefabricated PUFJ at 4 interfaces as an anti-seismic protection system before proceeding with the execution of the infill masonry wall; therefore at the beginning of the building's life cycle, there is a large initial cost for this variant which, however, reduces the costs that may arise after each earthquake occurrence; the effect of using this anti-seismic protection system is the limitation to no more than 25% of material losses related to damage to the masonry wall and the cost of removal of debris after each damage to the wall, including the scope of concrete edge repair, as well as limitation up to no more than 10% of the cost of rebuilding the installation; V1 is dedicated especially to newly constructed buildings and corresponds to the strategy of maintenance preventive activities in intention and due to the use of an efficient anti-seismic protection system the building's lifetime is forecasted at 60 years,
- V2-V5 variants assume execution of the injected PUFJ at 3 interfaces anti-seismic protection system in an existing building as a protection intervention before an earthquake ; however in the V2 variant the application of FRPU is not used, in V3 there is an additional application of FRPU only at infill diagonals, in V4 – additional application of FRPU only at infill edges and in V5 – additional application of FRPU as a combination of the systems V3 and V4; the scale of material damage is therefore limited, but only after 10 years of use; damage related to the masonry wall and the cost of removal of debris after each damage to the wall, including the scope of concrete edge repair is reduced to no more than 25% for the variant V2, no more than 15% for V3-V4 and no more than 10% for V5; the costs of rebuilding the installation are in turn no more than 10% for the variant V2 and no more than 5% for the V3-V5 due to the use of very efficient anti-seismic protection systems; all above-mentioned variants are dedicated especially to existing buildings and correspond to both strategies of maintenance, i.e. corrective (up to 10 years of use) and preventive in intention (after 10 years

of use), and the building's lifetime is forecasted at 50 years for variants V2-V4 and 60 years for V5.

In all of the life cycle scenarios described above, a withdrawal type called “from cradle to grave” was assumed. According to this approach, the phase of decommissioning the building from use is finished with its demolition, followed by the utilization and management of demolition materials.

4. LIFE CYCLE COSTS ANALYSIS METHOD AND RESULTS

4.1. Description of the methods for the LCCA

To calculate the value of the life cycle costs for all variants (V1-V5) of the innovative anti-seismic protection systems, application presented in Figure 1 and the variant corresponding to the reference scenario (V0), the Net Present Value (NPV) method recommended by ISO 15686-5:2017 (ISO, 2017), was applied. According to the method, the net present value (NPV) may be described as the sum of the discounted benefit of a given variant of the investment project (or construction system implementation) less the sum of the discounted costs. In the case of where costs only are taken into account, the NPV may be called the net present cost (NPC). The NPV or NPC is calculated using the following formula:

$$X_{NPV(NPC)} = \sum(C_n \cdot q) = \sum_{n=0}^p \frac{C_n}{(1+d)^n} \quad \text{Equation 1}$$

where:

- C_n – cash flow (the difference between benefit and cost) or cost in year, n
- q – discount factor
- d – expected real discount rate per annum
- n – number of years between the base date and the occurrence of the cost
- p – period of analysis (lifetime)

Due to the attempt to compare the obtained results of life cycle costs analysis with the reference scenario with application of traditional wall system without anti-seismic protection and the fact that the lifetimes of some variants of anti-seismic protection systems are 60 years and not 50 years, the annual cost indicator (AC) was also applied. The annual cost (AC) or annual equivalent value (AEV) is an uniform annual amount equivalent to the investment project costs, taking into account changing the value of money over time throughout the period of analysis when lifetimes of a given variant of the investment project (or construction system

implementation) are different. The AC or AEV is calculated using the following formula:

$$X_{AC(AEV)} = \frac{X_{NPC} \cdot d}{1 - (1+d)^{-n}} \quad \text{Equation 2}$$

where:

X_{NPC} – net present cost

d – expected real discount rate per annum

n – number of years between the base date and the occurrence of the cost

4.2. Detailed assumptions adopted for the LCCA

In order to be able to carry out life cycle costs analysis (LCCA) using the methods and economic indicators recommended by ISO 15686-5:2017 (ISO, 2017), it is necessary to adopt the following time and cost parameters:

- length of the life cycle (lifetime) of a given building variant (or construction system implementation) in years as a period of analysis (p), after which costs of decommissioning the building from use and the utilization and management of demolition materials are calculated,
- times of calculating subsequent operating costs taken as n -values (numbers of years between the base date and the occurrence of the cost),
- initial costs incurred in the building implementation phase immediately before the start of its use phase (C_n in the so-called zero year),
- periodic operation costs (C_n) corresponding to the values of costs incurred during the use of the building after n -years,
- withdrawal costs (C_n) charged after building's lifetime (p),
- expected real discount rate per annum (d).

The time and cost data adopted for the calculations for “set A” of works are presented in Table 1 for all six variants (V0 and V1-V5).

The input data sets for the remaining sets of works (“set A” and “set B”) were prepared in the same way.

All cost data ($C_{n,0}$, $C_{n,n}$ and $C_{n,p}$) included in Table 1 and for other sets of works include the sum of the costs: labor, purchase of building materials (including transport costs), equipment work and general construction costs along with the calculation profit taking into account the risk of construction companies that can perform specific ranges of construction and installation works. For the implementation of the innovative anti-seismic protection system application, solutions were adopted based on systems using materials produced by SIKA, i.e. Sika PM – flexible, high elasticity two-component adhesive material based on polyurathane resins (for the implementation of prefabricated PUFJ and injected

PUFJ anti-seismic systems) and Sika PS – solvent-free flexible two-component adhesive material based on polyurathane resins for the implementation of FRPU repairs. In the case of prefabricated PUFJ, the costs of prefabricating a joint with a cross-section of approx. 2×15 cm were added, and in the case of injected PUFJ – the costs of making cuts and injections around the perimeter of the wall at three edges of contact with a reinforced concrete frame with a cross-section of approx. 2×10 cm.

Table 1. Data assumed for life cycle costs analysis (own study).

Variant	V0	V1	V2	V3	V4	V5	
Type of the innovative anti-seismic protection system application	no anti-seismic protection system applied	prefabricated PUFJ at 4 interfaces	injected PUFJ at 3 interfaces and application of FRPU				
			no application of FRPU	only at infill diagonals	only at infill edges	as a combination of the systems V3 and V4	
Lifetime (p)	50 yrs.	60 yrs.	50 yrs.	50 yrs.	50 yrs.	60 yrs.	
Discount rate (d)	8%	8%	8%	8%	8%	8%	
Initial costs ($C_{n,0}$)	1,440 EUR	2,314 EUR	1,440 EUR	1,440 EUR	1,440 EUR	1,440 EUR	
Periodic operation costs ($C_{n,n}$) after	10 yrs.	2,010 EUR	445 EUR	2,682 EUR	3,090 EUR	3,230 EUR	3,592 EUR
	20 yrs.	2,110 EUR	467 EUR	467 EUR	276 EUR	276 EUR	191 EUR
	30 yrs.	2,215 EUR	490 EUR	490 EUR	290 EUR	290 EUR	200 EUR
	40 yrs.	2,325 EUR	515 EUR	515 EUR	304 EUR	304 EUR	210 EUR
	50 yrs.	not applicable	541 EUR	not applicable	not applicable	not applicable	221 EUR
Withdrawal costs ($C_{n,p}$)	404 EUR	425 EUR	404 EUR	404 EUR	404 EUR	425 EUR	

Periodic operation costs ($C_{n,n}$) are calculated with a time interval of 10 years, which corresponds to the assumption described in chapter 3 according to which the frequency of earthquakes causing significant material and social losses can be as high as 9 to 12 years (that is, on average, 10 years).

Withdrawal costs ($C_{n,p}$), as well as part of periodic operation costs ($C_{n,n}$) related to removal of debris after each damage to the wall and installation, include the costs of construction waste disposal, including environmental charges.

It is worth also emphasizing that the discount rate (d) allows to take into account the impact of economic phenomena such as inflation or deflation if the nominal costs instead of the real costs are used. However, inflation (or deflation) is not the only factor that can affect the real cost value of a building element or technology. Therefore, it is natural to forecast the value of future costs based on i.e. valorization indicators. In this analysis, a “hybrid approach” was used, according to which it was assumed that: the discount rate (d) is 8%, and the forecast increase in the prices of

building elements or their technology amounts to an average of 5% for each of the following 10 years ($1,05^{[1, 2, \dots, p/10]}$).

In accordance with the provisions of ISO 15686-5: 2017 (ISO, 2017), life cycle costs analysis (LCCA) should also include elements of maintenance management, i.e. the costs of all activities necessary to organize, prioritize, resources or control maintenance, such as: periodic inspections (including condition inspections, detailed inspections, condition monitoring), maintenance planning (including planning, resources, procurement) and design, and management of major replacements. Since in this article, LCCA is only a simulation of cost-effectiveness and efficiency of the presented solutions in seismic areas compared to the traditional system without anti-seismic protection, the authors did not take into account the above-mentioned cost elements.

4.3. Discussion of the results

For each of the defined variants of innovative anti-seismic protection systems (V1-V5) and the reference scenario with application of traditional system without anti-seismic protection (V0), a life cycle costs analysis (LCCA) was carried out to determine:

- (i) net present cost (X_{NPC}) in EUR,
- (ii) annual cost (X_{AC}) in EUR,
- (iii) payback period (PP) in years, after which the cumulative net present cost (X_{NPC}) for the reference scenario (V0) exceeds the X_{NPC} for the innovative anti-seismic protection system (V1-V5), which proves the profitability of a given innovative anti-seismic protection system in relation to the reference scenario (if applicable).

Table 2 presents the results of the analysis in terms of the values calculated for the X_{NPC} and X_{AC} comparative criteria for each set of works.

Table 2. Results of life cycle costs analysis (own study).

Set of works	Economic comparative criteria	V0	V1	V2	V3	V4	V5
A	X _{NPC}	2,260 EUR	2,251 EUR	2,169 EUR	2,304 EUR	2,369 EUR	2,505 EUR
		100.00%	99.60%	95.97%	101.95%	104.82%	110.84%
	X _{AC}	184.74 EUR	181.88 EUR	177.30 EUR	188.34 EUR	193.65 EUR	202.40 EUR
		100.00%	98.45%	95.97%	101.95%	104.82%	109.56%
B	X _{NPC}	2,953 EUR	2,651 EUR	2,728 EUR	2,856 EUR	2,921 EUR	3,057 EUR
		100.00%	89.77%	92.38%	96.72%	98.92%	103.52%
	X _{AC}	241.39 EUR	214.20 EUR	222.99 EUR	233.46 EUR	238.77 EUR	247.00 EUR
		100.00%	88.74%	92.38%	96.72%	98.92%	102.33%
C	X _{NPC}	3,159 EUR	2,704 EUR	2,863 EUR	2,982 EUR	3,047 EUR	3,179 EUR
		100.00%	85.60%	90.63%	94.40%	96.45%	100.63%
	X _{AC}	258.23 EUR	218.48 EUR	234.03 EUR	243.76 EUR	249.07 EUR	256.86 EUR
		100.00%	84.61%	90.63%	94.40%	96.45%	99.47%

The life cycle costs analysis conducted shows that for “set A” of works:

- the lowest X_{NPC} value was obtained for the variant V2 – 2,169 EUR (95.97% in relation to reference scenario – V0) and the highest – 2,505 EUR for V5 (110.84% in relation to V0),
- the lowest X_{AC} value was calculated for the variant V2 – 177.30 EUR (95.97% in relation to V0) and the highest – 202.40 EUR for V5 (109.56% in relation to V0),

for “set B” of works:

- the lowest X_{NPC} value was obtained for the variant V1 – 2,651 EUR (89.77% in relation to V0) and the highest – 3,057 EUR for V5 (103.52% in relation to V0),
- the lowest X_{AC} value was calculated for the variant V1 – 214.20 EUR (88.74% in relation to V0) and the highest – 247.00 EUR for V5 (102.33% in relation to V0),

for “set C” of works:

- the lowest X_{NPC} value was obtained for the variant V1 – 2,704 EUR (85.60% in relation to V0) and the highest – 3,179 EUR for V5 (100.63% in relation to V0),
- the lowest X_{AC} value was calculated for the variant V1 – 218.48 EUR (84.61% in relation to V0) and the highest – 256.86 EUR for V5 (99.47% in relation to V0).

It should be noted that the variant V0 (the reference scenario) did not generate the lowest X_{NPC} and X_{AC} values in any case. However, for the “set C” of works, the X_{NPC} value for V5 is very close to the X_{NPC} value for the variant V0 (it is only 20.00 EUR higher, i.e. +0.63%), but the X_{AC} value for V5 is lower only 1.37 EUR lower (-

0.53%) than V0, which is the effect of extending the lifetime for variant V5 by 10 years (up to 60 years).

Figure 2, Figure 3 and Figure 4 present charts of cumulative cost values (to the X_{NPC} value at the end of lifetime) for all analyzed variants for each set of works (for “set A”, “set B” and “set C”, respectively).

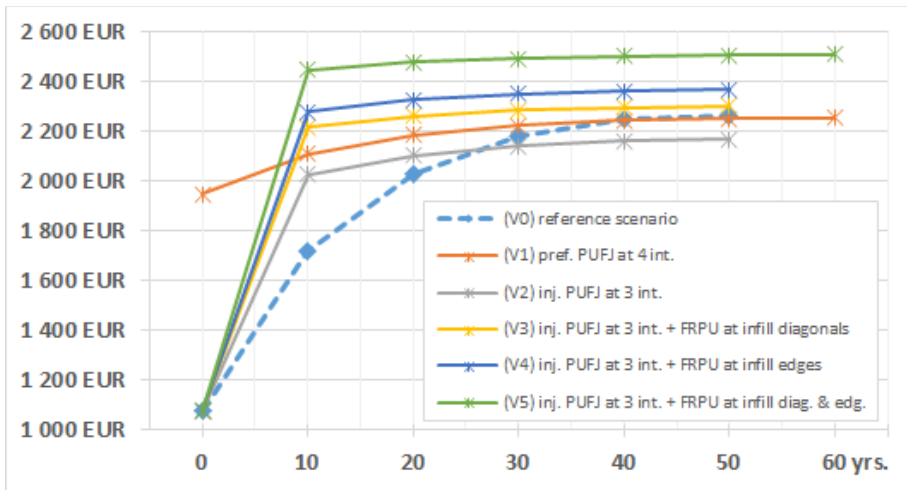


Figure 2. Cumulative cost of X_{NPC} for “set A” of works (own study).

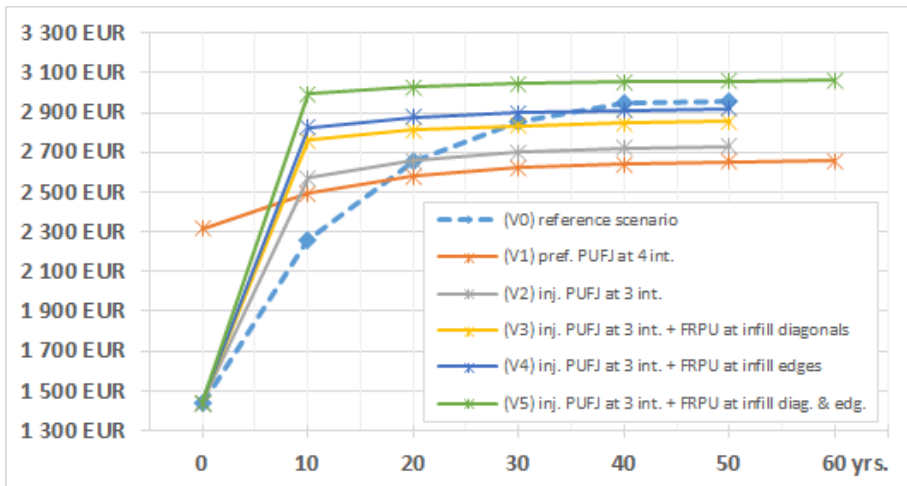


Figure 3. Cumulative cost of X_{NPC} for “set B” of works (own study).

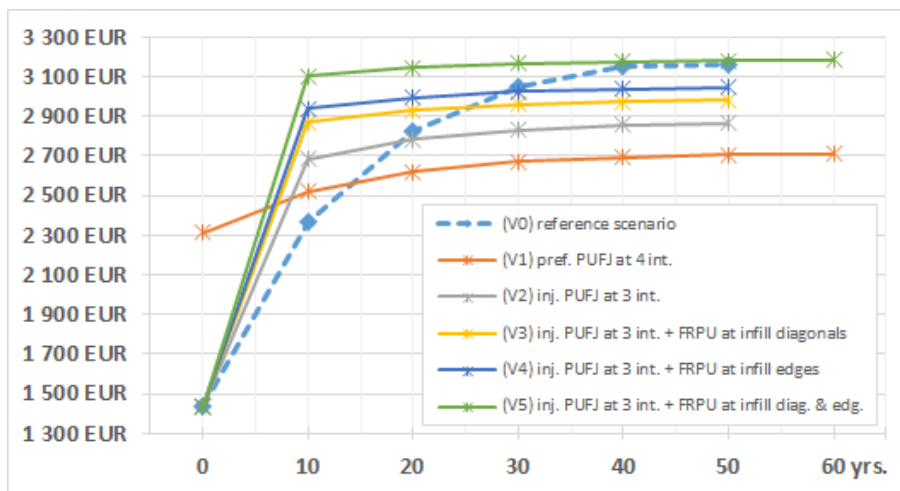


Figure 4. Cumulative cost of X_{NPC} for “set C” of works (own study).

Table 3 shows the results of linear interpolation for the value of payback periods (PP) in years, after which the cumulative net present cost (X_{NPC}) for the reference scenario (V0) exceeds the X_{NPC} for the innovative anti-seismic protection system (V1-V5), which proves the profitability of a given innovative anti-seismic protection system in relation to the reference scenario. The calculations were made on the basis of the charts presented above (Figure 2, Figure 3 and Figure 4).

Table 3. Linear interpolation for the value of payback periods (PP) (own study).

Set of works	V1	V2	V3	V4	V5
A	38.4 yrs.	26.8 yrs.	–	–	–
B	17.5 yrs.	20.0 yrs.	29.0 yrs.	36.0 yrs.	–
C	14.3 yrs.	18.8 yrs.	25.6 yrs.	29.0 yrs.	–

The lowest value of payback period (PP) of only 14.3 years was obtained for variant V1 (prefabricated PUFJ at 4 interfaces) with “set C” of works. In the case of “set B” and “set C” of works, the V1-V4 of innovative anti-seismic protection system variants turn out to be favorable in relation to the reference scenario (maximum PP

value is 36.0 years). Only in the case of the variant V5 (injected PUFJ at 3 interfaces and application of FRPU as a combination of the systems V3 and V4), the value of payback period (PP) was not obtained. On the other hand, as shown above, for the “set C” of works, the X_{NPC} value for V5 is very close to the X_{NPC} value for the variant V0 (the X_{NPC} value for V5 is 100.63% in relation to V0) and the X_{AC} value for V5 is slightly lower than for V0 (the X_{AC} value for V5 is 99.47% in relation to V0). It should be also noted that as the value of the cost of works on an earthquake wall element increases, the value of payback period (PP) decreases. Thus, even those anti-seismic protection systems that require the use of more material intended for the implementation of PUFJ and FRPU (i.e. V4 and V5) turn out to be profitable in relation to the reference scenario (V0).

5. CONCLUSIONS

Taking into account the results of life cycle costs analysis described in Chapter 4 (comparison of X_{NPC} , X_{AC} and PP values to the application of traditional wall system without anti-seismic protection), it can be concluded that in the perspective of the long-term life cycle of a building exposed to severe effects of earthquakes, the application of innovative anti-seismic protection systems using PolyUrethane Flexible Joints (PUFJ) at the frame-infill interface and for bonding of glass fiber meshes to the weak masonry substrate to form Fiber Reinforced PU (FRPU) is cost effective from an economic point of view.

As shown in Table 2, even the highest net present cost (X_{NPC}) value – 2,505 EUR for variant V5 (injected PUFJ at 3 interfaces and application of FRPU as a combination of the systems V3 and V4) for the smallest scope of works (“set A”), i.e. 110.84% in relation to V0 (2,260 EUR), is a value slightly exceeding (by about 10%) the sum of the costs incurred in the life cycle of a building exposed to the destructive force of repeated earthquakes.

If, on the other hand, the scope of works related to RC frames with infills increases in terms of costs, it turns out that the potentially most expensive solutions will generate savings.

In addition, the most advanced anti-seismic protection systems allow to extend the lifetime of masonry walls filling reinforced concrete frames, and at the same time reduce the amount of debris from the demolition of parts or entire buildings damaged or destroyed as a result of earthquakes.

Economical aspects aside, an important element associated with earthquakes is the prevention of major damage and collapse of buildings or their components. It is difficult to underestimate the meaning of human life, which can be saved if the structure withstands the shaking of earth, and this is the case with the presented innovative solutions. In this case, there are also often damages to external elements, i.e. cars or external infrastructure, damaged as a result of i.e. falling out of external infill walls.

Another important element worth considering is the protection of monuments. The collapse of a part or the entire historic building may be an irreparable loss from the historical point of view.

All the above-mentioned basic arguments decide that, according to the authors, the cost-effectiveness and efficiency of the presented solutions in seismic areas, both in the case of a low-intensity earthquake and with relatively high vibration amplitudes.

RESOURCES

Atmaca, B., Demir, S., Günaydın, M., Altunışık, A.C., Hüsem, M., Ates, S., Adanur, S., & Angın, Z. (2020). Lessons learned from the past earthquakes on building performance in Turkey. *Journal of Structural Engineering & Applied Mechanics*, 3(2), 61-84, <https://doi.org/10.31462/jseam.2020.02061084>.

Bostenaru Dan, M. (2018). Decision Making Based on Benefit-Costs Analysis: Costs of Preventive Retrofit versus Costs of Repair after Earthquake Hazards. *Sustainability*, 10(5), 1537. <https://doi.org/10.3390/su10051537>.

De Martino, G., Di Ludovico, M., Prota, A., Moroni C., Manfredi G., Dolce M. (2017). Estimation of repair costs for RC and masonry residential buildings based on damage data collected by post-earthquake visual inspection. *Bulletin of Earthquake Engineering*, 15, 1681-1706. <https://doi.org/10.1007/s10518-016-0039-9>.

Günaydın, M., Atmaca, B., Demir, S., Altunışık, A.C., Hüsem, M., Adanur, S., Ates, S., & Angın, Z. (2021). Seismic damage assessment of masonry buildings in Elazığ

and Malatya following the 2020 Elazığ-Sivrice earthquake, Turkey. *Bulletin of Earthquake Engineering*, 19, 2421-2456. <https://doi.org/10.1007/s10518-021-01073-5>.

ISO 15686-5:2017. (2017). “Buildings and constructed assets – Service-life planning – Part 5: Life-cycle costing”.

Kwiecień, K., Kwiecień, A., Stryzewska, T., Szumera, M., & Dudek, M. (2020). Durability of PS-Polyurethane Dedicated for Composite Strengthening Applications in Masonry and Concrete Structures. *Polymers*, 12(12), 2830. <https://doi.org/10.3390/polym12122830>.

Makra, K., Rovithis, E., Riga, E., Raptakis, D., & Ptilakis, K. (2021). Amplification features and observed damages in İzmir (Turkey) due to 2020 Samos (Aegean Sea) earthquake: identifying basin effects and design requirements. *Bulletin of Earthquake Engineering*, 19, 4773-4804. <https://doi.org/10.1007/s10518-021-01148-3>.

Plebankiewicz, E., Zima, K., & Wieczorek, D. (2018). Life Cycle Equivalent Annual Cost (LCEAC) as a comparative indicator in the life cycle cost analysis of buildings with different lifetimes. In *MATEC Web of Conferences*, 196, 04079. EDP Sciences. <https://doi.org/10.1051/mateconf/201819604079>.

Ramirez, C.M., Liel, A.B., Mitrani-Reiser, J., Haselton, C.B., Spear, A.D., Steiner, J.L., Deierlein, G., & Miranda, E. (2012). Expected earthquake damage and repair costs in reinforced concrete frame buildings. *Earthquake Engineering & Structural Dynamics*, 41, 1455-1475. <https://doi.org/10.1002/eqe.2216>.

Rousakis, T., Ilki, A., Kwiecien, A., Viskovic, A., Gams, M., Triller, P., Ghiassi, B., Benedetti, A., Rakicevic, Z., Colla, C., Halici, O. F., Zajac, B., Hojdys, Ł., Krajewski, P., Rizzo, F., Vanian, V., Sapalidis, A., Papadouli, E., & Bogdanovic, A. (2020). Deformable Polyurethane Joints and Fibre Grids for Resilient Seismic Performance of Reinforced Concrete Frames with Orthoblock Brick Infills. *Polymers*, 12(12), 2869. <https://doi.org/10.3390/polym12122869>.

Wieczorek, D., Plebankiewicz, E., & Zima, K. (2019). Model estimation of the whole life cost of a building with respect to risk factors. *Technological and Economic Development of Economy*, 25(1), 20-38. <https://doi.org/10.3846/tede.2019.7455>.

Yön, B., Onat, O.E., Emin Öncü, M., & Karasin, A. (2020). Failures of masonry dwelling triggered by East Anatolian Fault earthquakes in Turkey. *Soil Dynamics and Earthquake Engineering*, 133, 106126. <https://doi.org/10.1016/j.soildyn.2020.106126>.

SEISMIC PERFORMANCE OF THE POLYMER FLEXIBLE JOINTS IN RC FRAMES WITH VARIOUS INFILL WALL ASPECT RATIOS

A. Tugrul Akyildiz¹, Arkadiusz Kwiecień²

¹*Cracow University of Technology, Warszawska 24, 31-155 Cracow, Poland, tugrulakyildiz@gmail.com*

²*Cracow University of Technology, Warszawska 24, 31-155 Cracow, Poland, akwiecie@pk.edu.pl*

*Responsible author: *tugrulakyildiz@gmail.com*

ABSTRACT

Earthquakes affect buildings in variety of ways. Among those, infill wall failures constitute a high proportion of the total visible damages in multi-story constructions, which can be easily observed even under low or moderate intensity earthquakes. The failures occur as a result of the interaction forces emerging at the interfaces of surrounding frame and walls, and mainly attributed to the brittle intrinsic characteristics of the materials. In order to overcome this challenge, an innovative solution aiming to mitigate damages on the structural components of the infilled RC buildings from the hazardous effects of seismic motions is investigated. The solution proposes to use a material called Polyurethane PM as the flexible joint between different structural members i.e., infill walls and concrete frames, in reinforced-concrete (RC) buildings. The material has high ductility features that allow deformability capacity to reach remarkable levels. Thus, earthquake induced lateral displacement demands on the structural systems can be satisfied by means of dissipating the seismic energy up to the high drift levels, which is a crucial point from the earthquake engineering perspective. In this study, performance of the aforementioned PolyUrethane Flexible Joint (PUFJ) is examined in single-bay and single-story RC frames with different width-height infill wall aspect ratios. Three dimensional models are created numerically in the finite elements method (FEM) environment and gradually increasing monotonic horizontal loads are imposed on the top-beam level of the frames. For the comparison purposes, Stiff (STF) type of frames are also created which represent the traditional mortar joint implementation between the frame and infill walls. Moreover, as a reference, analyses on the Bare-Frame (BF) systems are conducted, too. The results are evaluated in terms of the stiffness and strength status of the frames as a whole system and besides, performances of the different materials are discussed on the individual component level.

KEYWORDS: Polymer flexible joints, infill walls, earthquake damage, seismic protection, RC buildings, wall aspect ratio

1. INTRODUCTION

Masonry as a construction technique is being used across the globe for many years, perhaps since the very first periods of the human civilization. Common reasons of preferring this method can be stated as; easy accessibility, different formation and configuration options, fireproof and thermal insulation features. Following the technological developments throughout the ages, masonry utilization areas have also been evolved and this ancient method has started to be adopted for various structural solutions. Among those, arranging blocks for creating infill walls in multi-story frames is one of the most popular options. Such infilled systems are preferred particularly for creating dwellings as well as for the architectural purposes. Although there are variety of advantages of using this technique, today it is a known fact that infill walls are vulnerable against earthquakes especially if the brittle materials such as clay bricks are used for constituting the masonries. Structural engineers most often consider these walls as non-structural components with their additional mass effects on the buildings only, hence designing phase primarily focus on the other structural parts [1]. This approach might be appropriate in many circumstances if the vertical loads are the only concern, yet strong lateral loads such as earthquakes trigger additional mechanisms on the structural systems which cannot be neglected. Because, high inertial characteristics of the walls lead to receive seismic effects more severely on buildings compared to the bare-framed systems. Under such conditions, the infill walls which are initially assumed to provide an auxiliary load carrying source might reveal substantial risks for the building stability, since relatively low ductile capacities of the walls cannot withstand the earthquake induced displacement demands. In this case, negative effects outweigh the positive ones, especially if the infills are severely damaged and eventually lose their load carrying capacities [2]. Past earthquakes showed us the fatal consequences of this drawback that infill wall related failures caused either partial or total collapse of the multi-story buildings. The failure mechanisms could be categorized under different types including but not

limited to in-plane and out-of-plane damages, soft-story effects and short-column shear damages on columns, see Figure 1 [3-5].



Figure 1. Infill wall related failures after earthquakes; in-plane and out-of-plane damages (left) [3], corner crushing of the wall and shear damage on column (middle) [4], and soft-story mechanism (right) [5].

Multi-story reinforced concrete (RC) buildings comprise of various materials, such as concrete, reinforcing steel and infill wall – which is also a heterogenous component itself. Naturally, each material has different ductility features, though it is desired that structural elements constructed by those to exhibit similar displacement behaviors under the earthquake loads. However, this expectation cannot be actualized easily in real-life scenarios unless an appropriate solution is utilized which can prevent the negative interaction effects occurring as a result of the aforementioned ductility variations. That being said, it can be stated that infill wall related damages are the outcomes of those interaction forces arising between the frames and masonries. A crucial aspect at this point is the bonding efficiency between the surrounding frame and infill wall. In this way, it can be possible to sustaining the wall stability thanks to the sufficient connection. On the other hand, such joint detail should also satisfy the frame protection needs, particularly when

strong bricks are preferred in the wall. In Figure 2, typical infilled system damages are illustrated.

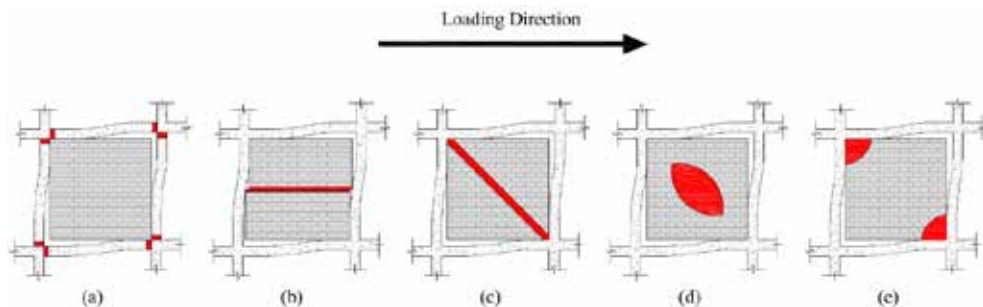


Figure 2. Common infill wall related failure mechanisms; (a) frame damage, (b) horizontal shear, (c) diagonal crack, (d) mid-height diagonal compression, (e) corner crushing.

Aforementioned concerns about the infill masonries lead engineers to develop preventative solutions in order to mitigate such damages. Among those; carbon fiber reinforced polymer (CFRP) wrapping sheets on the walls [6-8], special connection detailing for separating masonries from the frames [9] or enhancing the sliding capacity of infills with special joints [10] are some of the popular methods. Accordingly, this paper also focuses on another alternative solution in this regard. PolyUrethane Flexible Joints (PUFJ) – made by the Polyurethane PM, a product of Sika Company – are designed for replacing the traditional mortar placed between the frame and infill walls. In this way, ductility level of the frames is aimed to be enhanced while sustaining the load carrying capacity. Simultaneously, concrete and brick elements are also protected by means of distributing the stress concentrations around the masonry boundaries. Previous experimental [11-12] and numerical [13-14] studies on this specific material revealed promising results. Hyper-elastic features of the material ensure to resisting against the large deformations. Details of the material properties can be found elsewhere [15-17].

This study presents the numerical results of single-bay and single-story frames which had real-size dimensions and constructed with the joint type of traditional stiff (STF) mortar and PUFJ. Frames and masonry details were identical for both frame types, though frame-to-masonry connection detailing constituted the only difference. In

order to investigate the efficiency of the proposed solution with various configurations, three different wall width-to-height aspect ratios were considered for each joint type of frames. Accordingly, rectangular shaped walls were categorized as follows; the masonry wall with the edge lengths of vertical 1950mm and horizontal 2000mm was labeled as the wall with the aspect ratio of 1.0, since it almost represents the exact square shape. On the other hand, the height of the wall was kept constant whereas the width dimension was modified for designing the other aspect ratios. In this way, the width of the square shaped wall was reduced to the half – from 2000mm to 1000mm, thus the frame with the wall aspect ratio of 0.5 was obtained. Similarly, the width of the wall was modified once again, but this time the length was increased from 2000mm to 3000mm; hence, the aspect ratio of 1.5 was achieved. The wall was created by forming brick units with dimensions of 65mm x 120mm x 250mm in single wythe vertically, thus the wall thickness was 120 mm. Beam and column elements had the same dimensions and 250mm x 250mm section area was provided for each. However, reinforcement detailing was different for those. Reinforcement ratio for the frames was intentionally left relatively deficient, thus the effect of masonries could be more visible. Joint thickness between the frame and infill wall was determined as 20 mm, for both traditional mortar and PUFJ. Details of the dimensions of frames are shown in Figure 3.

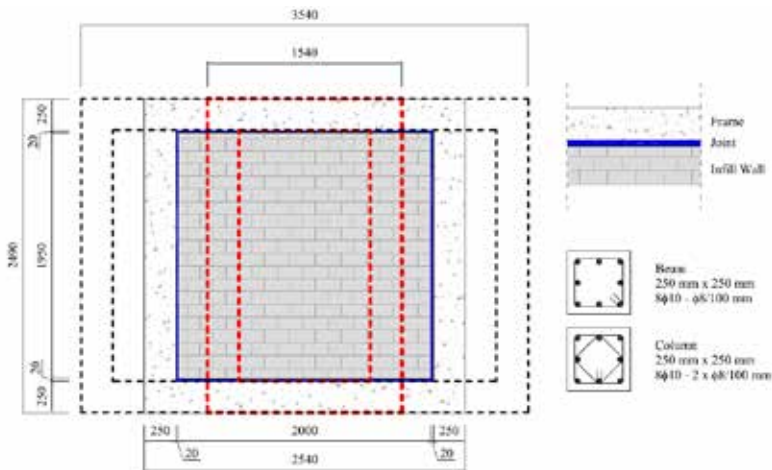
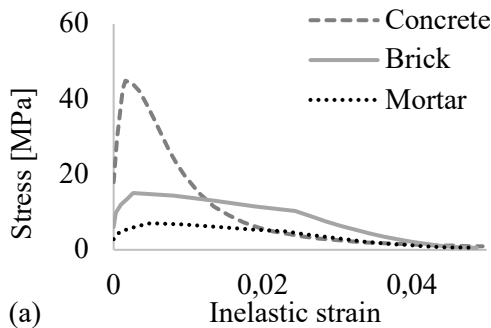


Figure 3. Details of the frames; red-dotted, black-line and black-dotted for the aspect ratios of 0.5, 1.0 and 1.5, respectively [mm].

2. NUMERICAL MODELS

The analyses were performed by ABAQUS [18] software, which is a commercially available Finite Elements Method (FEM) based program. Although the analyses were run for a single direction only – in-plane of the masonry – 3D numerical elements were used throughout the simulations. In this way, the stress distributions as well as the material distortions could be captured more accurately compared to the 2D modeling strategy, though it led to higher computational efforts. Hexahedral solid elements with reduced integration (C3D8R) were utilized while creating the concrete, brick units and joint parts. Moreover, reinforcement bars were modeled by using the 2-node 3D truss elements (T3D2) embedded in the concrete matrix which are also available in the element library of the program and designed to carry merely the axial loads. Non-linearity on the material level as well as geometrically (second order effects) were considered during all analyses.

In order to achieve reliable results from the numerical models, particularly the composite systems such as masonries, calibration with the experimental tests is essential. Therefore; the results from the previous researches [13, 19] were derived and adapted to this study while determining the material constitutive properties for the numerical modeling. Further details can be found in these references. Concrete class of C35/45 was used for the frames. Various sizes of reinforcement steel bars had the type of B500B, which is commonly preferred in the construction sector. Moreover, polyurethane PM properties for the PUFJ were derived from another work [20]. Stress-strain relations of these materials are given in Figure 4 and Figure 5.



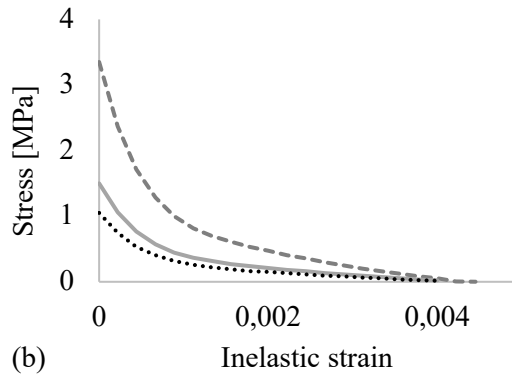


Figure 4. Concrete, brick and mortar mechanical properties; (a) compressive, (b) tensile.

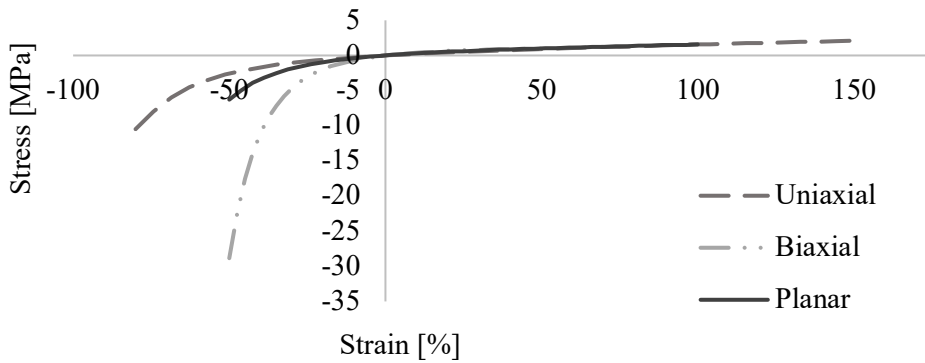


Figure 5. Polyurethane PM mechanical properties.

Additionally to the individual material constitutive properties, interactions among the different materials are also need to be defined for obtaining accurate results. Accordingly, simplified micro modeling technique was followed for the infill walls. In this way, brick units were modeled separately; however, interaction between the units were actualized by the contact pairs assuming mortars had zero thickness. Exterior boundary of the infill walls was assigned to the same contact pair approach,

which was in contact with the surrounding frame. Traction-separation law, which is largely used for defining the cohesive surfaces was enforced on those parts. In terms of the PUFJ interaction with the other parts, perfect bonding assumption was determined which is in line with the experimental results [20]. Therefore, the joints were assumed to be tied to the rest of system.

Frames were restrained at the bottom beam level and the rest of system was able to move freely in any direction. First, all frames were exposed to the vertical loads affecting on the columns. Total amount of 60kN loading was distributed equally on those, for representing upper stories in a building. Following that, while the vertical loads were still effective, the frames were loaded with the identical monotonically increasing horizontal loading procedure in a single direction. This was done by means of forcing the frames on top-beam level with gradually increasing displacement targets. The ultimate displacement was determined relatively very high for such systems – as 150mm, which corresponds to a drift ratio slightly greater than the 6.8%. Hence, an extreme condition could be examined.

3. RESULTS OF THE ANALYSES

Outcomes were evaluated on the global level by means of comparing between the horizontal load carrying capacities of the frames as well as on the individual level in terms of overviewing the damage status of the different units that constitute the frames.

For the case of load capacities; peak values of the curves were considered for identifying the maximum load levels. In addition, initial stiffness values of the frames were determined by calculating the slopes of tangent lines correspond to the 10% of maximum load values of those curves [21]. Secant stiffness values were also determined in a similar way; yet this time, the loads at the ultimate horizontal displacements were utilized. These curves are presented in Figures 6-7.

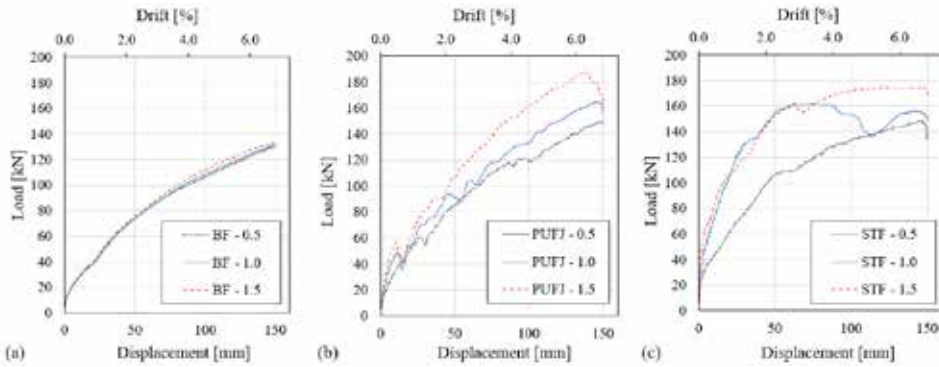


Figure 6. Load – displacement curves of the frames based on the aspect ratio variations; (a) BF, (b) PUFJ and (c) STF.

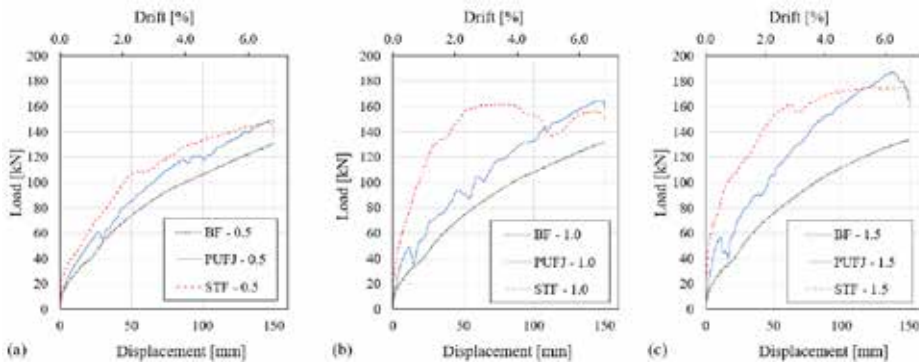


Figure 7. Load – displacement curves of the frames based on the joint connection types; (a) aspect ratio: 0.5, (b) aspect ratio: 1.0 and (c) aspect ratio: 1.5.

According to the results; it was seen that aspect ratio practically did not make any differences for the frame type of BF. This was an expected outcome, since the columns were the only horizontal load carrying members in the absence of infill walls and they had the identical length and section dimensions for the case of each aspect ratio, hence the overall shear capacities of the frames were similar. Peak loads were reached to values slightly higher than 130kN. On the other hand, variations of the aspect ratios led to obtain different results for the frames PUFJ and STF. In both

frame types, greater aspect ratios increased the horizontal load carrying capacities due to the fact that shear area of the infill walls in the direction of loading was also enhanced. This trend was smoother for the PUFJ frame, whereas for the case of STF type, difference between the aspect ratios of 1.0 and 1.5 was marginal until the load drop started to occur for the frame with the aspect ratio of 1.0 just after 3.5% drift ratio.

Although STF frame exhibited higher initial stiffness at the beginning of analyses compared to the other frames, relative stiffness drop at the ultimate point was mostly accounted for this type and it is represented here as the secant stiffness. Accordingly, in the extreme case, STF frame experienced the declining of the initial stiffness value from the levels of 50kN/mm to 1.1kN/mm which corresponds to 2.2% of the initial value. The other frame types, BF and PUFJ, showed rather ductile behavior since the beginning of loading, thus smaller stiffness drops were observed. The greatest decreases were seen for the case of frames with the aspect ratio of 1.5, as the secant stiffness values were 13.0% and 9.0% of the initial ones for the BF and PUFJ frames, respectively.

Unlike the trend of initial stiffness values, PUFJ type which initially prone to behave ductile compared to STF frame, exhibited greater peak load performance for the case of each aspect ratio. The difference was rather marginal for the aspect ratios of 0.5 and 1.0; however, it was reached to around 7% when the aspect ratio was 1.5%. On the other hand, BF type which performed the lowest initial stiffness values in each aspect ratio, also could withstand relatively lower loads. In terms of the peak loads, those values were less than the other frames in a range of approximately 10% to 30%, depends on the wall aspect ratio.

Details of the load – displacement results are given in tabular format too, see Table 1.

Table 1. Load – displacement results of the frames.

Frame	Aspect Ratio	Max. Load [kN]	Relative Max. Load [%]	Initial Stiffness [kN/mm]	Secant Stiffness [kN/mm]	Secant / Initial Stiffness [%]
BF		130.7	87.5	6.65	0.87	13.1
PUFJ	0.5	149.4	100.0	6.86	0.98	14.3
STF		148.1	99.1	20.66	0.90	4.4
BF		131.8	80.1	6.70	0.88	13.1
PUFJ	1.0	164.6	100.0	9.78	1.04	10.6
STF		162.1	98.5	34.37	0.99	2.9
BF		133.5	71.2	6.83	0.89	13.0
PUFJ	1.5	187.5	100.0	11.74	1.06	9.0
STF		174.8	93.2	50.16	1.12	2.2

Furthermore, damage status of the frames was evaluated in terms of the cracking occurrence on the structural units. Accordingly, influence of the flexible joints was visible regardless of the wall aspect ratio, though the damage patterns were slightly different for those. The damages were distributed rather evenly across the infill walls for the case of PUFJ type of frames. The failures were not accumulated on a specific zone, and particularly the brick units in the vicinity of the wall perimeters were able to sustain their strength thanks to the effectiveness of flexible joints while mitigating the stress concentrations. This potentially prevents the out-of-plane failures in a real-life scenario. On the other hand, damages were more intense for the case of STF type, and different failure patterns could be stated. Regarding the frame with the aspect ratio of 0.5, the damages on the brick units were mostly concentrated on the central zone of the wall in a similar manner of typical diagonal compression failure. For the STF type of frames with the other aspect ratios; it was seen that damages were accumulated in different parts of the walls. Those were formed in a double-

strut shape for the aspect ratio of 1.0, and an irregular mix of sliding-shear and diagonal compression could be stated as the failure of the frame with the aspect ratio of 1.5. It is also worth to mention that the connection loss between the frame and wall was encountered in these frames as a result of the implementation of stiff joints which were not able to resist the larger displacement demands and could not distribute the stresses. Moreover, in both PUFJ and STF frames, the columns were severely damaged due to the plastic hinges occurred starting the column ends, and later spreading along these vertical members, though the beams were in good condition at the end of analyses. These damages are presented in Figures 8-9.

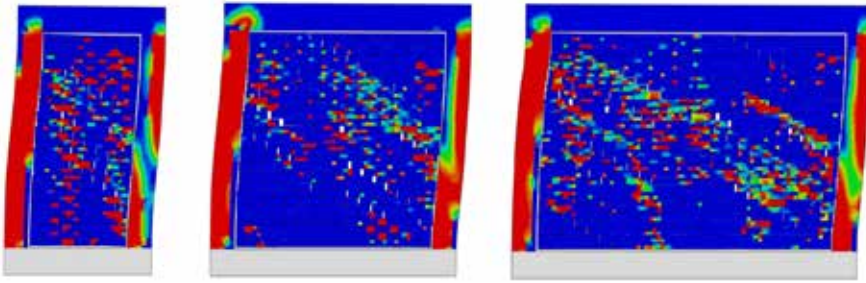


Figure 8. Cracking damage status of the PUFJ frames at the end of analyses; aspect ratio: 0.5 (left), aspect ratio: 1.0 (middle) and aspect ratio: 1.5 (right).

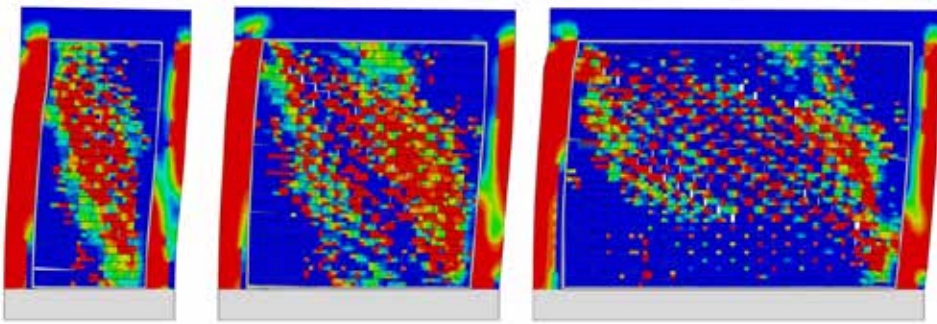


Figure 9. Cracking damage status of the STF frames at the end of analyses; aspect ratio: 0.5 (left), aspect ratio: 1.0 (middle) and aspect ratio: 1.5 (right).

4. CONCLUSIONS

In this study, polymer based flexible joint approach (PUFJ) which is developed for providing an alternative solution for protecting buildings against the earthquakes was tested through monotonically increasing horizontal loads. For this purpose, numerical models were created while adhering to the real-size dimensions and actual material properties. In order to compare this innovative solution with the existing construction techniques, traditionally constructed stiff mortar (STF) and bare-frame (BF) options were also analyzed. Findings are summarized as below:

- Infill walls increased the lateral load carrying capacity thus BF exhibited lower peak loads, which is a well-known phenomenon. On the other hand, this study shows that PUFJ effectiveness in terms of load carrying capacity is around the similar levels or even higher compared to the traditionally constructed STF frame.
- Ductility is a key element in terms of earthquake engineering. Because, enormous amount of energy is spread around during a ground shake and reliable energy absorption mechanisms are required while resisting such forces. Therefore, force-based design (FBD) approach has lost its popularity in the recent years while the importance of the displacement-based design (DBD) method has started to be better comprehended [22-24]. In this regard, PUFJ implementation exhibits promising results that ductility is possible to be enhanced close to the BF levels without compromising the structural load carrying capacity.
- Aspect ratio variation was not effective on the results of the BF type, since the columns were the only horizontal load carrying members and their dimensions were identical regardless of the aspect ratio. On the other hand, effect of this difference was clearly visible for the PUFJ and STF frames. Both types exhibited higher lateral load resistance for the greater aspect ratios, since the shear area of the walls were enhanced, too.
- Positive effects of flexible joints were also encountered in terms of mitigating local damages occurring on the individual masonry parts; i.e., brick units. High displacement demands could be successfully achieved thanks to the hyper-elastic features of the joints. In this way, the wall stability could also be sustained regardless of the aspect ratio, which traditional stiff joint method failed.

REFERENCES

- [1] Sucuoğlu, H. (2013). Implications of Masonry Infill and Partition Damage in Performance Perception in Residential Buildings after a Moderate Earthquake. *Earthquake Spectra*, 29(2), 661–667. <https://doi.org/10.1193/1.4000147>
- [2] Hermanns, L., Fraile, A., Alarcón, E., & Álvarez, R. (2013). Performance of buildings with masonry infill walls during the 2011 Lorca earthquake. *Bulletin of Earthquake Engineering*, 12(5), 1977–1997. <https://doi.org/10.1007/s10518-013-9499-3>
- [3] Doğangün, A., Ural, A., Sezen, H., Güney, Y., & Fırat, F. (2013). The 2011 Earthquake in Simav, Turkey and Seismic Damage to Reinforced Concrete Buildings. *Buildings*, 3(1), 173–190. <https://doi.org/10.3390/buildings3010173>
- [4] Gur, T., Pay, A., Ramirez, J. A., Sozen, M. A., et. al. (2009). Performance of School Buildings in Turkey During the 1999 Düzce and the 2003 Bingöl Earthquakes. *Earthquake Spectra*, 25(2), 239–256. <https://doi.org/10.1193/1.3089367>
- [5] Sezen, H., Elwood, K. J., & Whittaker, A. S. et. al. (2000, September). *Structural Engineering Reconnaissance of the August 17, 1999, Kocaeli (Izmit), Turkey, Earthquake* (No. 2000/09). Pacific Earthquake Engineering Research Center.
- [6] Altın, S., Anil, Z., Kara, M. E., & Kaya, M. (2008). An experimental study on strengthening of masonry infilled RC frames using diagonal CFRP strips. *Composites Part B: Engineering*, 39(4), 680–693. <https://doi.org/10.1016/j.compositesb.2007.06.001>
- [7] Erdem, I., Akyuz, U., Ersoy, U., & Ozcebe, G. (2006). An experimental study on two different strengthening techniques for RC frames. *Engineering Structures*, 28(13), 1843–1851. <https://doi.org/10.1016/j.engstruct.2006.03.010>
- [8] Yuksel, E., Ozkaynak, H., Buyukozturk, O., Yalcin, C., Dindar, A., Surmeli, M., & Tastan, D. (2010). Performance of alternative CFRP retrofitting schemes used in infilled RC frames. *Construction and Building Materials*, 24(4), 596–609. <https://doi.org/10.1016/j.conbuildmat.2009.09.005>

- [9] Tasligedik, A. S., Pampanin, S., & Palermo, A. (2013, 28–30 August). *Low damage seismic solutions for non-structural drywall partitions*. In Proceedings of the Vienna Congress on Recent Advances in Earthquake Engineering and Structural Dynamics, Vienna, Austria.
- [10] Preti, M., Bolis, V., & Stavridis, A. (2016, 26–30 June). *Design of masonry infill walls with sliding joints for earthquake structural damage control*. In Proceedings of the 16th International Brick and Block Masonry Conference, Padova, Italy.
- [11] Akyildiz, A. T., Kwiecień, A., Zając, B., et. al. (2020, 5–8 July). *Preliminary in-plane shear test of infills protected by PUFJ interfaces*. In Proceedings of the 17th International Brick/Block Masonry Conference (17thIB2MaC 2020), Kraków, Poland.
- [12] Rousakis, T., Ilki, A., Kwiecien, A., Viskovic, et. al. (2020). Deformable Polyurethane Joints and Fibre Grids for Resilient Seismic Performance of Reinforced Concrete Frames with Orthoblock Brick Infills. *Polymers*, 12(12), 2869. <https://doi.org/10.3390/polym12122869>
- [13] Akyildiz, A. T., Kowalska-Koczwara, A., & Hojdys, Ł. (2021). Seismic Protection of RC Buildings by Polymeric Infill Wall-Frame Interface. *Polymers*, 13(10), 1577. <https://doi.org/10.3390/polym13101577>
- [14] Rousakis, T., Vanian, V., Fanaradelli, T., & Anagnostou, E. (2021). 3D FEA of Infilled RC Framed Structures Protected by Seismic Joints and FRP Jackets. *Applied Sciences*, 11(14), 6403. <https://doi.org/10.3390/app11146403>
- [15] Kwiecień, A. (2012). *Polymer flexible joints in masonry and concrete structures*, Monography No. 414, Wyd. Politechniki Krakowskiej, Seria Inżynieria Łądowa, Kraków, (in Polish).
- [16] Kwiecień, A., Gams, M., & Rousakis, T. (2017). Validation of a new hyperviscoelastic model for deformable polymers used for joints between rc frames and masonry infills. *Engineering Transactions*, 65(1), 113–121.
- [17] Kwiecień, A., Gams, M., Viskovic, A. et. al. (2017). Use of polymer flexible joint between RC frames and masonry infills for improved seismic performance, Zurich: SMAR.
- [18] Dassault Systèmes. Abaqus v2016 Analysis User's Manual. (2015). Dassault Systèmes: Vélizy Villacoublay, France.

- [19] Viskovic, A., Zuccarino, L., Kwiecień, A., Zajac, B., & Gams, M. (2017). Quick Seismic Protection of Weak Masonry Infilling in Filled Framed Structures Using Flexible Joints. *Key Engineering Materials*, 747, 628–637. <https://doi.org/10.4028/www.scientific.net/kem.747.628>
- [20] Kisiel, P. (2018). *Model Approach for Polymer Flexible Joints in Precast Elements Joints of Concrete Pavements*. Ph.D. Thesis, CUT, Cracow, Poland.
- [21] Mondal, G., & Jain, S. K. (2008). Lateral Stiffness of Masonry Infilled Reinforced Concrete (RC) Frames with Central Opening. *Earthquake Spectra*, 24(3), 701–723. <https://doi.org/10.1193/1.2942376>
- [22] Moehle, J. P. (1992). Displacement-Based Design of RC Structures Subjected to Earthquakes. *Earthquake Spectra*, 8(3), 403–428. <https://doi.org/10.1193/1.1585688>
- [23] Priestley, M. J. N. (1993). Myths and fallacies in earthquake engineering. *Bulletin of the New Zealand Society for Earthquake Engineering*, 26(3), 329–341. <https://doi.org/10.5459/bnzsee.26.3.329-341>
- [24] Priestley, M. J. N. (2020). *Performance based seismic design*. Paper No. 2831. Proceedings of 12th World Conference on Earthquake Engineering, New Zealand.

EARTHQUAKE PROTECTION OF RC FRAMES WITH INFILLS JOINED BY PUFJ AND FRPU SYSTEMS

Arkadiusz Kwiecień^{1*}

¹*Cracow University of Technology, Faculty of Civil Engineering, Warszawska 24, 31-155 Cracow, Poland, akwiecie@pk.edu.pl*

*Responsible author: *akwiecie@pk.edu.pl*

ABSTRACT

Infill structures consisting of reinforced concrete (RC) frame and masonry infill walls are very popular structures, especially in seismic areas. In such structures, RC skeleton plays load-bearing role and infill walls play significant role as secondary elements stiffening the entire building during earthquakes, when they are in good shape and structural condition. Their damages lead to reducing of stiffness and thus to reducing of seismic resistance of RC frame structures with infills. They should also be resistant to cyclically repeating earthquakes to reduce economic losses. In this paper, innovative solutions protecting infill structures are presented with results of their examination on a shake table, and especially damage and stiffness parameters changing with repeating seismic excitations are discussed. Their analysis confirmed that these introduced anti-seismic solutions based on flexible bonding are able to protect infill structures against serious damage and failure (in-plane or out-of-plane) and protect RC columns against damages under repeating strong seismic action, assuring safe level of load bearing capacity. Obtained results indicate that these anti-seismic solutions can be used efficiently in damaged or newly constructed infill structures in seismic areas.

KEYWORDS: infill walls, seismic protection, flexible joints, global stiffness ratio, damage indicator, shake table

1. INTRODUCTION

Infill structures consisting of reinforced concrete (RC) frame and masonry infill walls are very popular structures, especially in seismic areas. In such structures, RC skeleton plays load-bearing role and infill wall is treated as a non-structural element. Inspections of damaged structures in post-earthquake areas show that the damage pattern of infill walls is usually characterized by oblique fractures from in-plane shear or out-of-plane collapse, slippage of joints at the joint with a reinforced concrete frame or a combination of the above [1,2]. These damages lead to infills falling out of the frames. Non-structural infill walls are more prone to damage and fail faster compared to reinforced concrete load-bearing elements. The insufficient ability of the rigid elements to transmit forces due to the relatively large displacement (imposed by the RC columns) is the main cause of failure of infills. Stress concentrations at the contact of reinforced concrete elements with filling walls cause damage even at very small horizontal drifts, below 0.5% [3]. When the fillings are strong and stiff enough, they can cause harmful destruction of reinforced concrete columns (due to local stress concentration), and even the collapse of the building (the so-called soft-story). The cost of repairing fillings is very high, even in the case of moderate earthquakes, which leads to an urgent need to consider the impact of non-structural filler walls on the overall behavior of the structure and to use innovative solutions to protect them from damage during repeated strong earthquakes [4]. Infill walls play significant role as secondary elements stiffening the entire building [5] during earthquakes, when they are in good shape and structural condition. Their damages lead to reducing of stiffness and thus to reducing of seismic resistance of RC frame structures with infills. In this paper, innovative solutions protecting infill structures are presented with results of their examination on a shake table, and especially damage and stiffness parameters changing with repeating seismic excitations are discussed.

2. INNOVATIVE SOLUTION PROTECTING INFILL STRUCTURES

In the last decade, a new innovative solution was developed, creating bonding structural connectors, able to withstand large deformation. In the past, connectors of brittle structural members were belonging to opposite areas: stiff joints (capable to

carry high loads but unable to carry high deformations) and sealants (capable to carry high deformations but unable to carry high loads). The gap between them was empty in the case of construction industry, whereas in motor and marine industries this gap was fulfilled by flexible connectors. Following those branches, a new sort of structural joints was introduced in construction industry, named Polymer Flexible Joints – PFJ (Fig. 1a). They are capable to carry high loads and large deformations simultaneously. They also allow for reducing of stress concentrations and redistributing them over large bonding area (Fig. 1b).

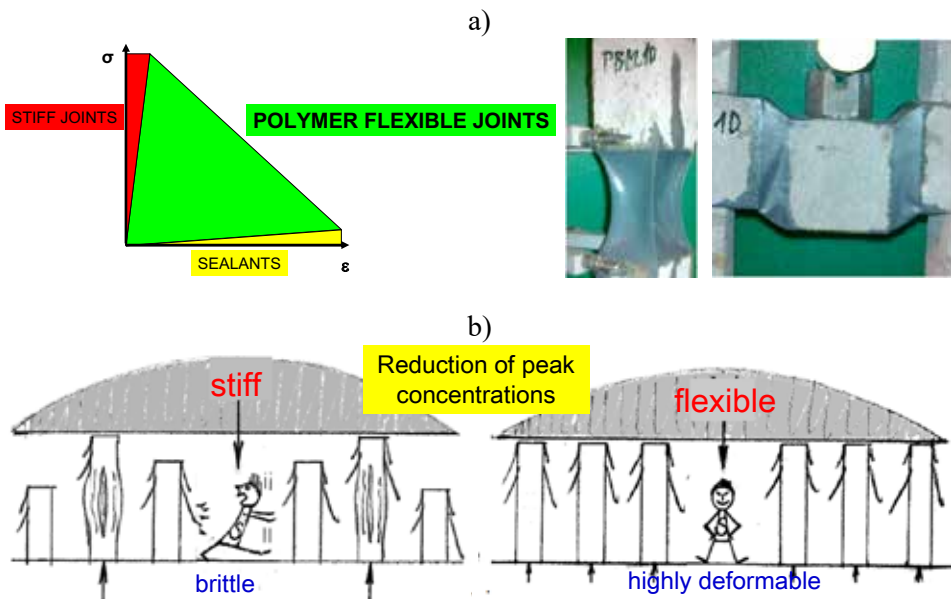


Figure 1. Polymer Flexible Joints (PFJ) transferring loads and large deformations simultaneously (a), schematically presented idea of reduction of stress concentrations and even redistribution of stress by highly deformable flexible polyurethanes (b).

2.1. PUFJ and FRPU systems

Polymer Flexible Joints (PFJ) and is dedicated to structural and non-structural bonding of elements constructing civil engineering structures, made of various materials (concrete, masonry, wood, metal). The specially designed connectors are able carry static, dynamic and cyclic loads and simultaneously transfer large deformations. They are resistant to elevated temperatures and reduce stress concentrations by redistributing them for large bonding area. These connectors made of special polyurethanes distributed by SIKA Poland occur in three forms: PolyUrethane Flexible Joints (PUFJ) – injected (Fig. 2a) and prefabricated (Fig. 2b) and Fiber Reinforced PolyUrethanes (FRPU) – composite (Fig. 2c). These three innovative products of FlexAndRobust Systems are also examined by Cracow University of Technology and other research and development partners in frame of H2020 project MEZeroE, as proper solutions for nearly zero energy buildings (nZEB) in seismic areas.

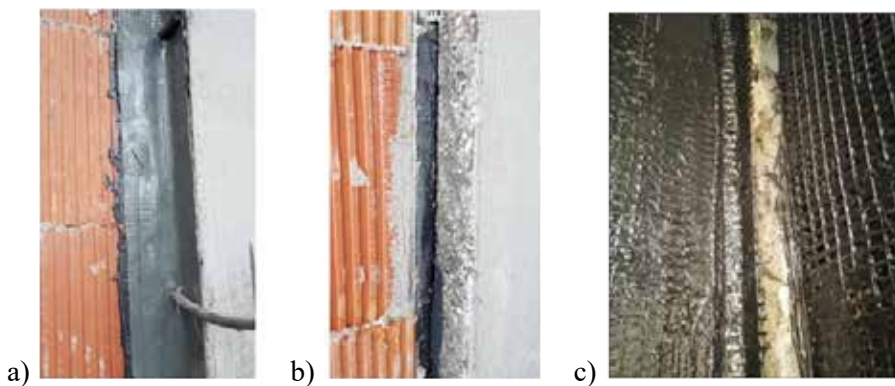


Figure 2. Injected PUFJ (a), prefabricated PUFJ (b) and FRPU composite (c).

Injected PUFJ (Fig. 2a) is liquid inject able material of fast curing time, suitable for filling gaps and bonding of structural and non-structural elements, as well as for repair of damaged (cracked) elements. It can fill cracks or gaps between structural elements (e.g. RC skeleton and infill) and can be used for seismic improvement of

existing infill structures. Application of this system at 3 interfaces (top and two side) between RC elements and a masonry infill is visible in Fig. 3a (at right hand site). Cracks of a damaged structure can be filled by injected PUFJ and can protect it efficiently against strong dynamic loads (Fig. 4).

Prefabricated PUFJ (Fig. 2b) is a flexible layer constructed on site or in a factory, which connects structural and non-structural elements with special adhesives and can be adjusted to any bonding surface shapes and thicknesses. It can be installed on all RC frame elements' surfaces and then the space can be filled with masonry (Fig. 3a). It is dedicated for seismic improvement of existing RC frame structures (new or old after an earthquake), before an infill installation.



Figure 3. Installation of: injected and prefabricated PUFJ (a), FRPU composite (b).



Figure 4. Seriously cracked masonry building repaired by injected PUFJ and efficiently protected against dynamic loading caused by a caterpillar [6].

FRPU composite (Fig. 2c) is prefabricated or constructed on site composite material, consisted of strengthening fibers and flexible polyurethane matrix, fastened to structural and non-structural elements by flexible adhesives. It can be installed on infill walls' surfaces in various pattern (Fig. 3b). FRPU is dedicated for seismic improvement of existing infill walls (even seriously cracked) and for protection of them against out-of-plane failure.

2.2. Shake table tests of PUFJ and FRPU systems on real scale specimen

Dynamic tests on natural 3D specimen consisting of a RC frame with infill walls protected by PUFJ and FRPU systems were carried out in the laboratory of IZIIS Skopje in North Macedonia in frame of the H2020 SERA project. A symmetrical building with B and C type infill walls was tested in 4 PHASES (Fig. 5) on an one-direction shake table using acceleration of a scaled 77% Kefallonia 2014 Earthquake (77%KEF) [7]. The infill of type B was created by cutting 3 furrows 2 cm wide on the top and side edges of the wall, which were then filled with injected PUFJ (simulation of wall protection in an existing building). In the infill of type C, the inside of the frame was first lined with prefabricated PUFJ laminates of 2 cm thickness and then the wall was built (simulation of wall protection in a newly constructed building). More details of the specimen construction, materials' parameters and testing procedure can be found in [7,8].

In PHASE 1 (10 gradually increasing seismic excitations up to 77%KEF), the infill walls of type B were tested in-plane and the infill walls of type C were tested out-of-plane. In PHASE 2 (3 gradually increasing seismic excitations up to 18%KEF), the heavily damaged B-type walls (Fig. 6a) were reinforced with FRPU on both sides (B_FRPU – Fig. 6b) and the 3D specimen was excited again, but to a level that was safe for the building specimen. After rotating the building by 90 degrees, the type C walls were tested in-plane until the moment when bonds in the mortar joints between the wall blocks were opened (Fig. 6c) - PHASE 3 (3 gradually increasing seismic excitations up to 16%KEF). In the same phase, B_FRPU specimens were tested out-of-plane. After the FRPU reinforcement of the type C walls (C_FRPU – Fig. 6d), the tests were continued in PHASE 4 (7 gradually increasing seismic excitations up to 45%KEF) up to the maximum load capacity of the seismic table (limitation caused by the failure of an actuator). Maximum values recorded during the dynamic tests on the shake table in four phases are presented in Table 1.

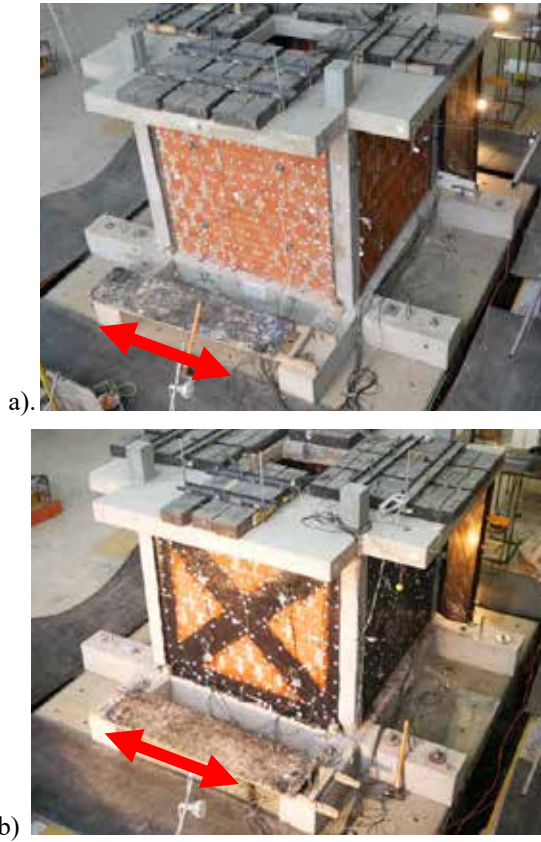


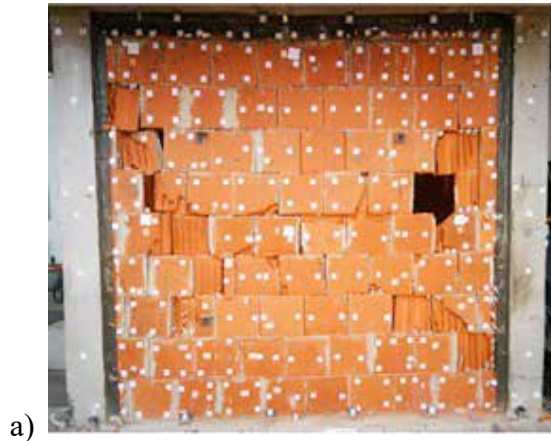
Figure 5. View of the RC building with infill walls protected by PUFJ and FRPU on the shake table in IZIIS: PHASE 1 - B (in-plane) and C (out-of-plane) (a), PHASE 4 - B_FRPU (out-of-plane) and C_FRPU (in-plane) (b).

Table 1. Maximum values recorded during tests on the shake table.

PHASE	Infill type (excitation direction)	Shake table acceleration [g]	RC slab acceleration [g]	RC slab displacement [mm]	RC frame drift [%]
1	B (in-plane) C (out-of-plane)	1.64	1.52	88.9	3.7
2	B_FRPU (in-plane) C (out-of-plane)	0.39	0.89	38.9	1.6

3	B_FRPU (out-of-plane) C (in-plane)	0.35	0.48	16.0	0.7
4	B_FRPU (out-of-plane) C_FRPU (in-plane)	0.95	1.25	21.0	0.9

The presented maximum values indicate that the PUFJ kept a very badly damaged B-type infill in the plane of the frame, even for accelerations above 1.5 g and the building deflection of 3.7%, and the C-type infill withstood the same excitation in out-of-plane mode.



a)



b)

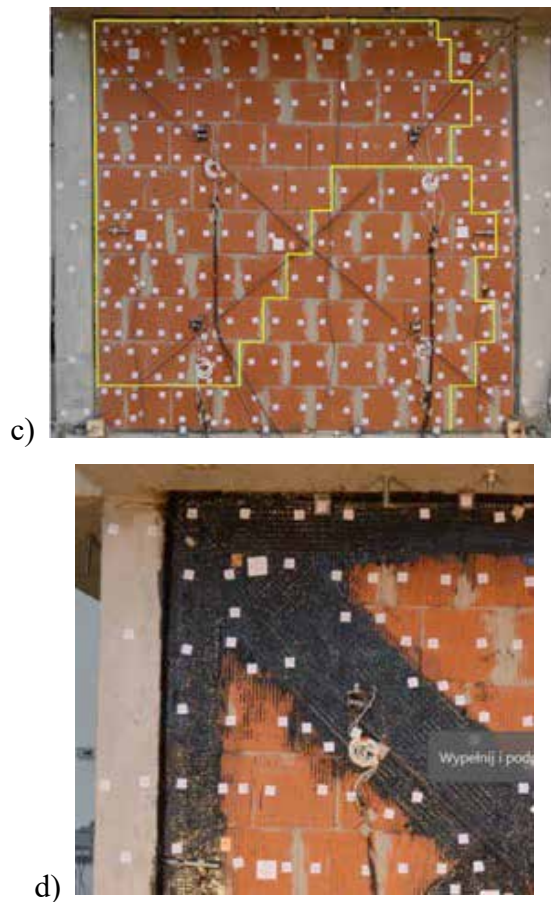


Figure 6. Views of in-plane tested faces of the 3D specimen: in PHASE 1 – seriously damaged infill B (a), in PHASE 2 – damaged infill B protected by FRPU (b), in PHASE 3 –infill C with opened mortar joints (c), in PHASE 4 - cracked infill C protected by FRPU (d).

3. MODIFICATION OF STIFFNESS AND DAMAGE CHARACTERISTICS

3.1. Global stiffness ratio and damage indicator

Useful measure of building condition in seismic areas are two factors: a global stiffness ratio EI_n/EI_0 (defined by Equation 1) and a damage indicator d_n (defined by Equation 2).

$$\frac{EI_n}{EI_0} = \frac{f_n^2}{f_0^2} \quad \text{Equation 1}$$

$$d_n = 1 - \frac{f_n}{f_0} \quad \text{Equation 2}$$

Both factors are dependent on an initial first natural frequency f_0 and a current first natural frequency f_n of the analyzed structure, which can be determined by dynamic diagnostic methods (e.g. ambient vibrations). These factors were used in analysis of stiffness changes and correlated with them changes of damage intensity, determined in two perpendicular X and Y directions of the 3D specimen, after different levels of excitation on the shake table.

3.2. Analysis of changes in stiffness and damage of the 3D specimen in testing phases

Analysis was carried out for four phases separately, taking into consideration changes of global stiffness of the tested 3D specimen. Damages occurred in the specimen structure (in infill walls and in RC columns) after series of shake table excitations with various KEF levels caused changes in global stiffness measure.

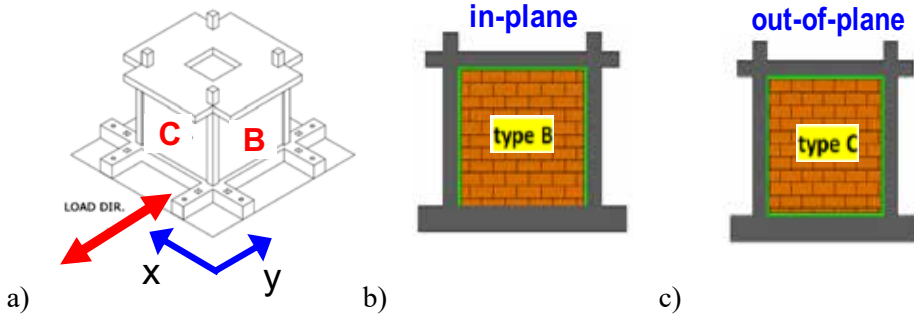


Figure 7. Setup of the full scale specimen on a shake table in PHASE 1: Position of the type B and type C infills in relation to load direction (a); infill type B excited in-plane (b); infill type C excited out-of-plane (c).

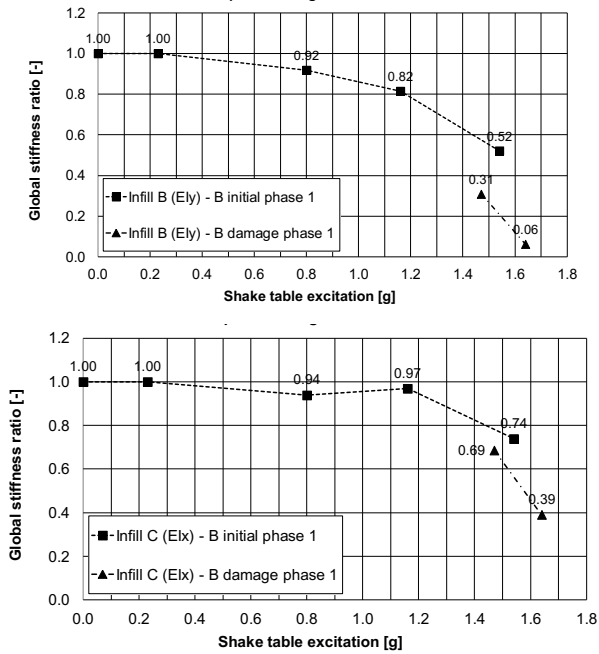


Figure 8. Change of global stiffness ratio of the full scale specimen on a shake table in PHASE 1: EI_Y - infill type B excited in-plane (left); EI_X - infill type C excited out-of-plane (right).

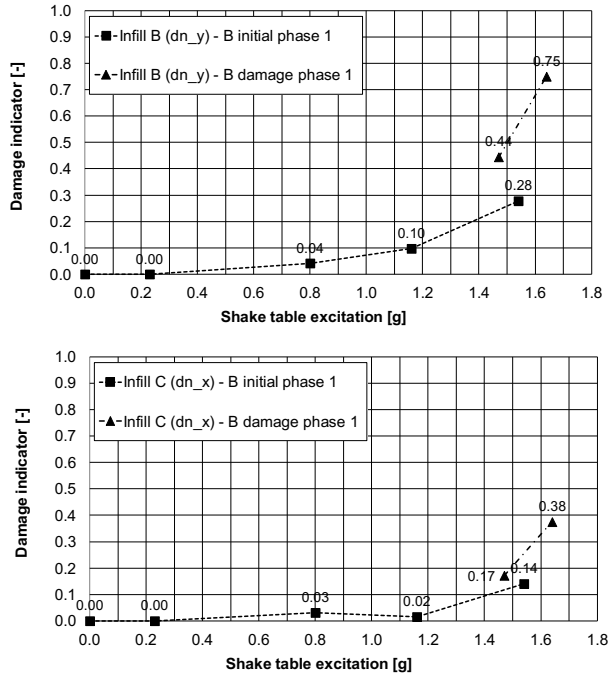


Figure 9. Change of damage indicator of the full scale specimen on a shake table in PHASE 1: d_{nY} - infill type B excited in-plane (left); d_{nX} - infill type C excited out-of-plane (right).

The testing methodology for determination of frequencies f_0 and f_n and of dynamic characteristics of the system used shake table tests by means of white noise of acceleration. The determined frequencies were used in Equation 1 and Equation 2 for determining damage level increase causing stiffness changes in directions X (perpendicular to the shake table excitation) and Y (parallel to the shake table excitation). Analyzing each testing phase separately, location of infill walls of types B and C related to excitation direction is presented in Figures 7a, 10a, 13a and 16a for phases 1, 2, 3 and 4, respectively.

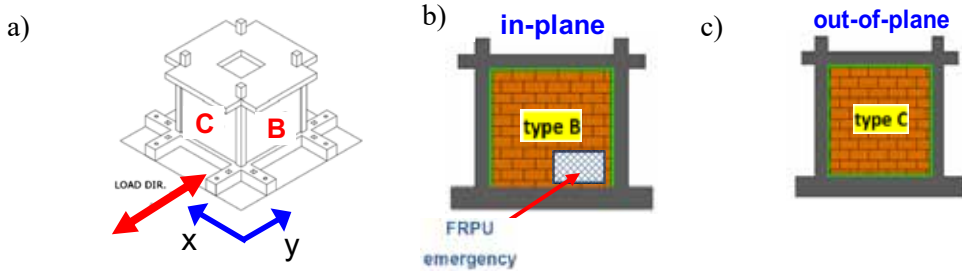


Figure 10. Setup of the full scale specimen on a shake table in PHASE 2: Position of the type B and type C infills in relation to load direction (a); infill type B protected by FRPU excited in-plane (b); infill type C excited out-of-plane (c).

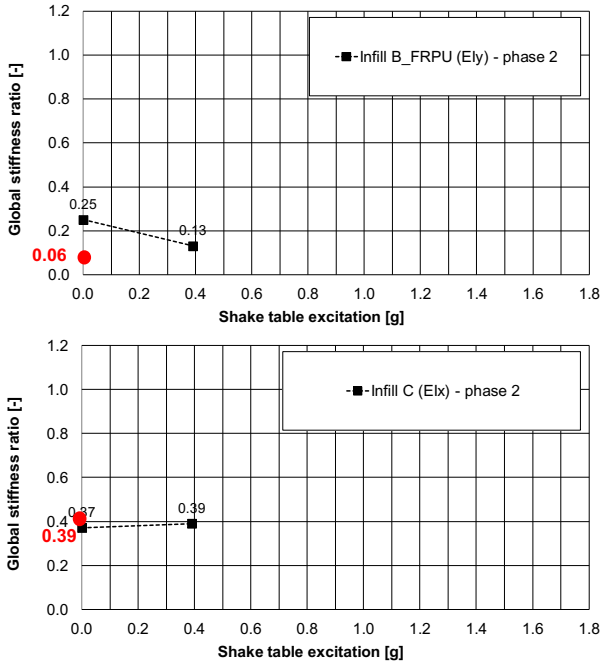


Figure 11. Change of global stiffness ratio of the full scale specimen on a shake table in PHASE 2: EI_Y - infill type B protected by FRPU excited in-plane (left); EI_X - infill type C excited out-of-plane (right). Red dot indicates final global stiffness ratio from previous phase.

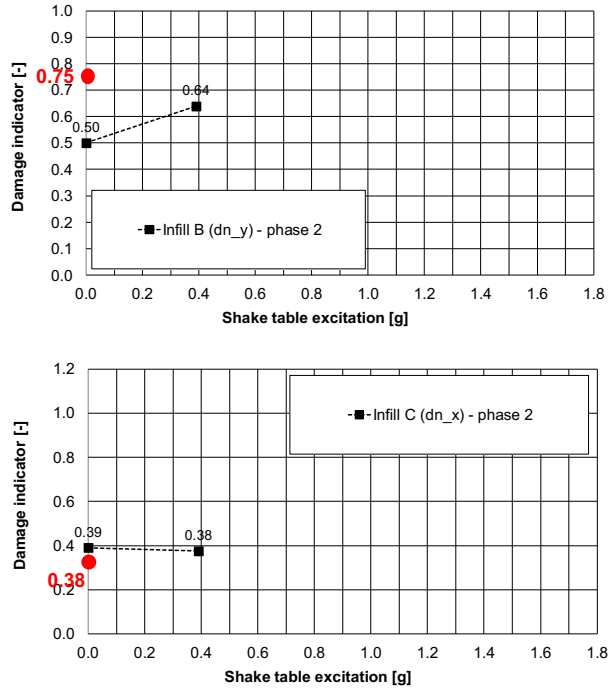


Figure 12. Change of damage indicator of the full scale specimen on a shake table in PHASE 2: d_{nY} - infill type B protected by FRPU excited in-plane (left); d_{nX} - infill type C excited out-of-plane (right). Red dot indicates final damage indicator from previous phase.

Positions in tests of infill walls of type B and C, with FRPU protection or without, in relation to in-plane and out-of-plane modes, are presented in Figures 7bc, 10bc, 13bc and 16bc.

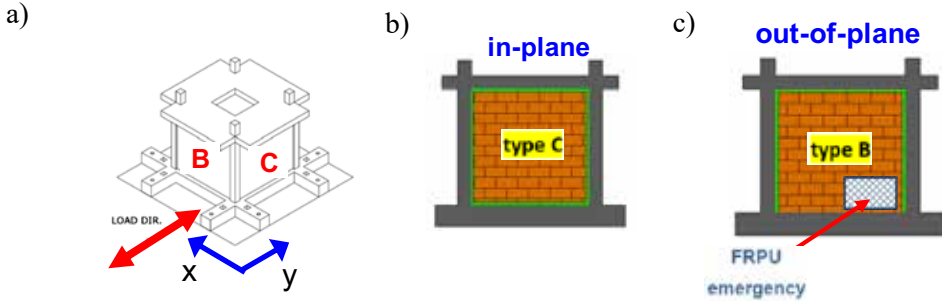


Figure 13. Setup of the full scale specimen on a shake table in PHASE 3: Position of the type B and type C infills in relation to load direction (a); infill type C excited in-plane (b); infill type B protected by FRPU excited out-of-plane (c).

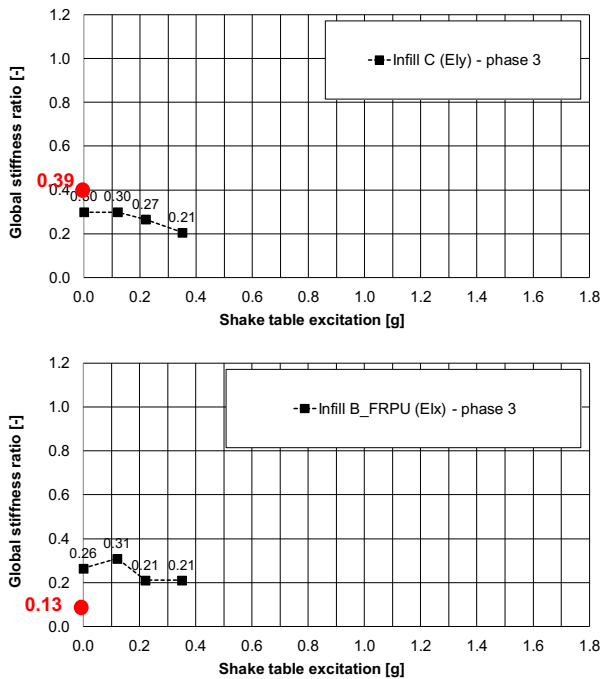


Figure 14. Change of global stiffness ratio of the full scale specimen on a shake table in PHASE 3: EI_y - infill type C excited in-plane (left); EI_x - infill type B protected by FRPU excited out-of-plane (right). Red dot indicates final global stiffness ratio from previous phase.

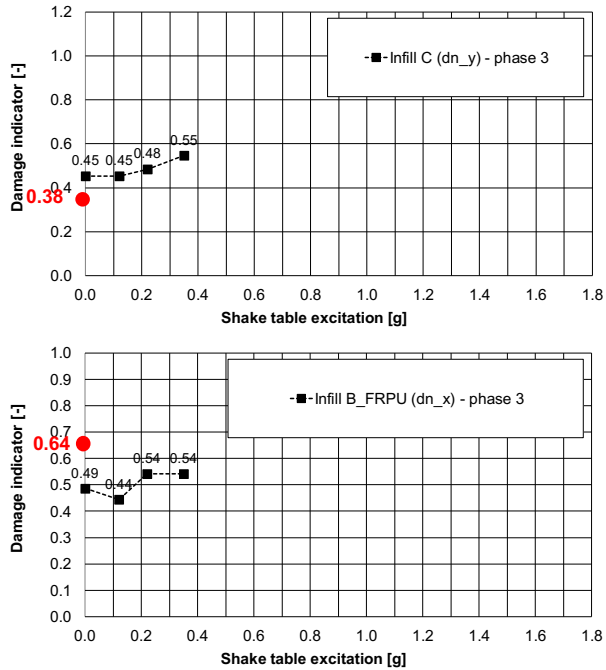


Figure 15. Change of damage indicator of the full scale specimen on a shake table in PHASE 3: d_{nY} - infill type C excited in-plane (left); d_{nX} - infill type B protected by FRPU excited out-of-plane (right). Red dot indicates final damage indicator from previous phase.

Following this phase presentation order, the global stiffness ratio EI_{Yn}/EI_{Y0} in Y direction and the ratio EI_{Xn}/EI_{X0} in X direction are presented in Figures 8, 11, 14 and 17, respectively. Similarly, the damage indicator d_Y in Y direction and the indicator d_X in X direction are presented in Figures 9, 12, 15 and 18, respectively.

The stiffness and damage parameters recorded at the end of each phase are presented in graphs of the next phase with red dots and parameters' values for comparison.

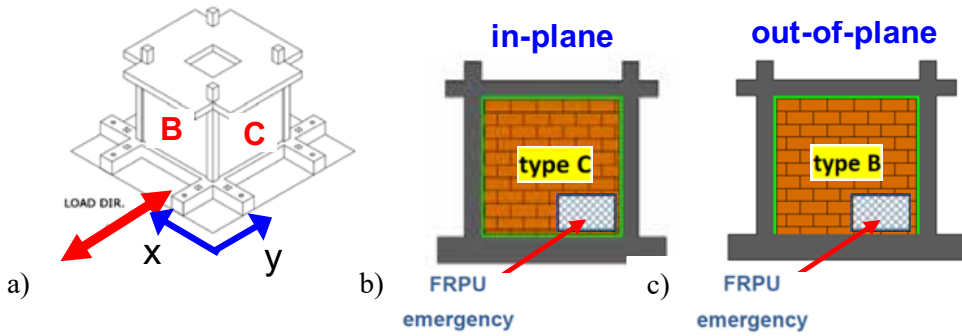


Figure 16. Setup of the full scale specimen on a shake table in PHASE 4: Position of the type B and type C infills in relation to load direction (a); infill type C protected by FRPU excited in-plane (b); infill type B protected by FRPU excited out-of-plane (c).

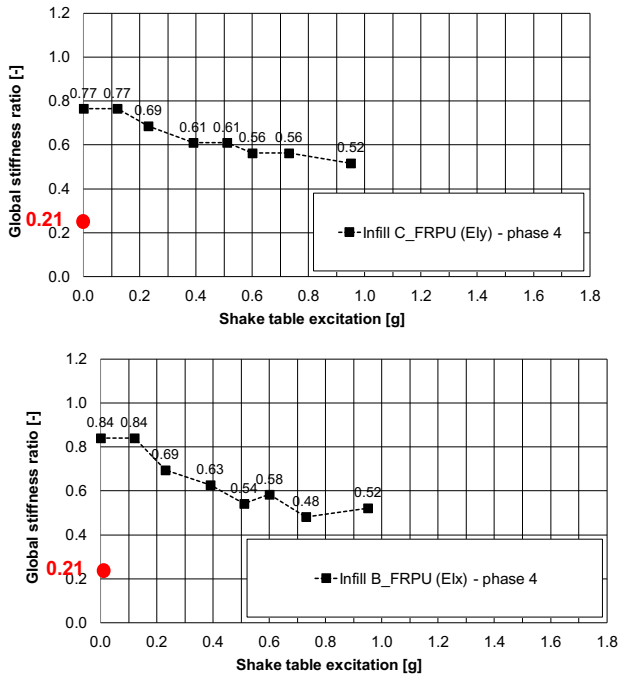


Figure 17. Change of global stiffness ratio of the full scale specimen on a shake table in PHASE 4: EI_Y - infill type C protected by FRPU excited in-plane (left); EI_X - infill type B protected by FRPU excited out-of-plane (right). Red dot indicates final global stiffness ratio from previous phase.

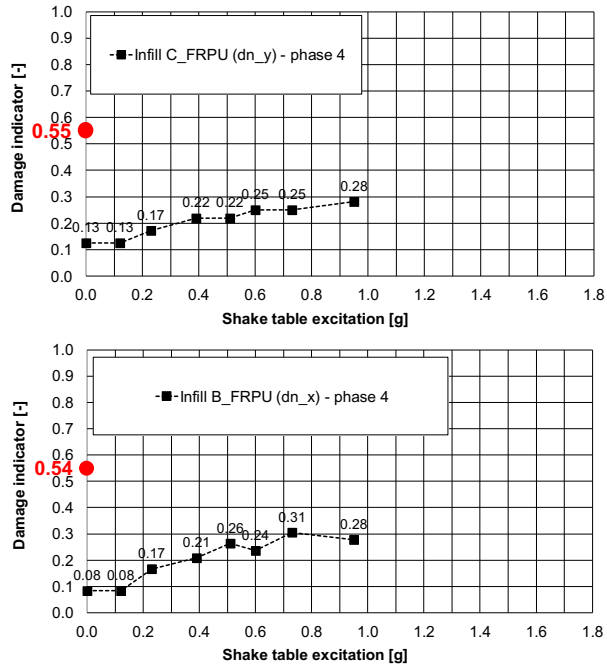


Figure 18. Change of damage indicator of the full scale specimen on a shake table in PHASE 4: d_{nY} - infill type C protected by FRPU excited in-plane (left); d_{nX} - infill type B protected by FRPU excited out-of-plane (right). Red dot indicates final damage indicator from previous phase.

In PHASE 1, after 10 series of shaking up to 77%KEF, the global stiffness ratio reduced from 1 to 0.06 in Y direction (serious damages of infills B protected by injected PUFJ – Fig. 6a) and to 0.39 in X direction (lack of out-of-plane failure of infills C protected by prefabricated PUFJ), respectively (Fig. 8). Accordingly, the damage indicator increased from 0 to 0.75 in Y direction and to 0.38 in X direction (Fig. 9).

In PHASE 2, seriously cracked infills B were strengthened by FRPU intervention (Fig. 5b, 6b and 10b). This action caused visible increase of the global stiffness ratio from 0.06 to 0.25 in Y direction and negligible change from 0.39 to 0.37 in X direction (Fig. 11). The damage indicator decreased from 0.75 to 0.50 in Y direction and changed from 0.38 to 0.39 in X direction (Fig. 12). After 3 series of shaking up

to 18%KEF, the global stiffness ratio reduced from 0.25 to 0.13 in Y direction and changed from 0.37 to 0.39 in X direction (Fig. 12).

Accordingly, the damage indicator increased from 0.50 to 0.64 in Y direction and changed from 0.39 to 0.38 in X direction (Fig. 12).

The test was stopped to avoid irreversible destruction and to allow for further testing. The specimen was next rotated by 90 degree, thus infills B_FRPU were tested out-of-plane and infills C in-plane (Fig. 13). This process changed a little initial parameters after rotation. The global stiffness ratio decreased from 0.39 to 0.30 in Y direction (for infills C) and surprisely increased from 0.13 to 0.26 in X direction (for infills B_FRPU) - Fig. 14. The damage indicator increased from 0.38 to 0.45 in Y direction and decreased from 0.64 to 0.49 in X direction, respectively (Fig. 15) – see [7] for details.

In PHASE 3 (Fig. 13), after 3 series of shaking up to 16%KEF, the global stiffness ratio reduced from 0.30 to 0.21 in Y direction and from 0.26 to 0.21 in X direction (Fig. 17). Accordingly, the damage indicator increased from 0.45 to 0.55 in Y direction and from 0.49 to 0.54 in X direction (Fig. 18). The test was stopped due to visible plastic hinges at tops and bottoms of columns, bed mortar joints opening (Fig. 6c) and low global stiffness of the specimen, which was in danger of collapsing. In this phase, infills C were decided to be strengthened with FRPU solution (Fig. 5b and 6d).

In PHASE 4 (Fig. 16), moderate cracked infills C were strengthened by FRPU intervention in smaller amount than applied in B_FRPU (Fig. 5b). This action caused significant increase of the global stiffness ratio from 0.21 to 0.77 in Y direction and from 0.21 to 0.84 in X direction (Fig. 17), because of application of FRPU strengthening also to columns with plastic hinges. The damage indicator decreased significantly from 0.55 to 0.13 in Y direction and changed from 0.54 to even 0.08 in X direction (Fig. 18). Such big changes in stiffness and damage parameters indicates very high efficiency of applied FRPU in recovery of structural safety.

After 7 series of shaking up to 45%KEF in PHASE 4, the global stiffness ratio reduced from 0.77 to 0.52 in Y direction and from 0.84 to 0.52 in X direction (Fig. 17). Accordingly, the damage indicator increased from 0.13 to 0.28 in Y direction and from 0.08 to 0.28 in X direction (Fig. 18). The experimental campaign was stopped due to actuator failure of the shake table and impossibility of testing continuation. The remained parameters of the 3D specimen in both directions X and Y ($EI_{Yn}/EI_{Y0}=EI_{Xn}/EI_{X0}=0.52$ and $d_{nX}=d_{nY}=0.28$) indicates that the RC frame

structure with infill walls protected by PUFJ and FRPU is able to withstand further serious dynamic loading. This was confirmed by further testing campaign carried out on this not collapsed specimen using forced harmonic vibration tests in resonance (excitations for the total period of over 2 hours). The tested structure survived without collapse withstanding: max. acc. = 0.77g, max. disp. = 30.15mm and max. drift = 1.3% [3].

4. CONCLUSIONS

Infill walls play significant and efficient role in seismic protection of RC structures when are protected against serious damage and failure (in-plane or out-of-plane) and do not cause damages to RC columns assuring load bearing capacity. They should also be resistant to cyclically repeating earthquakes to reduce economic losses. Presented innovative seismic protection of infill structures by PUFJ and FRPU solutions manifested their high efficiency in tests on the shake table and discussed damage and stiffness parameters lead to conclusions:

- PUFJ effectively protects infills against in-plane and out-of-plane failure even when high accelerations (over 1.5g) and large drifts (over 3.5%) occur.
- FRPU composites are able to protect even seriously damaged infills against failure excited by repeating strong seismic loads and partially recover initial object stiffness.
- Presented parameters: global stiffness ratio and damage indicator are useful tools in evaluation of changes in structural condition of seismically excited infill structures.
- Analyzed comparison of these parameters (in four phases of testing on the shake table) confirmed that proposed PUFJ and FRPU solutions can efficiently protect damaged or newly constructed infill structures against repeating strong earthquakes.

RESOURCES

[1] Hermanns L., Fraile A., Alarcón E., Álvarez R.: Performance of buildings with masonry infill walls during the 2011 Lorca earthquake. Bulletin of Earthquake Engineering, (2014) vol. 12, no. 5, pp. 1977–1997.

- [2] Ricci P., De Luca F., Verderame G.M.: 6th April 2009 L'Aquila earthquake, Italy: reinforced concrete building performance. *Bulletin of Earthquake Engineering*, (2011) vol. 9, no. 1, pp. 285–305.
- [3] Kwiecień A., Rakicevic Z., Bogdanovic A., Manojlovski F., Poposka A., Shoklarovski A., Rousakis T., Ilki A., Gams M., Viskovic A.: PUFJ and FRPU earthquake protection of infills tested in resonance. 1st Croatian Conference on Earthquake Engineering 1CroCEE, 22-24 March 2021, Zagreb, Croatia, pp. 465-475.
- [4] Varum H., Furtado A., Rodrigues H., Dias-Oliveira J., Vila-Pouca N., Arêde, A.: Seismic performance of the infill masonry walls and ambient vibration tests after the Ghorka 2015, Nepal earthquake. *Bulletin of Earthquake Engineering*, (2017) vol. 15, no. 3, pp. 1185–1212.
- [5] Akyildiz A.T., Kowalska-Koczwara A, Hojdys Ł.: Seismic Protection of RC Buildings by Polymeric Infill Wall-Frame Interface. *Polymers*. 2021; 13(10):1577.
- [6] Kwiecień A., Kuboń P.: Dynamic analysis of damaged masonry building repaired with the flexible joint method. *Archives of Civil Engineering*, (LVIII), 1/2012, ISSN 1230-2945, pp. 39-55.
- [7] Rousakis T., Ilki A., Kwiecień A., Viskovic A., Gams M., Triller P., Ghiassi B., Benedetti A., Rakicevic Z., Colla C., Halici O.F., Zając B., Hojdys Ł., Krajewski P., Rizzo F., Vanian V., Sapalidis A., Papadouli E., Bogdanovic A.: Deformable polyurethane joints and fibre grids for resilient seismic performance of reinforced concrete frames with orthoblock brick infills. *Polymers* 2020, 12, 2869; doi:10.3390/polym12122869, pp. 1-20.
- [8] Triller P., Kwiecień A., Bohinc U., Zając B., Rousakis T., Viskovic A.: Preliminary in-plane shear test of damaged infill strengthened by FRPU. 10th International Conference on FRP Composites in Civil Engineering (CICE 2020/2021), Istanbul 8-10 Dec. 2021.

ACKNOWLEDGEMENT

This project has received funding from the European Union's Horizon 2020 research and innovation programme under grant agreement No 953157.

SEISMIC RETROFIT OF LOW- AND MID-RISE RC BUILDINGS BY ENCASEMENT TECHNIQUE

Mahmood Hosseini¹, Almotasim Billah Alabeidy² and Mehmet Cemal Genes³

¹*Professor, Dept. of Civil Eng., Faculty of Eng., Eastern Mediterranean University (EMU), Famagusta 99628, North Cyprus via Mersin 10, Turkiye, Email: mahmood.hosseini@emu.edu.tr*

²*Assoc. Prof., Dept. of Civil Eng., Faculty of Eng., Eastern Mediterranean University (EMU), Famagusta 99628, North Cyprus via Mersin 10, Turkiye, Email: cemal.genes@emu.edu.tr*

³*Graduate Student, Dept. of Civil Eng., Faculty of Eng., Eastern Mediterranean University (EMU), Famagusta 99628, North Cyprus via Mersin 10, Turkiye, Email: almotasim.billah@emu.edu.tr*

*Responsible author: mahmood.hosseini@emu.edu.tr

ABSTRACT

Existing reinforced concrete buildings designed either considering gravity-only loads or following provisions of the outdated design codes are deemed seismically deficient, especially if they are located in a highly seismic region. Consequently, many researchers have studied the possibility of strengthening these seismically weak structures to enhance their performance and mitigate losses in an intense seismic event. However, most of the available retrofitting techniques in practice hinder the functionality of the building and interrupt their daily usage during the upgrading process. Therefore, this research was conducted to propose an efficient non-destructive seismic retrofitting technique to externally strengthen seismically deficient reinforced concrete moment frame buildings. The primary goal of this research was to develop a strategy where the entire retrofitting process is accomplished outside the building, so that the activities inside the building can be continued with minimum interruption. The proposed technique which can be called ‘building encasement’ is based on adding a stiff peripheral framing system that

confines the existing structure to reduce the inter-story drift values, and enhance the global seismic behavior of the building. To show the efficiency of the proposed retrofit technique it was applied to a set of RC buildings, having 3, 5 and 7 stories, designed by an old version of seismic design code. For seismic evaluation of the buildings in both non-retrofitted and retrofitted states a series of nonlinear time history analysis (NLTHA) was conducted by using three-dimensional accelerograms of a set of selected earthquakes, compatible with the considered site of the buildings. The performance-based assessment, by using the results of NLTHA, showed the capability of the proposed retrofit technique for strengthening of the weak RC buildings. It was shown that by appropriate design of the encasing frames the seismic performance of the retrofitted buildings can be kept mostly in IO performance level, particularly for low-rise buildings.

KEYWORDS: Vulnerable RC buildings, Peripheral frames, Nonlinear time history analysis, Performance-based seismic evaluation

1. INTRODUCTION

1.1 Statement of the problem

Existing moment frame reinforced concrete (MFRC) buildings, built in the era prior to the enactment of modern seismic codes are mostly considered seismically vulnerable due to their limited ductility or strength. In the event of strong ground motions, these buildings pose a significant risk to the life safety and economic wellbeing of societies since the buildings prone to damage include residential, commercial, and other critical facilities such as hospitals. The creation of such structural weaknesses could be attributed to several factors, with the most concerning being the prescriptive code design approach where the simpler linear static method is often adopted in seismic design. However, the inadequacies in this elastic design approach led to the development of a more viable and comprehensive Performance-Based Design (PBD) methods to design and assess the response of buildings, particularly in seismogenic areas. This method is based on the premise that the structure's ability to survive an earthquake is essentially a function of its inherent inelasticity (nonlinear behavior) and deformation capacity rather than the initial yield strength (linear elastic behavior). In other words, ductile design and detailing

requirements are the major focus in the newer codes to better mitigate seismic demands and reduce vulnerabilities. As a result, the rehabilitation of older reinforced concrete (RC) structures has been a topic of concern for civil engineers worldwide, and over the last few decades a lot of work has been put into developing retrofitting techniques and strategies as a means to control lateral deformations, and improve seismic capacity of these existing structures. An effective seismic risk mitigation begins with vulnerability assessment so that seismic retrofit techniques can be implemented appropriately.

The addition of RC elements, or sometimes steel elements, to increase the overall strength and stiffness of the structure is one of the retrofit techniques implemented to upgrade the seismic behavior of weak existing multi-story buildings. However, these additions need destruction of some parts of the existing building (Pincheira & Jirsa, 1995; Tena-Colunga et al., 1996), which in practice hamper the functionality of the building and interrupt its regular operations during the upgrading process, which may take several months. Obviously, this interruption is troublesome for the buildings' owners and users, since finding a substitute buildings is difficult, and evacuation of the building and transferring the contents and/or facilities to the substitute building is very costly. In the case of some essential buildings like hospitals, it is actually impossible to find the substitute building, and as a result the users of the building lose their staying or working place for a relatively long time. Therefore, a retrofit technique, which does not necessitate the evacuation of the building is quite desired. This research was conducted to propose an efficient non-destructive seismic retrofitting technique to externally strengthen seismically deficient reinforced concrete moment frame buildings. The primary goal of this research was to develop a strategy where the entire retrofitting process is accomplished outside the building, so that the activities inside the building can be continued with minimum interruption. The proposed technique which can be called 'building encasement' is based on adding a stiff peripheral framing system that confines the existing structure to reduce the inter-story drift values, and enhance the global seismic behavior of the building. Fortunately, many of the existing essential buildings, which need retrofitting, are located in open areas, and therefore, the proposed encasement technique is quite applicable to them.

1.2 Background

Since the 1970s, researchers worldwide have studied the possibility of externally upgrading the seismically weak structure to mitigate the structural response and enhance the performance of the structure as a whole. The primary goal of those studies was to develop retrofitting strategies that do not require interrupting the inner workings with the entire upgrading process being completed outside the building. To date, external strengthening techniques have concentrated on system-based structural retrofitting, featuring distinctive forms such as external shear walls (Kaplan et al., 2011), external bracing (Elbahy et al., 2019) and external moment frames or braced frames (Cao et al., 2020) and. With the considerable increase in lateral stiffness and the ease of connection to the existing building, RC braced frames, as shown in Figure 1, have been the most commonly used in practice (Cao et al., 2020).



Figure 1. External retrofitting by RC braced frames (Cao et al., 2020)

Nonetheless, many studies have indicated that the primary failure mechanism of the external braced frames due to ground shaking is the out-of-plane buckling of braces. This received widespread attention and led to the development of Assembled Buckling-Restrained Braces (ABRB) as an alternative to the steel bracing typically used. ABRB delivered superior mechanical properties under compressive stresses and provided the choice of replacing the damaged plates after failure (Iwata & Murai, 2006; Usami et al., 2012). Despite the studies that proved the immaculate energy-dissipation capacities of such elements, the applications of this type of braced frames in seismic retrofitting might yield immense residual deformations, demanding costly repairs following a seismic event. Moreover, most of the aforementioned

experimental studies were conducted in comparison to bare frames without infills and facades; however, in real cases, these components cannot be overlooked, which may leave no room for the addition of braces (Xie, 2005).

Cao et al. (2019) proposed an innovative external retrofitting method that employs self-centering precast bolt-connected steel-plate reinforced concrete buckling-restrained-brace-frame (PBSPC BRBF) (Figure 2).

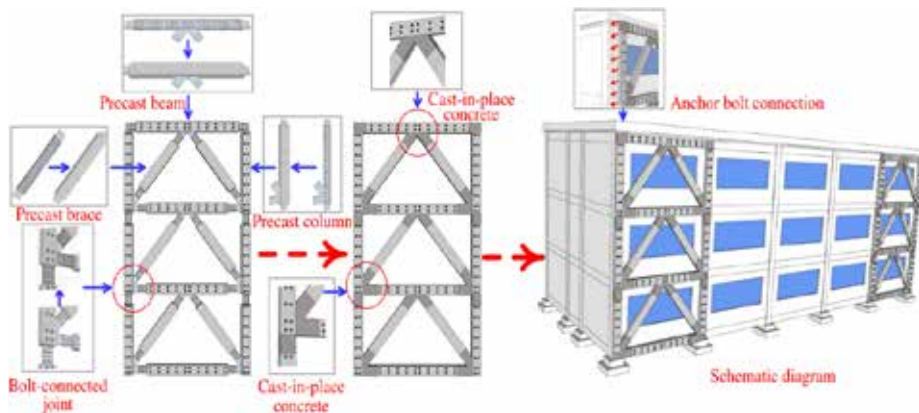


Figure 2. Schematic diagram of the retrofitting mechanism of the SC-PBSPC braced frame (Cao et al., 2019)

This method combines the energy dissipation capacity of the ABRB with the ample displacement control of the prestressed tendons and precast assembly to acquire the ideal lateral force resisting capacity. The combination of these technologies together with the existing MFRC boosts the overall structural performance of the integrated system as a global or system-based retrofit in terms of residual deformations and stiffness characteristics.

It can be understood from Figures 1 and 2 that to use those proposed external frames for retrofitting they should to be connected firmly to the main structure of the building, and this in turn needs some specific connections with high strength. Creation of such connections is a major challenge. This is while in encasement

technique, proposed in this paper, no connection is required, and it is enough to only remove the external cover/façade of the building partially, so that the added external frames can be tightly in touch with the existing frames.

1.3. Research strategy

The application of the proposed encasement technique to the vulnerable buildings was carried out through a computer-based finite element simulation. The considered buildings, having 3, 5 and 7 stories, and designed based on the provision of an old version of seismic design code, were modeled using CSI-ETABS V19.0 software. The equivalent lateral force method was used for design of buildings, and nonlinear time history analysis (NLTHA) was used for evaluating the seismic behavior of the original as well as retrofitted buildings, by the proposed encasement technique, and the efficiency of this technique was shown by comparison of the performances of original and retrofitted buildings through a performance-based approach. Details of design and analyses are presented briefly in the next section.

2. THE CONSIDERED BUILDINGS AND THEIR DESIGN AND ANALYSIS

2.1. Conventional design of the considered buildings

The general plan and beam and columns layout of the considered RC buildings, having 3, 5 and 7 stories, and moment frames structures, is illustrated in Figure 3.

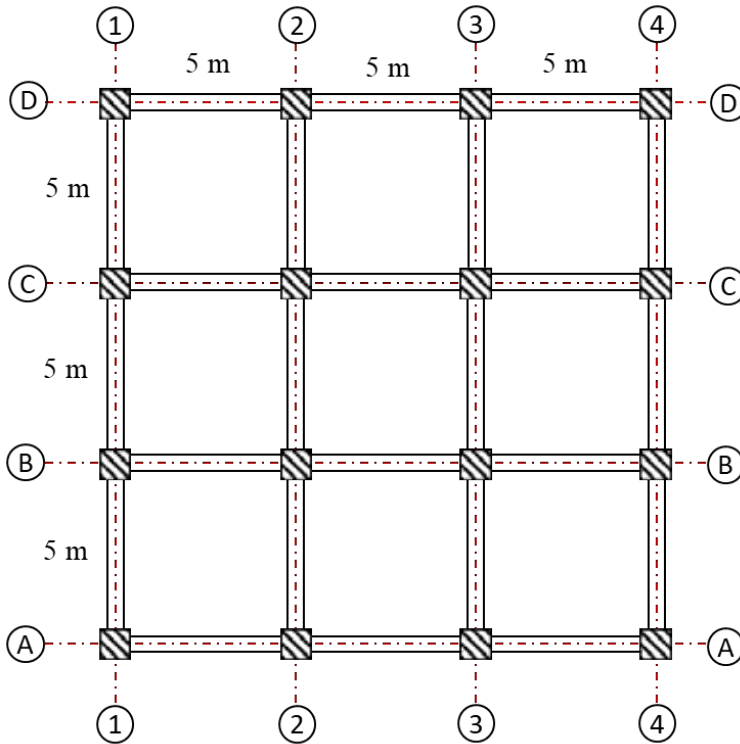


Figure 3. General plan, and beam and columns layout of the considered buildings

As shown in Figure 3, the moment frames spanning three bays in both perpendicular directions, with 5 m spans. All stories' height were assumed to be 3 m. Details of the applied dead and live, as well as seismic loads are not presented here for the sake of brevity, and can be found in the main report of the study (Alabeidy, 2022). In order to design the conventional building the equivalent linear procedure according to EC8 was used. All the buildings' frames were designed as regular moment frames classified as Medium Ductile Structures, according to ACI Standard 318-02 (2002), with an importance factor of 1.

2.2. Ground motion selection for NLTHA

For conducting the NLTHA of the original and retrofitted buildings a suite of seven earthquake records, acquired from the Pacific Earthquake Engineering Research

(PEER) Center database, was selected to cover a wide range of frequencies and accelerations. Measures were taken to select include near-fault, far-fault, as well as records that possess pulse-like frequencies in the selected suite of actual earthquake data. Specifications of the selected records are given in Table 1, while their spectral acceleration response curves after scaling are presented in Figure 3.

Table1. General information for the chosen ground motion records

Event Name	Date	Rrup (km)	Vs ₃₀ (m/sec)	Magnitude Mw	Record type
Imperial Valley	1940	6.09	213.44	6.95	Near-fault
Imperial Valley	1979	7.29	242.05	6.53	Near-fault
Superstition Hills	1987	18.48	266.01	6.54	Pulse-like
Spitak Armenia	1988	23.99	343.53	6.77	Near-fault
Cape Mendocino	1992	41.97	337.46	7.01	Far-fault
Northridge	1994	6.5	282.25	6.69	Pulse-like
Taiwan				7.3	
SMART1	1986	55.55	306.38		Far-fault

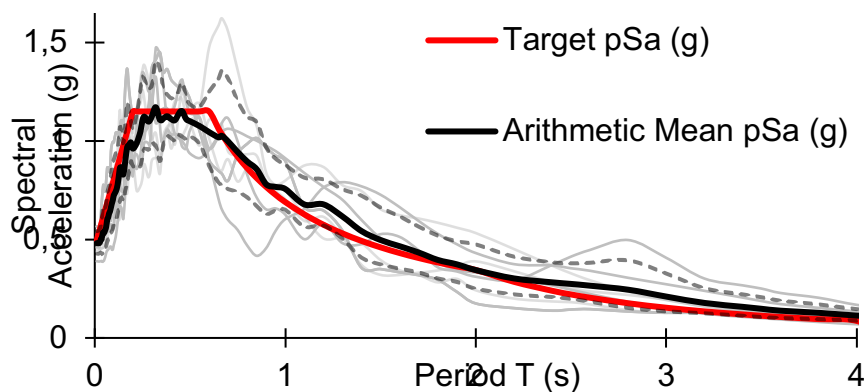


Figure 3. Mean spectral acceleration spectrum for the scaled ground motion records

The selected records were scaled to match the elastic target spectrum of the EC8 code by using the approach of minimizing the mean-square error (Michaud & Léger, 2014). This method results in a more convenient scaling where it matches the target response without affecting the frequency of the ground motion records. The scaling was carried out for the periods between 0.10 and 2.5 sec, covering the fundamental periods for all three buildings under evaluation, including the retrofitted ones.

2.3. Modeling the nonlinear behavior of materials and elements

There were two cases of nonlinearity in the analyzed buildings of this study. The first case was the elastic-plastic behavior of materials, and the other case was related to behavior of gap elements between the encasing and original frames in retrofitted buildings. To model the nonlinear behavior of the RC structural elements the idealized concentrated inelasticity technique was adopted according to ATC 70 (2010). This technique utilizes uniaxial fiber hinges that can explicitly capture some features of the nonlinear behavior according to the nonlinear stress-strain curves of materials, while other effects are considered by integrating the flexural stresses developed over the cross-section of the element and along the fiber's length. In this modeling approach, a single cross-section consisting of discretized fibers is used along a fraction of the member's length, mainly where the inelastic action is anticipated, which is typically located at the ends of the elements in RC moment frames. For reinforced concrete beams and columns, a fiber segment may be composed of several discrete concrete and steel reinforcement fibers, given their respective stress-strain relationships. The number of fibers used in each cross-section heavily influences the accuracy of the analysis; however, based on previous data available on NIST guidelines (2017), an optimal number of 56 for the beams and 28 fibers for the columns is used to ensure accurate results with a minimal computational burden as depicted in Figure 4.

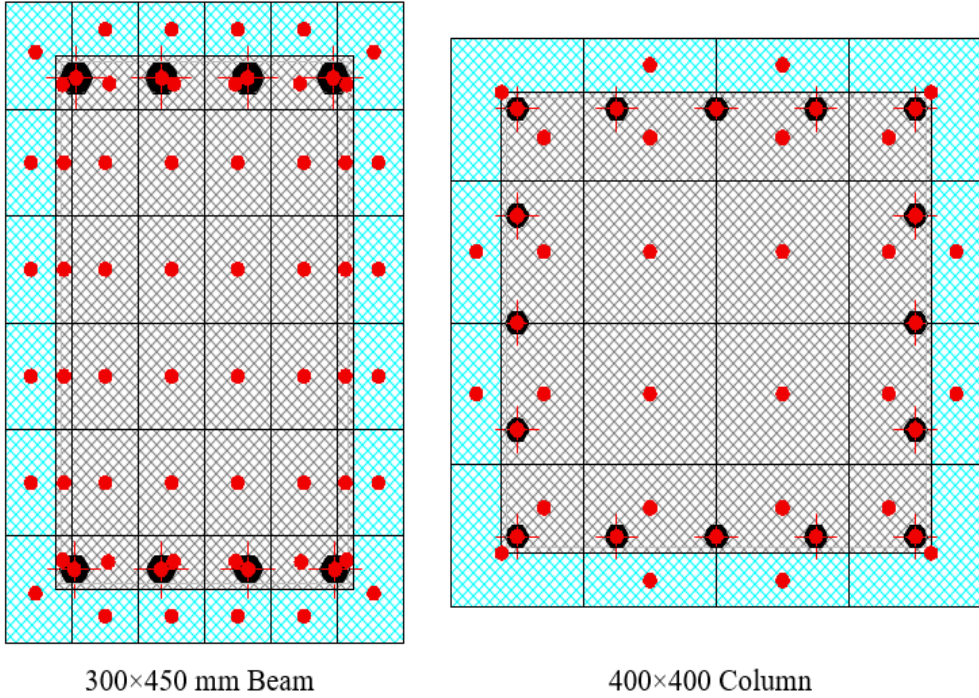


Figure 4. Discretization of fibers in beams and columns of the analyzed buildings

The other nonlinear behavior was related to the connection interface between the existing structure and the retrofitting peripheral encasement, which was modeled using nonlinear link elements of gap type. Gap elements simulate the contact between the outer elements of the existing building and elements of the encasing frames by creating restoring forces when the elements are in contact and releasing them when the elements move away from each other. Therefore, the gap should inherently have a large stiffness when the surfaces are in touch and zero when they are separate as depicted in Figure 5.

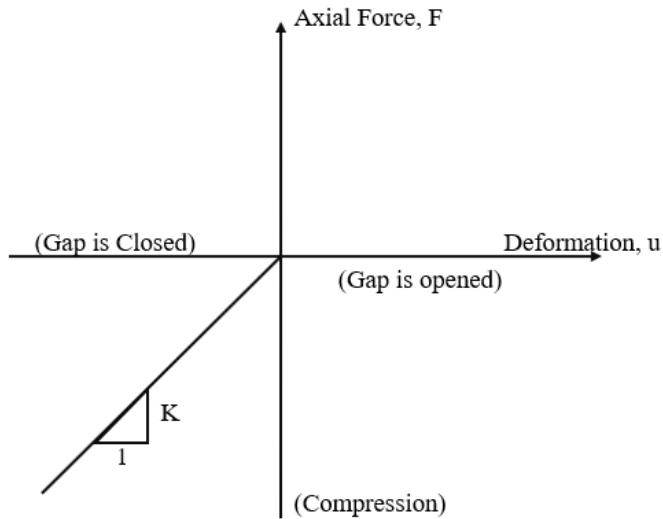


Figure 5. The force-deformation relationship in the gap element

The nonlinear gap stiffness is a key parameter in the analysis as it often controls the solution of the entire equation of motion. It is often tempting to define a very large stiffness value as recommended in many published research; however, too large stiffness may lead to numerical difficulties in the analysis due to a phenomenon called bouncing in which the state of the gap interchanges back and forth (closed/open) with each iteration of the solution (Rizzo, 1991). As such, calibration has been done to select the most appropriate stiffness value for the gap elements to deliver accurate results without sacrificing much time. This was achieved by creating a retrofitted building model and subjecting it to arbitrary lateral loading. By gradually increasing the stiffness of the gap elements and monitoring the forces generated and displacement encountered at one of the nodes, it was clear that choosing a stiffness 100 times (two orders of magnitude) greater than the corresponding stiffness of any connected elements is sufficient to obtain reasonably accurate results as quickly as possible. It should be noted that this value was also one of the recommended stiffness values highlighted by CSI ETABS analysis reference (2019).

3. RESULTS AND DISCUSSIONS

Within this section, the results obtained from the finite element simulations by means of linear and nonlinear analyses are presented together with a brief comprehensive explanation regarding the observed seismic performance of the original and retrofitted buildings. The considered seismic responses and performance indices include roof relative displacement, roof absolute acceleration, drift ratios and finally plastic hinges' states. It is worth mentioning that for the sake of brevity, in each case only one sample of the numerical results is presented, however, the complete results can be bound in the main report of the study (Alabeidy, 2022).

3.1 Seismic vulnerability of the original buildings

As mentioned in the previous section, the first stage in the study was to conduct a preliminary economic design for the selected buildings in line with the Eurocodes standards. After that, the structures were intentionally weakened by reducing the materials' strength, and then linear analysis employing was used to investigate the vulnerability of the structure under seismic actions. Figure 6 shows the demand/capacity (D/C) ratios based on PMM interaction in frames elements for the weakened 5-story building as a sample.

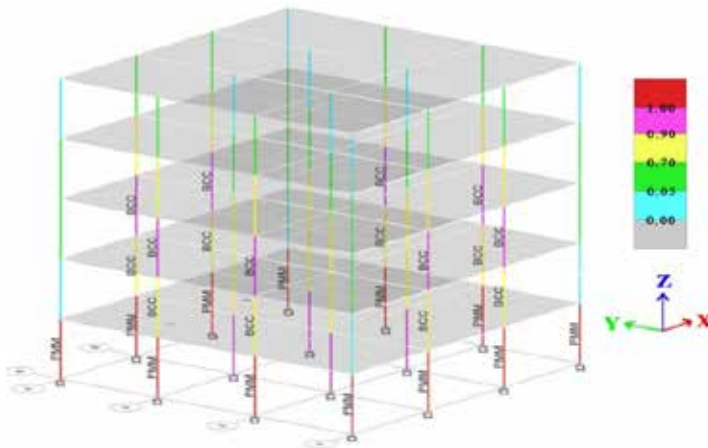


Figure 6. Deficiencies identified by the linear analysis of the 5-story bare structure

It can be seen in Figure 6 that many element of the building, particularly peripheral columns of the lowest story, are seismically weak, and therefore, the building needs to be retrofitted. The same is true for 3- and 7-story buildings, but the results are now shown here.

3.2. The retrofitted buildings by encasement technique

Seismic behavior of the retrofitted building was evaluated by a series of NLTHA, as mentioned in the previous section, by using the scaled records of selected earthquakes, given there in Table 1. To find the appropriate features of the elements of the RC encasing frames to enhance the seismic capacity of the vulnerable structures a cycle of trial and error was followed for each building. For all buildings the cycles started with a uniform dimension of 800×250 mm for the beams and columns, and by changing the dimensions and reinforcement details, and checking the performance level based on the results of NLTHA the final cross-sectional properties were finalized. Table 2 shows the final acquired geometry and detailing requirements for the retrofitting elements that satisfy Eurocode8 provisions and meet the performance objectives to minimize damage to structural members, and Figures 7 to 9 show schematically the retrofitted buildings by encasement technique. It is worth mentioning that for 3-story building it was not necessary to cover the whole body of the building structure by the encasing frames, and it was enough to encase just two lower stories as shown in Figure 7, and it is also noticeable that in case of 7-story building the cross-sectional dimensions of elements of the encasing frame at upper stories were smaller than lower stories, as shown in Table 2 and Figure 9.

Table 2. Optimized column cross-sections for the proposed retrofitting system

Section type (Dimensions are in mm.)	Column section of 3-story building: 950 × 400	Column section of 5-story building: 1000 × 425	Column section of 7-story building (1 st , 2 nd & 3 rd story): 1100 × 550	Column section of 7-story building (4 th & 5 th story): 900 × 500	Column section of 7-story building (6 th & 7 th story): 600 × 350
Section layout (2 and 3 red axes indicate the major and minor axes of the section.)					
Reinforcement details	Main bars: 20φ22 Transverse bars: 2φ10/100	Main bars: 18φ26 Transverse bars: 2φ10/100	Main bars: 20φ26 Transverse bars: 2φ10/100	Main bars: 16φ26 Transverse bars: 2φ10/100	Main bars: 12φ20 Transverse bars: 2φ10/100

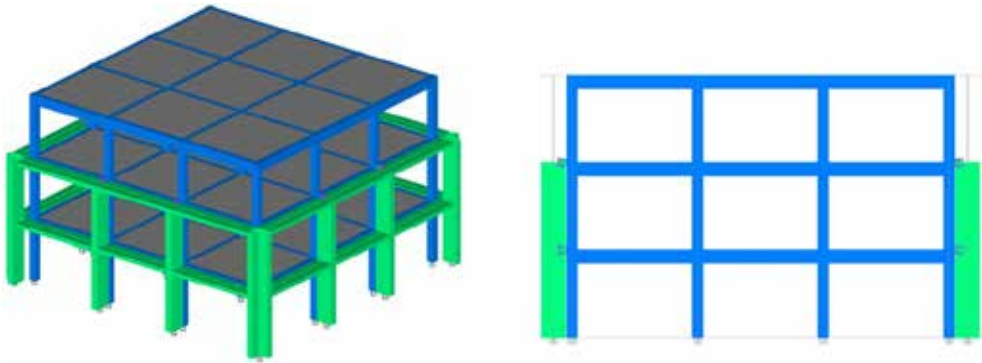


Figure 7. 3D view and section of the retrofitted 3-story building by encasement technique

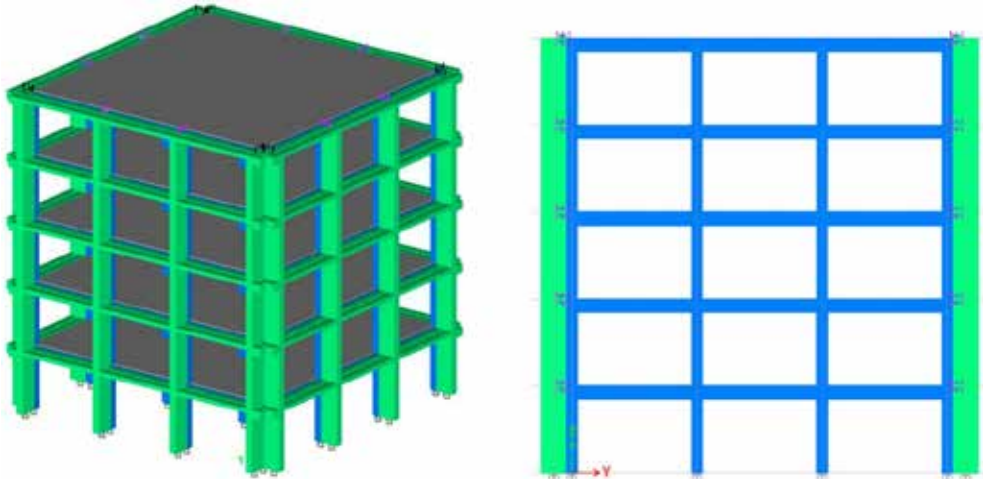


Figure 8. 3D view and section of the retrofitted 5-story building by encasement technique

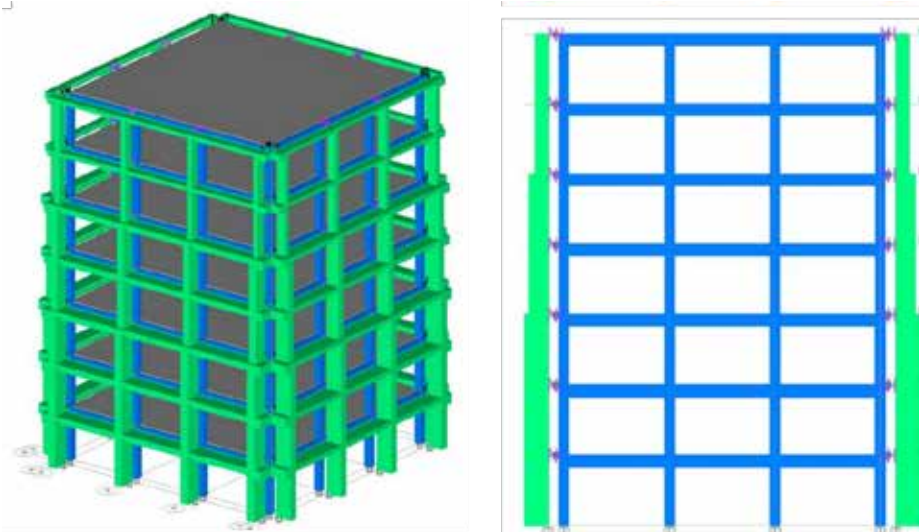


Figure 9. 3D view and section of the retrofitted 7-story building by encasement technique

The used gap elements between existing and encasing frames can be seen in Figures 7 to 9. Retrofitted buildings were seismically evaluated and compared with the original vulnerable building as described in the next part of this section.

3.3. Seismic evaluation of buildings' structures

Before conducting NLTHA for the original and retrofitted buildings, their fundamental periods were obtained to see the effect of encasement on the period values. Table 3 presents the period values before and after retrofitting.

Table 3. Fundamental periods (in sec) of original and retrofitted buildings' structures

3-story buildings	Original	0.706
	Retrofitted	0.512
5-story buildings	Original	1.238
	Retrofitted	0.727
7-story buildings	Original	1.602
	Retrofitted	0.883

As shown in Table 3, the buildings' periods decreased after retrofitting, due to the increase of the lateral stiffness, as expected. Samples of seismic responses, obtained by NLTHA, are shown in Figures 10 and 11.

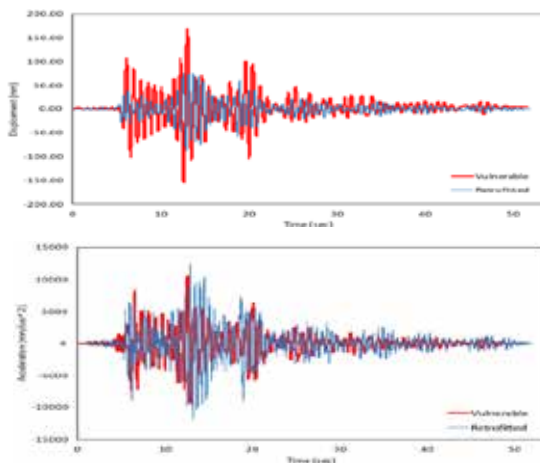


Figure 10. Roof relative displacement (left) and roof absolute acceleration (right) time histories of 3-story buildings subjected to "Imperial Valley-06" earthquake record

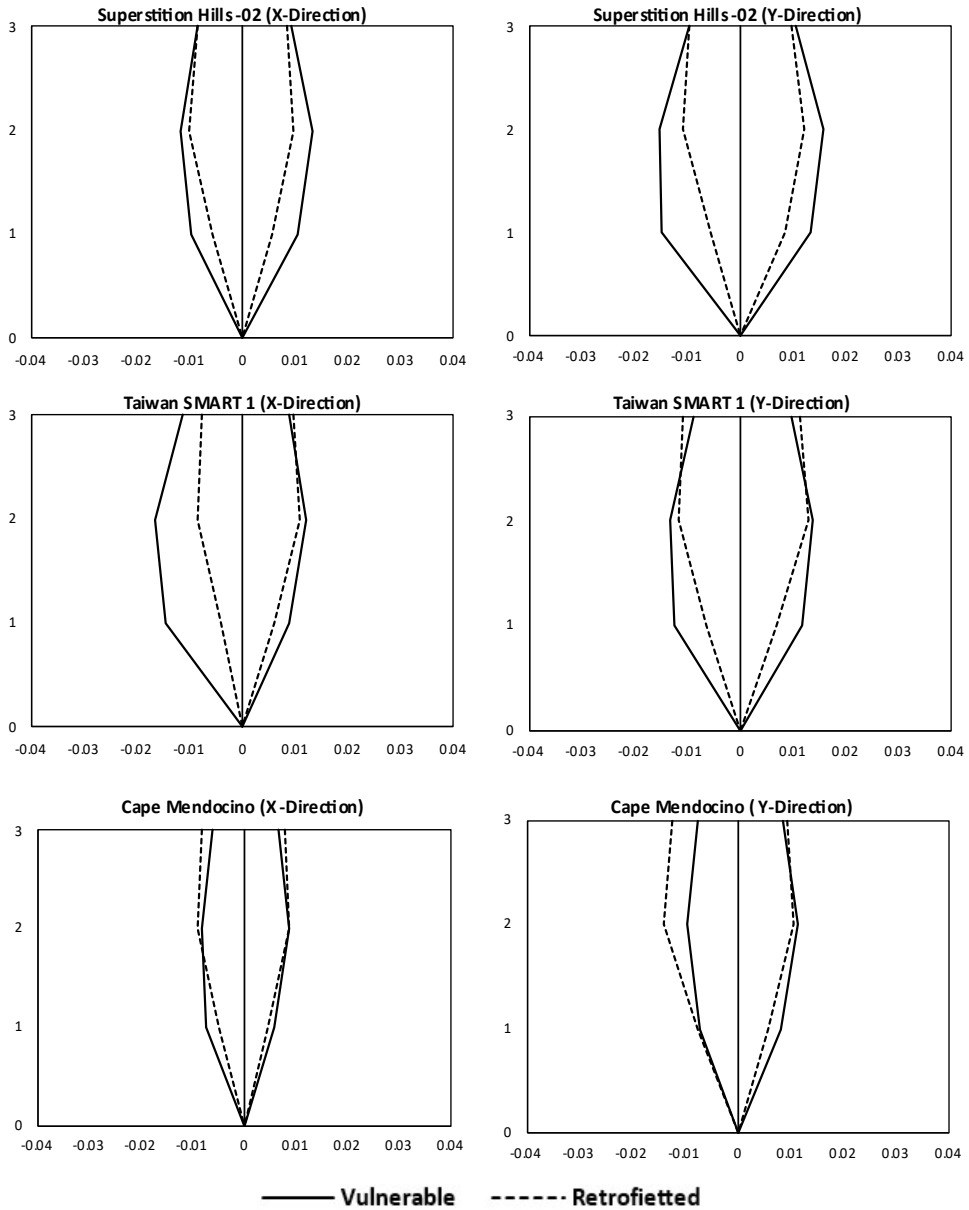
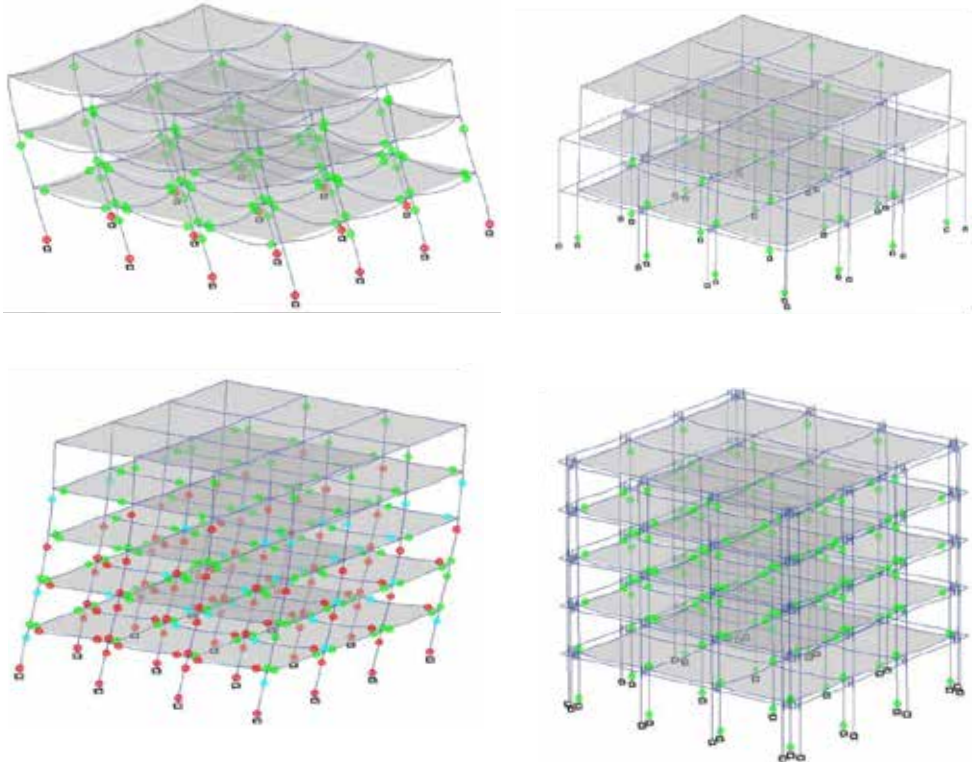


Figure 11. Inter-story drift ratios of the 3-story buildings in X and Y directions, subjected to three of the seven elected earthquakes

It can be seen in Figure 10 that the relative displacement response of the retrofitted building has drastically decreased. Obviously, this means less deformation in the body of the building structure and, therefore, less damage. However, it can also be seen in Figure 10 that the absolute acceleration response has not decreased, which is because of higher stiffness of the retrofitted buildings, as expected. Finally, it can be seen in Figure 11 that the inter-story drift values have generally decreased because of retrofitting, although in some cases a slight increase in drift values is also observed.

The last set of seismic evaluation results are the plastic hinges (PHs) formed in the structural elements, which shows the performance level of the building. Figure 12 shows the PHs formed in the original and retrofitted buildings subjected to Superstition Hills 02 earthquake as a sample of the seven selected earthquakes.



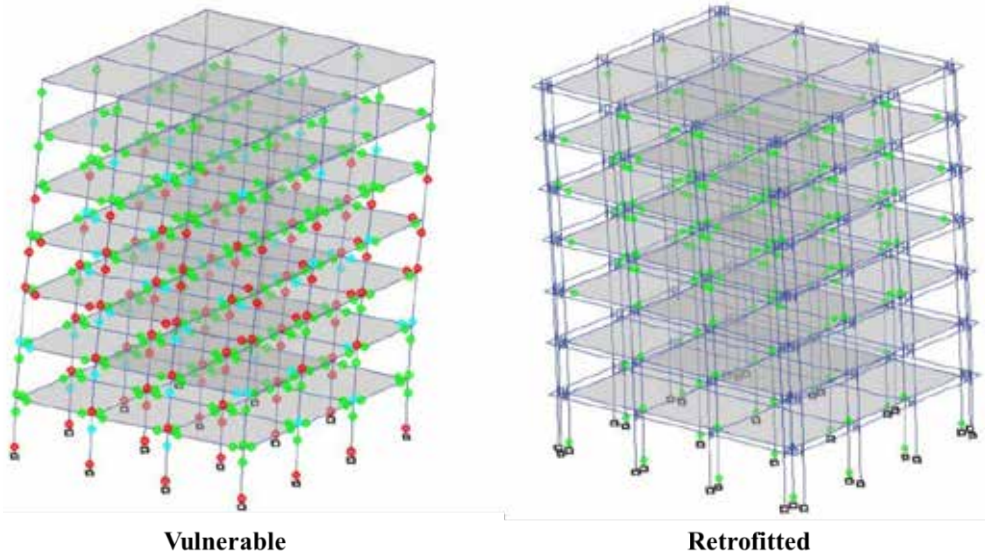


Figure 12. PHs formed in the buildings' structures at the end of Superstition Hills 02 earthquake record

It is observed in Figure 12 that the PHs in the original vulnerable buildings are at collapse level, while in the retrofitted buildings number of formed PHs is much lower, and they are all at immediate occupancy performance level. This clearly shows the effectiveness of the proposed encasement technique for retrofit of the existing vulnerable RC buildings.

4. CONCLUSIONS

This research sought to evaluate the seismic performance of a non-destructive retrofitting technique as a method for strengthening seismically deficient multi-story reinforced concrete moment-frame structure buildings. The proposed technique relies on confining the whole vulnerable building with stiff an encasing structure. To make the study more comprehensive, 3-, 5- and 7-story buildings were first designed utilizing the linear static method of analysis per Eurocode8 provisions, and then were made intentionally weak, by decreasing the strengths of the used material in the analysis software. After that, the proposed encasement technique was applied to the weakened building, and at the last step, the vulnerable and retrofitted buildings were

investigated under a suite of diverse ground motion records, employing a series of NLTHA. The findings of the study can be summarized as follows:

- In general, the retrofitted system immensely reduced the maximum roof displacement in both main orthogonal directions. However, in some scenarios, the retrofitted structures experienced an increase in roof displacement but without endangering the structural elements or causing permanent damage.
- The roof accelerations were observed to be slightly higher in the retrofitted structures due to the global higher stiffness upon incorporating the encasing frames. However, this higher acceleration was not sustained for a long period of time, unlike vulnerable buildings.
- The inter-story drift ratios of the vulnerable structures indeed exceeded the allowable limits of Eurocode8, particularly for the 5- and 7-story buildings, while the retrofitted structures remained below the allowable limits for most of the applied earthquakes.
- The vulnerable bare structures developed many plastic hinges at Collapse limit states, while in the retrofitted hinges were dominantly at Immediate Occupancy performance level, although some Life Safety hinges were developed in 5- and 7-story buildings.

In brief, the proposed retrofitting technique proved its capability to rehabilitate existing seismically weak RC buildings, particularly low-rise ones. However, it should be noted that in this research some aspects were not covered, and can be suggested for future research work. These aspects are discussed below.

- Soil-structure interaction was not considered in this research, which might play a significant role in the overall behavior of the retrofitted system as two shallow foundations will be situated in vicinity.
- The influence of plan and elevation irregularities was not within the study's scope, and this influence can severely impact the structure's seismic performance.
- The numerical simulation findings of the proposed retrofitting technique should be verified with experimental work.

REFERENCES

- ACI Committee. (2002). Building code requirements for structural concrete: (ACI 318-02) and commentary (ACI 318R-02). American Concrete Institute.
- Alabeidy, A. B. (2022). Seismic retrofit of multi-story RC buildings by encasement technique, M.Sc. Thesis submitted to Dept. of Civil Eng., Eastern Mediterranean University (EMU), Famagusta, Northern Cyprus.
- Cao, X. Y., Wu, G., Feng, D. C. & Zu, X. J. (2019). Experimental and numerical study of outside strengthening with precast bolt-connected steel plate-reinforced concrete frame-brace. *Journal of Performance of Constructed Facilities*, 33(6), 04019077.
- Cao, X. Y., Wu, G., Feng, D. C., Wang, Z. & Cui, H. R. (2020). Research on the seismic retrofitting performance of RC frames using SC-PBSPC BRBF substructures. *Earthquake Engineering & Structural Dynamics*, 49(8), 794-816.
- CSI. (2019). ETABS Integrated Analysis, Design and Drafting of Building Systems. California: Computers and Structures Inc.
- Elbahy, Y. I., Youssef, M. A., & Meshaly, M. (2019). Seismic performance of reinforced concrete frames retrofitted using external superelastic shape memory alloy bars. *Bulletin of Earthquake Engineering*, 17(2), 781-802.
- Iwata, M., & Murai, M. (2006). Buckling-restrained brace using steel mortar planks; performance evaluation as a hysteretic damper. *Earthquake engineering & structural dynamics*, 35(14), 1807-1826.
- Kaplan, H., Yilmaz, S., Cetinkaya, N. & Atimtay, E. (2011). Seismic strengthening of RC structures with exterior shear walls. *Sadhana*, 36(1), 17-34.
- Michaud, D. & Léger, P. (2014). Ground motions selection and scaling for nonlinear dynamic analysis of structures located in Eastern North America. *Canadian journal of civil engineering*, 41(3), 232-244.
- NIST. (2017). Guidelines for Nonlinear Structural Analysis for Design of Buildings Part IIb-Reinforced Concrete Moment Frames. National Institute of Standards and Technology.

Pincheira, J. A & Jirsa, J. O. (1995). Seismic response of RC frames retrofitted with steel braces or walls. *Journal of Structural Engineering*, 121(8), 1225-1235.

Rizzo, A. R. (1991). FEA gap elements: Choosing the right stiffness. *Mechanical Engineering*, 113(6), 57.

Tena-Colunga, A., Del Valle, E. & Pérez-Moreno, D. (1996). Issues on the seismic retrofit of a building near resonant response and structural pounding. *Earthquake spectra*, 12(3), 567-597.

Usami, T., Wang, C. L. & Funayama, J. (2012). Developing high-performance aluminum alloy buckling-restrained braces based on series of low-cycle fatigue tests. *Earthquake Engineering & Structural Dynamics*, 41(4), 643-661.

Xie, Q. (2005). State of the art of buckling-restrained braces in Asia. *Journal of constructional steel research*, 61(6), 727-748.

FATIGUE BEHAVIOUR OF ULTRA-HIGH PERFORMANCE CONCRETE UNDER CYCLIC STRESS REVERSAL LOADING

Birol Fitik, Prof. Dr.-Ing.¹

¹*Dept. of Concrete Structure, Stuttgart University of Applied Sciences, Schellingstr. 24, 70174 Stuttgart, birol.fitik@hft-stuttgart.de*

ABSTRACT

For the first time comprehensive experimental research was performed on the fatigue behaviour of UHPC under cyclic reversal stress loading in tension-compression. During the research project the fatigue strength and the reduction of the uniaxial stiffness due to cyclic loading were examined in 195 force controlled fatigue tests on bone-shaped non-reinforced UHPC-specimens. Compared to similar previous examinations the fatigue tests were not restricted to 2 million load cycles. Testing an adequate number of tension-compression combinations in this first stage and an additional second stage the indication of approximately linearised limiting curves for defined number of load cycles in terms of Goodman diagrams is the long term objective of the research project.

KEYWORDS: Ultra High Performance Concrete (UHPC), Fatigue Behaviour, Cyclic Stress Reversal Loading

1. INTRODUCTION

The high strength of Ultra High Performance Concrete enables the economical design of slender structures with reduced self-weight. Compared to structures made of normal strength concrete (NSC) structures made of UHPC show a deviant ratio of dead load to live load. An auspicious design principle for the utilization of the

specific material properties of UHPC is its application combined with prestressing. Economic design of prestressed members made of UHPC may cause cyclic stress reversal loading.

It is well known that NSC shows reduced fatigue strength under cyclic reversal stress loading compared to threshold loading. Further the stiffness of structures is reduced gradually by the occurring damage progress under cyclic loading.

Tensile fatigue of NSC has been investigated in the past by means of bending tests or splitting tests. In both types of test, it is not possible or difficult to determine the actual stresses in the specimens during the course of the experiment.

For the first time comprehensive experimental research was performed on the fatigue behaviour of UHPC under cyclic reversal stress loading in tension- compression. In the first stage of the research project the fatigue strength and the reduction of the uniaxial stiffness due to cyclic loading were examined in load controlled fatigue tests on bone-shaped non-reinforced UHPC-specimens. The lower and upper stress levels were defined with respect to practical conditions and material properties such as the prestressed level and the assumed long term behaviour under tension loading. Compared to similar previous examinations the fatigue tests were not restricted to 2 million load cycles. Testing an adequate number of tension-compression combinations in this first stage and an additional second stage the indication of approximately linearised limiting curves for defined number of load cycles in terms of Goodman diagrams is the long term objective of the research project.

During the research project the effect of important parameters like stress range, fibre addition, fibre orientation and heat treatment on the fatigue behaviour have been investigated in different experimental series.

2. MATERIAL

CONCRETE COMPOSITION

The bone-shaped UHPC-specimens were composed according to [1]. The ingredients for the fine-grained mixture M2Q (UHPC with and without fibre), the mixture M3Q (M2Q with different silica fume) and the coarse-grained mixture B5Q are listed below in table 1. At the end of the first research period it became known that the silica fume used up to now is not produced any more. Hence, a new silica

fume was defined within the priority program and when the new UHPC mixture M2Qnew respectively M3Q was taken up in the test program. Furthermore the mixture B5Q was investigated in the second research period to check the influence of the concrete composition on the fatigue behaviour. The mixture B5Q was developed during the first research period by other main participants from the mixture B3Q.

Table 1: Composition of the mixtures M2Q, M3Q und B5Q (in kg/m³)

material	description	M2Q		M3Q	B5Q
		without fibre	with fibre	with fibre	with fibre
cement	CEM I 52,5 R - HS/NA	855,0	832,0	814,0	650,0
water	water	174,0	169,0	160,0	158,0
additive	silica fume Grade 983	139,0	135,0	-	-
	silica fume Grade 971 U	-	-	132,0	-
	silica fume Sika Silicol P	-	-	-	177,0
	silica dust (QM1) W12	213,0	207,0	203,0	325,0
	silica dust (QM2) W3	-	-	-	131,0
super plasticizer	Glenium 51	25,0	24,0	32,6	-
	ViscoCrete 20 Gold	-	-	-	30,4
fine aggregate	glass sand H33	1002,0	975,0	954,0	354,0
	Basalt 2/8	-	-	-	597,0
steel fibre	steel fibre Stratec 9/0,15	-	192,0	196,0	192,0

CONCRETE PROPERTIES

The consistency of fresh UHPC was determined by a slump flow test, executed immediately after mixing. The slump flow for UHPC with and without steel fibres was about 750 - 800 mm. The slump flow for the new mixtures M3Q and B5Q with steel fibres was about 600 - 700 mm.

In addition, the fresh concrete density, the air void contents, the air- and water temperature and the temperature of the aggregates was determined with every casting.

In figure 1 the development of the compressive strength of UHPC with steel fibres and heat treatment (wSF wHT) for M2Q, M3Q and B5Q, with steel fibres and without heat treatment (wSF oHT) and without steel fibres and with heat treatment (oSF wHT) for M2Q is shown. The compressive strength was determined on cubes with an edge length of 100 mm. As expected the addition of steel fibres and heat treatment led to an increase of the compressive strength. Even after 90 days of curing the compressive strength of UHPC without heat treatment is far below the compressive strength of UHPC with heat treatment.

The testing load levels for cyclic testing were defined in relation to the static strength values. The static compressive and tensile strength were determined in tests on reference specimens manufactured of the same concrete batch as the bone-shaped UHPC-specimens for the cyclic tests.

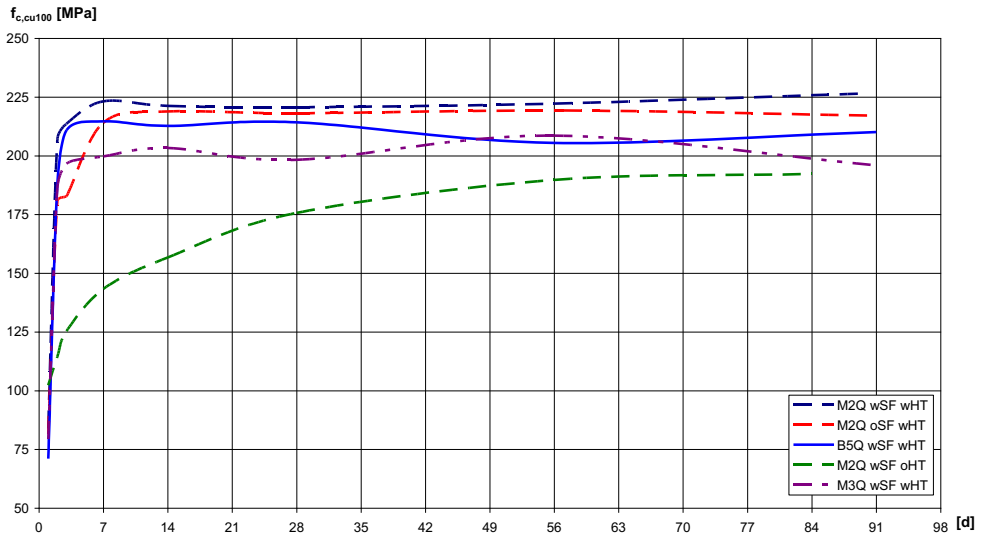


Fig. 1: Strength development of UHPC (mixture M2Q, M3Q and B5Q)

3. TEST PROGRAM

PRODUCTION OF TEST SPECIMENS

The bone-shaped UHPC-specimens were cast in the concrete laboratory. The formwork for nine specimens consisted of plastic (polyoxymethylen). The dimensions of the bone-shaped UHPC-specimens are shown in figure 2. The concrete was poured into the mould and compacted with an external vibrator. Simultaneously the reference specimens (cylinder, small bone-shaped UHPC-specimens and bending tensile prisms) were cast. One day after casting the specimens were stripped off and all cured under water till the 7th day (only for the series without heat treatment) or were subjected to a heat treatment for two days at 90°C (for the other series). Then the bone-shaped UHPC-specimens and the reference specimens were moved into the testing laboratory and stored under laboratory conditions until testing.

TEST ARRANGEMENT

The test rig for the main tests is shown in figure 2. The top and the bottom of the bone-shaped UHPC-specimens were bonded with the epoxy resin-based two-component adhesive MC-DUR 1280 (MC-Bauchemie Müller GmbH & Co. KG, Bottrop, Germany) to the testing machines adapters. Between the adapter and the ends of the specimen the adhesive was applied to compensate the uneven concrete surface and for bonding. Under the upper crosshead, a load cell with reference to the testing machines maximum load was arranged. Three different testing machines were used depending on required stress range.

After bonding the specimen to the adapter a curing period of 24 hours followed up. Then the gauges were prepared, the instrumentation applied and the first zero readings taken.

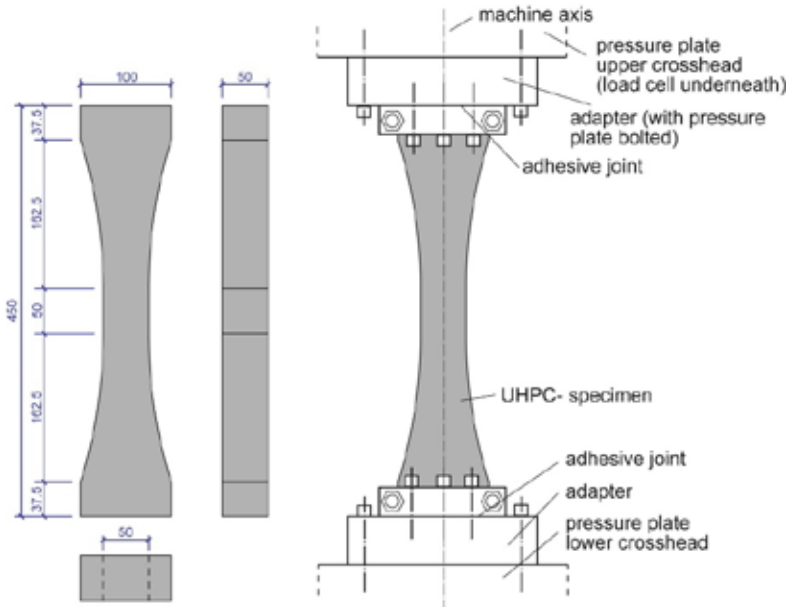


Fig. 2: Dimensions of bone-shaped UHPC-specimens [mm] and test arrangement

TEST PROCEDURE FOR M2Q, M3Q AND B5Q

With the background of the expected test duration and in combination with the necessary number of at least five specimens for a statistical analysis some parameters of influence have been examined during some of the tests. In figure 3 the researched load combinations are marked. The experimental tests included in the main series of the first research period 60 tests and the three additional test series each consisting of 20 tests. During the second research period 45 additional UHPC-specimens were tested (M3Q) and also 30 UHPC-specimens with the UHPC mixture B5Q. Altogether 195 fatigue tests were realized in both research periods.

The six test series are divided as follows:

Series 1 (A-T.H.): additional tests to check the influence of steel fibres (UHPC M2Q without fibres with heat treatment, cast horizontally)

Series 2 (M-F.T.H.): main tests (UHPC M2Q with fibres, with heat treatment, cast horizontally)

Series 3 (A-F.T.V.): additional tests to check the influence of fibre orientation (UHPC M2Q with fibres, with heat treatment, cast vertically)

Series 4 (A-F.H.): additional tests to check the influence of heat treatment (UHPC M2Q with fibres without heat treatment, cast horizontally)

Series 5 (M-M.F.T.H.): main tests second research period (UHPC M3Q with fibres, with heat treatment, cast horizontally)

Series 6 (M-B.F.T.H.): main tests second research period (UHPC B5Q with fibres, with heat treatment, cast horizontally)

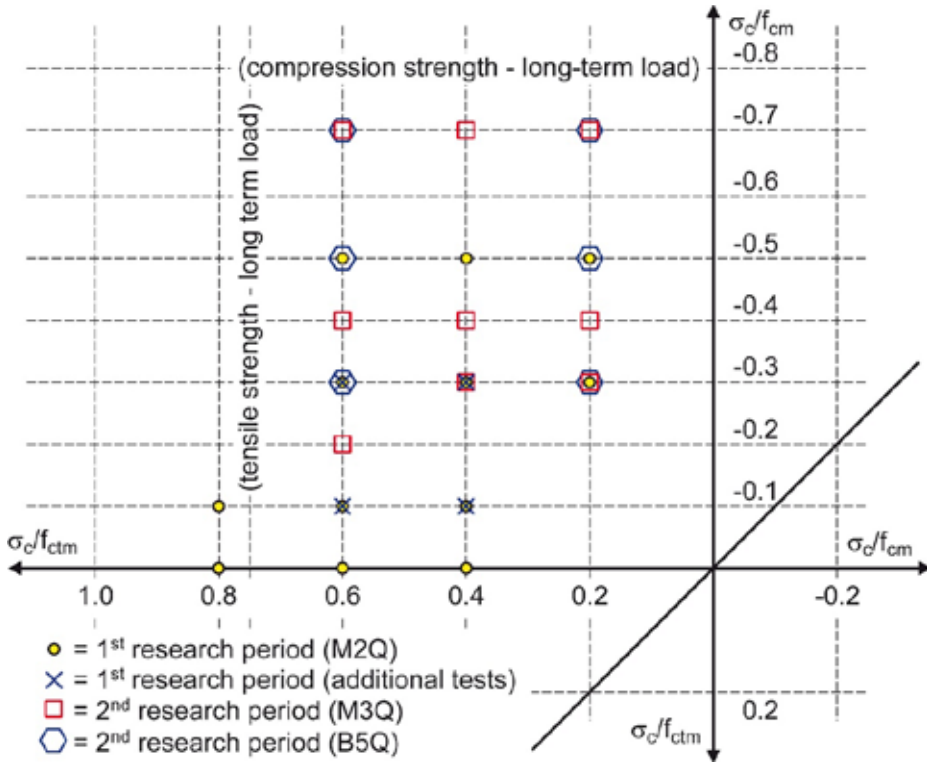


Fig. 3: Goodman diagram, researched combinations marked (M2Q, M3Q and B5Q)

In addition to the load the elongation of some specimens at a basic length of 50 mm on selected tests (range of constant cross section) has been measured. To measure the strain, four inductive displacement transducers were used. The measurements were recorded with digital measurement amplifiers and a sampling rate of 200 Hz. The strain measurements were only performed at some specimens of each series. The frequency of the testing machines varied between 8 and 10 Hz.

4. TEST RESULTS

SURVEY ON TEST RESULTS

Due to the large number of fatigue tests, only a small insight will be given on the most important test results. The test results of the main tests of the first research period were already presented i. a. in [2] and [3].

The linearised S-N-curves for the tests on specimens are represented in the semi logarithmic diagrams of figure 4 showing the number of load cycles to failure ($\log N$) against the specific tensile strength (σ_c/f_{ctm}). Figure 4 shows the results of main tests of the second research period on specimens with steel fibres and with heat treatment for the mixture B5Q (M-B.F.T.H.). The S-N-curves are drawn as dashed lines and the mean values of five tests as filled symbols. Remarkable is the large scatter of the number of load cycles. As a reason for these scatter local faults which initiate and accelerate the failure progress can be assumed.

Additionally in figure 4 the average number of load cycles to failure of normal strength concrete (NSC) is shown as black dashed line [4]. The number of load cycles found in the tests on UHPC exceeds the results of tests on NSC by far.

The number of load cycles reached depends on the upper stress level as well as on the stress range. Remarkable is also that some tests failed under compression. A couple of tests have been stopped after 100 million load cycles without failure as the research program could not be realized in the scheduled period otherwise.

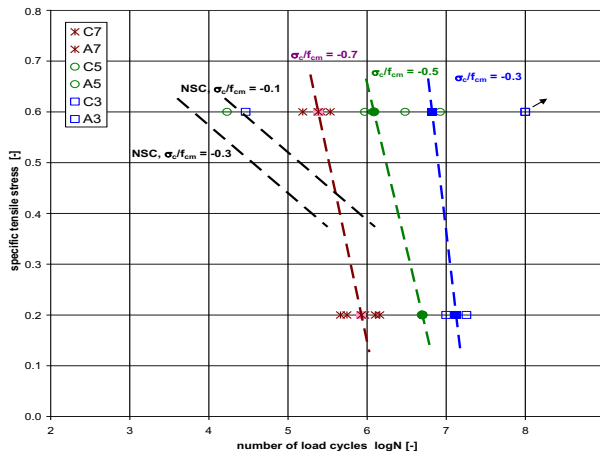


Fig. 4: S-N-curves of UHPC (B5Q) wSF wHT (M-B.F.T.H.)

Furthermore the test results of the fine-grained mixtures M2Q respectively M3Q and the results of the fatigue tests of the coarse-grained mixture B5Q are shown in figure 5 in a Goodman diagram. In addition the results for normal strength concrete (NSC) [4,5] are shown.

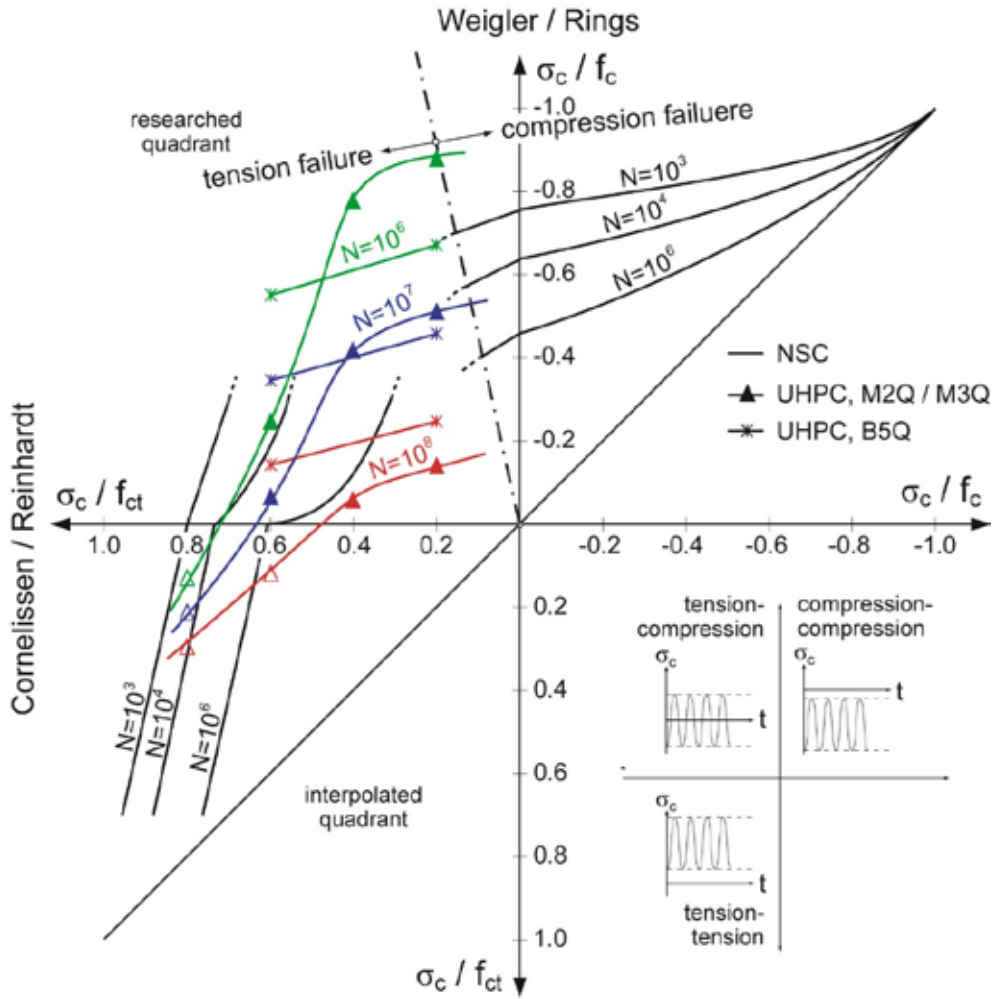


Fig. 5: Goodman diagram for NSC and UHPC under cyclic loading

RESULTS OF DEFORMATION MEASUREMENTS

The measurement of deformation performed on selected specimens showed damage progress similar to normal strength concrete (NSC) and high-strength concrete (HSC) subjected to cyclic loading. As known for normal concrete and high strength concrete, the increase of deformation to be observed in tests on UHPC can also be divided into three phases referred to as crack formation (phase I), constant crack propagation (phase II) and instable crack growth (phase III). Exemplifying the damage progress figure 6 shows the increase of deformation of a bone-shaped UHPC-specimen subjected to tensile threshold loading. Especially phase III is shorter as known for normal concrete. Figure 6 also shows the failure behaviour of normal concrete and high strength concrete [6].

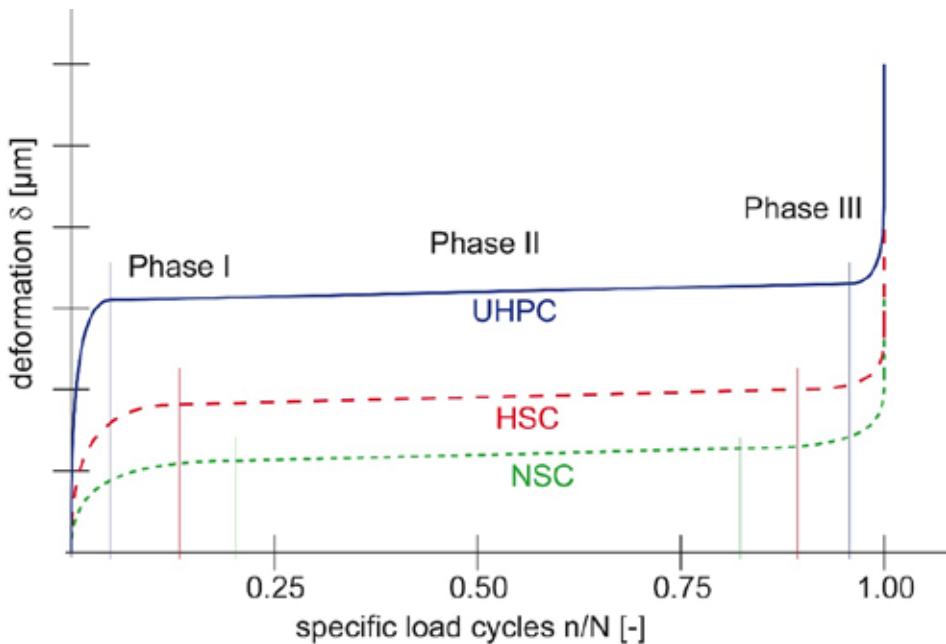


Fig. 6: Damage progress for single-level fatigue tests (model)

5. CONCLUSIONS

The tests carried out up to now already permit some conclusions which are examined, nevertheless, even more in detail. As expected the number of load cycles found in the tests on UHPC exceeds the results of tests on NSC by far (factor 100). Remarkable is also the large scatter of the number of load cycles. Local faults which initiate and accelerate the failure progress and the different kind of failure (compression or tension) can be assumed to be a reason for these large scatter.

Due to the addition of fibres the damage progress may be slowed down and exhibit a less brittle behaviour. Considering these test results economic design of UHPC structures under cyclic loading is possible.

The dependence known for normal strength concrete of the fatigue strength on the upper stress level as well as on the stress range could be confirmed.

In the carried out single-level fatigue tests very high load cycles were partially reached or the tests were finished after 10^7 or 10^8 load cycles without fatigue failure. Furthermore a changeover in failure was observed.

The validity of the well-known damage progress of concrete can also be divided in three phases for UHPC. Nevertheless, a relative shortening of the phases I and III of the crack formation and the instable crack growth could be observed respectively the phase II (the constant crack propagation) is clearly increased.

ACKNOWLEDGEMENT

The research project was funded by the German Research Foundation and was developed between 2005 and 2011 at the Technical University of Munich. The entire results were published in the dissertation [7].

REFERENCES

- [1] Fehling, E., and Schmidt, M., “Entwicklung, Dauerhaftigkeit und Berechnung Ultrahochfester Betone (UHPC),” *Bericht Universität Kassel*, DFG FE 497/1-1, 2005.
- [2] Fitik, B., “Fatigue behaviour of Ultra High Performance Concrete under alternating tensile and compressive loading,” In: *Proceedings of the 7th International PhD Symposium in Civil Engineering*, 11-13 September 2008, Stuttgart, Germany, edited by R. Eligehausen, C. Gehlen.
- [3] Fitik, B., Niedermeier, R., and Zilch, K., “Fatigue Behaviour of Ultra-High Performance Concrete under Cyclic Stress Reversal Loading,” In: *Proceedings of the Second International Symposium on Ultra High Performance Concrete*, 05-07 March 2008, Kassel, Germany, Structural Materials and Engineering Series, No.10, edited by E. Fehling, M. Schmidt, S. Stürwald, Kassel University Press.
- [4] Cornelissen, H., and Reinhardt, H., “Uniaxial tensile fatigue failure of concrete under constant-amplitude and programme loading,” In: *Magazine of Concrete Research*, V. 36, No. 129, 1984, pp. 216-226.
- [5] Weigler, H., and Rings, K., “Unbewehrter und bewehrter Beton unter Wechselbeanspruchungen,” *DAfStb-Heft 383*. Berlin, Ernst & Sohn (1987)
- [6] Kessler-Kramer, C., “Zugtragverhalten von Beton unter Ermüdungsbeanspruchung,” *Diss., Universität Karlsruhe*, 2002.
- [7] Fitik, B. (2012): Ermüdungsverhalten von ultrahochfestem Beton (UHPC) bei zyklischen Beanspruchungen im Druck-Zug-Wechselbereich. Dissertation, Lehrstuhl für Massivbau, Technische Universität München (2012)

ANTI-EARTHQUAKE MEASURES FOR THE HISTORICAL BUILDING OF ALI QAPU

Mehrdad Hejazi

Department of Civil Engineering, Faculty of Civil Engineering and Transportation, University of Isfahan, Isfahan, Iran, Email: m.hejazi@eng.ui.ac.ir

ABSTRACT

The Ali Qapu building has undergone two major restoration works. The first and more comprehensive restoration was carried out in the 1960s and 1970s and focused on the main masonry building. The restoration work on the wooden columnar structure remained incomplete. The main purpose of the restoration work was to retrieve the integrity of the masonry part, which was in a dangerous condition. The second restoration of the Ali Qapu building was undergone from 2005 to 2017 and it was concentrated on the wooden columnar structure and its supporting veranda. The main purpose of the work was to repair the damaged wooden part as well as the structural rehabilitation of the wooden structure. It also included the insertion of a lateral load bearing system of steel cables. The interventions partly aimed at improving the seismic behaviour of the building. This paper explained the interventions implemented during restoration works.

KEYWORDS: Ali Qapu building, Anti-earthquake, Measures, Restoration, Wood, Masonry

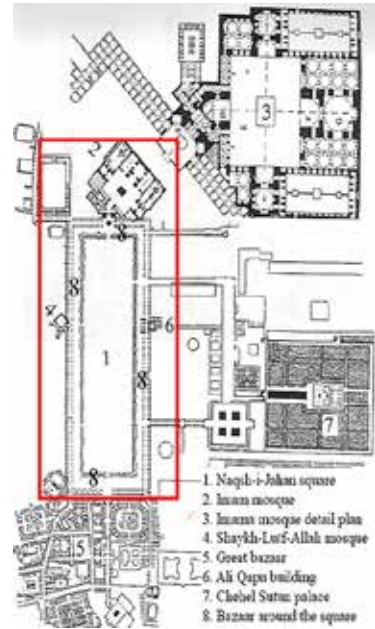
1. INTRODUCTION

The Naqsh-i-Jahan square in Isfahan, Central Iran, is a World Heritage Site registered in the UNESCO list in 1989. The square and its surrounding buildings were constructed in the earth sixteenth century. In addition to the bazaar around the square, four main buildings stand in the complex.

The palace of Ali Qapu (1597-1668 A.D.) with a high columnar *talar* (porch) at the middle of the western side looks over the square and used to be the main entrance to the royal palaces. Facing it on the east, is the mosque of Shaykh-Lutf-Allah (1601-28 A.D.), an excellent building with its exquisite *cafe au lait dome*, ornamented with arabesques. On the southern side of the maydan is the Imam mosque (1612-38 A.D.) with its beautiful dome and twin minarets and its imposing portal flanked by another pair of minarets. At the northern end of the maydan, is the tiled gateway of the Qaysariyah, the handsome bazaar [1-4] (Figure 1).



(a)



(b)



(c)

Figure 1. The World Heritage Site of the Naqsh-i-Jahan square: a) view from the south, b) plan, c) Ali Qapu building (1597-1668 A.D.).

2. ANTI-EARTHQUAKE MEASURES FOR THE ALI QAPU BUILDING

Two main restoration works have been carried out during the last six decades. The first and more comprehensive restoration on the whole building was done in the 1960s and 1970s. The second restoration work that focused on the wooden structure and its *talar* was in the 2000s, as described in the following.

2.1. Restoration Works in the 1960s and 1970s

The most comprehensive maintenance of the building started in 1964 and continued for six years. It covered the whole masonry section but the work on the wooden structure remained incomplete. The detailed process is reported by Galdieri [5] whose team was responsible for the maintenance of the Ali Qapu.

2.1.1. Rehabilitation of the Masonry Section in the 1960s

The load bearing masonry structure of the Ali Qapu is made of yellow-brown moderately fired bricks. They are 24 cm square and 5.5 cm thick. Gypsum mortar is used between bricks.

The maintenance of the Ali Qapu was offered to Italian experts, Istituto Italiano per il Medio ed Estremo Oriente (IsMEO), in 1964. At that time the masonry section, including the base of $22 \times 20 \times 33 \text{ m}^3$ and the part of $29 \times 17 \times 12 \text{ m}^3$ under the wooden structure, was damaged in all parts and two exposed cracks were observed on the northern and southern sides. It was supposed that the cause was the demolition of the lower load bearing walls or the settlement of the foundations.

The foundations of the Ali Qapu building rest on compacted clay soil. The thickness of the foundation varies from 1.2 m on the north-east part to 3.6 m on the south-east part. The foundations are made of lime. The system of foundations comprises of four cores placed on the four corners of the building. The four cores are inter-connected using thinner foundations. It was discovered by experimenting with the foundation that there was no possibility of settlement. However, the area of the foundation was still increased by 27%.

Then the maintenance concentrated on the upper structure and this continued from 1965 to 1970. The main aims in the programme were [5]:

1. Supporting the damaged or cracked parts of the building.
2. Repairing the worst damage in the building by using the same traditional materials.
3. Lightening the roofs and elements under thrust from excess loads (Figure 2).
4. Connecting the different parts of the building by using continuous spreaders in order to distribute the loads (Figure 3).
5. Creating a horizontal circumferential frame in the whole building in order to prevent the external parts from detaching (Figure 4).



Figure 2. Ali Qapu building, lightening the roofs at sixth floor, 1965-1970.

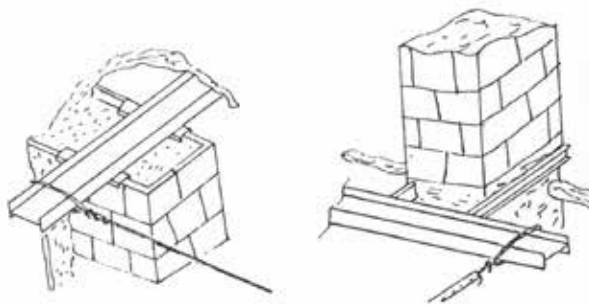
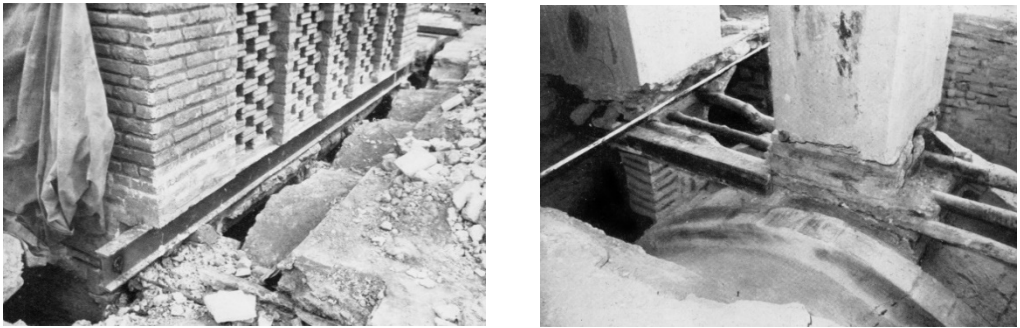


Figure 3. Ali Qapu building, using continuous spreaders in order to distribute the loads, 1964-1970 (after Galdieri [5]).



Figure 4. Ali Qapu building, using horizontal circumferential frame in the whole building in order to prevent the external parts from detaching, 1964-1970 (after Galdieri [5]).

2.1.2. Rehabilitation of the Wooden Columnar Structure in the 1970s

2.1.2.1. Description of the Wooden Columnar Structure

The wooden columnar structure covers the eastern veranda of the main building. It comprises columns, main beams, secondary beams on the top or between the main beams, and truss elements that transfer the load from the upper secondary beams to the lower main beams. A part of imposed load on the structure is supported by the side wall. A horizontal bracing system in the roof transfers the lateral load (Figure 5 and 6) [2, 6].

Eighteen columns (columns α' to η' , Figures 5 and 6(b)) along with the side wall (hatched section, Figures 5 and 6) carry the roof weight. Each column has a height of 10.5 m and an octagonal shape of cross-section with a diameter of 0.5 m at the base decreasing to 0.3 m at the top. Six columns (α' to ζ') were stiffened by cutting the wooden column into two parts, then emptying the central section of two parts and putting a \square -shape steel profile between them, connecting the wooden and steel

parts using bolts, and re-erecting the wood/steel column. The columns stand on a wooden spreader (Figure 6(c)) that was stiffened by I-shape steel profiles during the rehabilitation of the building.

There are two types of main beams. Perpendicular to the side wall, there are six beams of 17.5 m long of which 1.2 m are inside the side wall. The cross section of the beams is circular with a diameter of 0.4 m at the wall and 0.55 m at the other side (frames 1-6, beams a_7a_{10} to f_7f_{10} , Figs. 5 and 7). Parallel to the side wall, there are three lines of beams with a length of 28 m, each beam comprising three parts of 10 m, 8 m, 10 m long, and a diameter of 0.5 m (frames B-D, beams a_7f_7 , a_8f_8 and a_9f_9 , Figure 5).

Parallel to the main beams in lines 1 to 6 there are 10 lines of secondary beams with a cross-section of semi-circular shape and diameter 0.25 m (like beams a_1a_2 , a_2a_4 , a_4a_6 , g_1g_2 , g_2g_3 and g_3g_4 , Figure 5). Each secondary beam comprises of three parts and in frames 1 to 6 it lies at a distance of 0.2 m from the lower main beams near the wall and this distance gradually diminishes towards the other end (Figure 7).

There are 24 π -shape trusses which transfer the load from secondary beams to the main beams (a_8a_3 , a_3a_9 , a_9a_5 and ..., Figures 5 and 7).

All around the roof in the outer span there is a horizontal bracing for lateral loading. The rectangular cross section of the members is 0.1×0.15 m. The members form π or \times -shape trusses with beams (Figures 5 and 6(d)). As it is shown in Figure 6(d), a steel cable had previously been added to the structure to keep the f_7f_8 beam, which was cracked at one point, from moving outwards.

All the elements of the structure are made from the wood of sycamore (*platanus occidentalis*). Sycamore used to be an abundant species in Isfahan, capable of reaching 30 m in height, with tough, dense and hard wood. The connections between the elements are made by using iron nails. The roof structure is covered by an upper sloped plate and the lower wooden decorated roof of the veranda making a closed pyramid shape space with a maximum height of about 2 m.

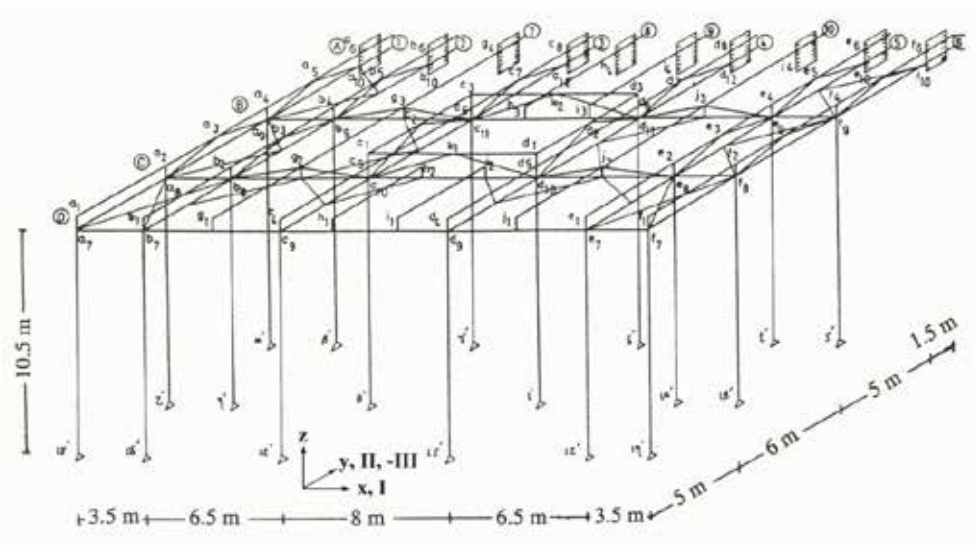


Figure 5. Ali Qapu building, the wooden columnar structure (after Hejazi [2, 6]).

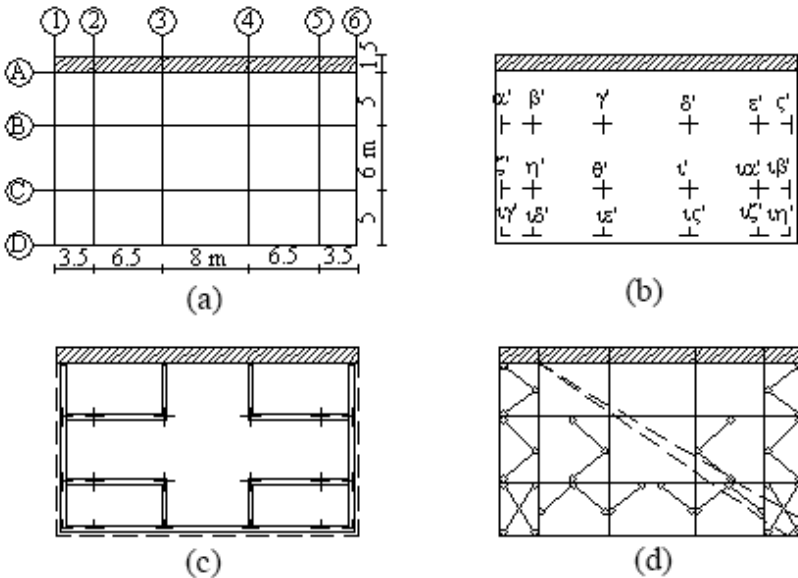


Figure 6. Ali Qapu building, wooden columnar structure: a) horizontal plan of the frames, b) horizontal plan of the columns, c) horizontal plan of the wooden spreaders under the columns, d) existing lateral bracing system before 2000 (after Hejazi [2, 6]).



(a)



(b)



(c)



(d)



(e)



(f)

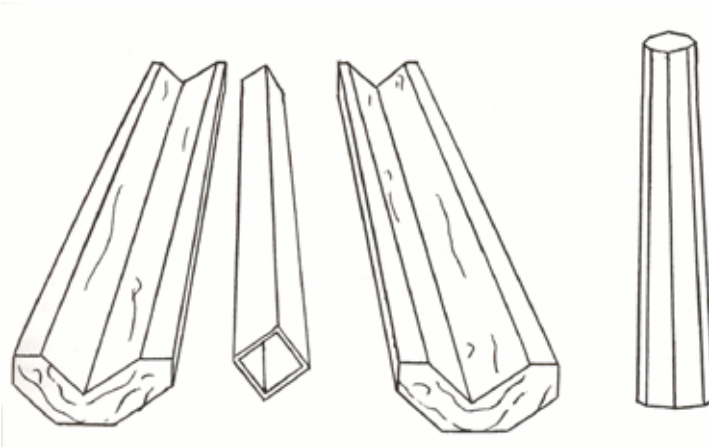
Figure 7. Ali Qapu building, wooden columnar structure: a) and b) wooden main and secondary beams in two directions (1990 and 2020), c) and d) a wooden truss (1990 and 2020), e) and f) wooden roof over the pond (1990 and 2020).

2.1.2.2. Load Bearing System

In the load bearing system of the wooden columnar structure, nine frames 1 to 6 and B to D participate (Figure 5 and 6(a)). The load on the upper sloped plate is transferred to the secondary beams, which in turn transfer the load to the lower main beams through π -shape trusses. Main beams also carry the weight of the lower wooden decorated roof of the veranda, which is connected to the main beams by iron connectors. Main beams are connected to the columns. The 18 columns of the structure along with the side wall support the load of the upper structure.

2.1.2.3. Strengthening the Wooden Columns in the 1960s and 1970s

During 1967 to 1968 and 1972 to 1975, six columns α' to ζ') were stiffened by cutting the wooden column into two parts, then emptying the central section of the two parts and putting a \square -shape steel profile between them and re-erecting the wood/steel column (Figure 8). The spreader under the columns was also stiffened by I-shape steel profiles.



(a)



(b)



(c)



(d)



(e)

Figure 8. Ali Qapu building, method of strengthening of wooden columns: a) schematics of the method (after Hejazi [2]), b) to e) the method (1960s and 1970s) (from the archives of the World Heritage Site of the Imam square).

2.2. Restoration Works in the 2000s

The last period of restoration of the building started in 2005 and completed in 2017. The restoration work focused on two parts: 1) the wooden columnar structure, and 2) the veranda on which the wooden structure stands.

2.2.1. Restoration of the Wooden Columnar Structure

The restoration of the wooden columnar structure involved the following parts.

2.2.1.1. Columns

The remaining wooden columns that were not stiffened by steel profiles, were cut longitudinally into two parts, emptied and embedded by □-shape profiles; the method similar to that implemented in the 1960s (Figure 9).







Figure 9. Ali Qapu building, stiffening wooden columns with steel profiles (2005 to 2017).

2.2.1.2. Supports and Connections of the Columns

For strengthening the connection between the steel profile inside the column and its support, a reinforced concrete foundation was constructed under each column and the connection was stiffened by welded steel stiffeners (Figure 10).

For the top of the column, a steel plate was connected to the beam above and the top of the steel profile was connected to the steel plate using welded steel stiffeners (Figure 11).



Figure 10. Ali Qapu building, strengthening the supports of the columns (2005 to 2017).

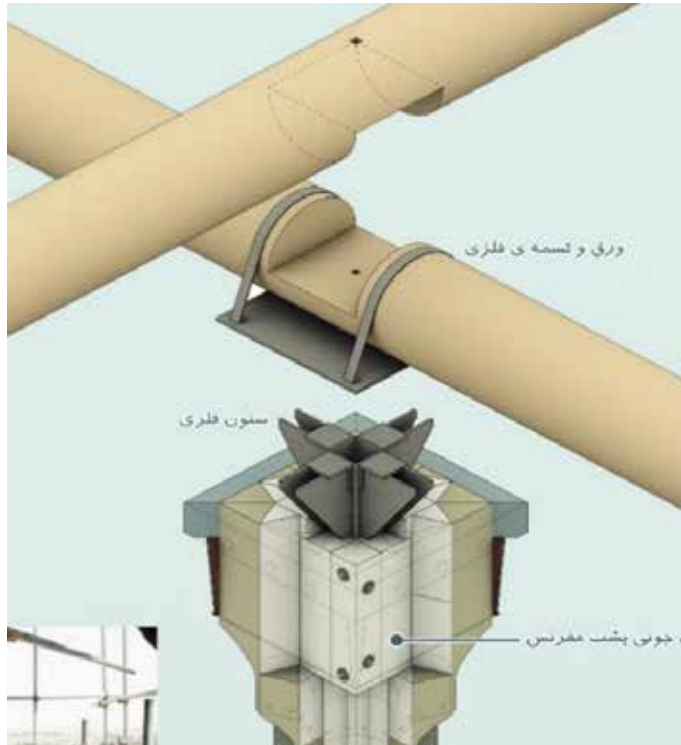




Figure 11. Ali Qapu building, strengthening the connections of the columns to top beams (2005 to 2017).

2.2.1.3. Lateral Load Bearing System in the Roof of the Wooden Structure

As shown in Figures 5 and 6(d), the original lateral load bearing system of the wooden columnar structure exists in the roof and consists of a number wooden members horizontally laid around the outer spans between main beams.

In the restoration works between 2005 and 2017, a horizontal system of steel cables consisting of ×-shape bracing in all spans, except the span over the pond, was added to the roof, as seen in Figures 12(a) and (b). It is expected that lateral load of wind and earthquakes is transferred by this system to the side thick masonry wall.

The decorated wooden ceiling is hanging and its weight is transmitted to the beams inside the roof by wooden connection and original iron strips. In the restoration work additional steel hangers were used to give additional strengthened the route of weight load from the ceiling to the upper beams (Figures 12(c) and (d)).



Figure 12. Ali Qapu building, the roof of the wooden columnar structure: a) and b) adding steel cables as the lateral load bearing system, c) and d) supporting the hanging ceiling by steel hangers (2005 to 2017).

2.2.1.4. Lightening the Floor of the Veranda

As shown in Figures 5 and 6(d), the original lateral load bearing system of the wooden columnar structure exists in the roof and consists of a number wooden members horizontally laid around the outer spans between main beams.



(a)



(b)



(c)



(d)

Figure 13. Ali Qapu building, the floor of the veranda under the wooden columnar structure: a) to c) lightening the floor, d) traditional pavement (2005 to 2017).

3. CONCLUSION

The Ali Qapu building has undergone two major restoration works. The first restoration, which was a comprehensive one, was carried out in the 1960s and 1970s and it focused on the main masonry building that was in a dangerous condition. The restoration work on the wooden columnar structure remained incomplete. The main purpose of the restoration work was to retrieve the integrity of the masonry part. The second restoration was carried out from 2005 to 2017 and it concentrated on the wooden columnar structure and its supporting veranda. The main purpose of the work was to repair the damaged wooden part as well as structural rehabilitation of the wooden structure, which also included the insertion of a lateral load bearing system of steel cables. A comprehensive seismic assessment of the building should be done in near future to evaluate the effectiveness of previous interventions.

REFERENCES

- [1] Pope, A. U. (1965). *Persian Architecture*. London: Thames and Hudson.
- [2] Hejazi, M. (1997). *Historical buildings of Iran: their architecture and structure*. Southampton and Boston: WIT Press (Computational Mechanics Publications).
- [3] Hejazi, M., and Mehdizadeh Saradj, F. (2014). *Persian architectural heritage: architecture*. Southampton and Boston: WIT Press.
- [4] Hejazi, M., Hejazi, B., and Hejazi, S. (2015). Evolution of Persian traditional architecture through the history. *Journal of Architecture and Urbanism*, Vol. 39, No. 3, pp. 188-207. DOI: 10.3846/20297955.2015.1088415.
- [5] Galdieri, E. (1979). *Esfahan: Ali Qapu, an architectural survey*. Rome.
- [6] Hejazi, M. (2003). Structural analysis of the wooden structure of the historical building of Ali Qapu. *Journal of Structural Engineering, ASCE*, Vol. 132, No. 11, pp. 1801-1805. DOI: 10.1061/(ASCE)0733-9445(2006)132:11(1801).

RESPONSE CONTROL ON SEISMIC UPGRADING OF LOW-RISE RC BUILDING IN THAILAND USING ELASTO-PLASTIC DAMPERS

Panumas Saingam¹

¹ *Department of Civil Engineering, School of Engineering, King Mongkut's Institute of Technology Ladkrabang, Bangkok 10520, Thailand, panumas.sa@kmitl.ac.th or panumas_saingam@hotmail.com*

ABSTRACT

Over the past half-century, many reinforced concrete (RC) buildings were damaged by the earthquakes in many unexpected countries. Therefore, seismic resistance and reinforcement requirements for RC buildings have significantly improved in many countries. Thailand has historically been considered to have a low seismic hazard which causes the majority of current existing RC buildings were not designed with seismic resistance. A recent seismic design specification was published in 2009; however, many older buildings do not satisfy the new code and require retrofit. This study proposes a response control method in order to seismic retrofit the existing RC building using elasto-plastic dampers to develop the seismic performance of the RC buildings. A retrofit method is introduced to efficiently distribute the dampers along with the building height. Design examples are introduced of 2-story RC school buildings in Thailand, which were damaged in the 2014 Mae Lao earthquake, and the predicted responses verified using time history analysis.

KEYWORDS: Low-rise RC building, Thailand, Response control, Seismic Upgrading, Elasto-Plastic Dampers

1. INTRODUCTION

Over the past half-century, many reinforced concrete (RC) buildings were damaged by the earthquakes in many regions. Therefore, seismic resistance and reinforcement requirements for RC buildings have significantly improved in many countries. The majority of currently existing buildings in Thailand were not designed with seismic resistance. However, there has been an increase in building damage during recent seismic events, and in 2009 the Department of Public Works and Town & Country Planning published a seismic design code for new buildings (DPT 1302-52, 2009), followed by a code for seismic retrofit (1303-57, 2014). Shortly after the May 15, 2014 Mae Lao earthquake struck, causing extensive damage in older buildings that were constructed before the current seismic code was implemented. Much of the damage was observed in reinforced concrete (RC) structures, as reported in Lukkunaprasit et al.(2015), and Ornthammarath et al. (2016), including some school buildings. Typical Thai school buildings are shown in Figure 1, constructed of non-ductile RC moment frames with vertical irregularities due to infill masonry walls. The 2-story building in Figure 1a received significant structural damage during Mae Lao earthquake, as indicated by the severe damage to the beam-column joint at the top of ground story columns.

A conventional retrofit solution for seismically deficient reinforce concrete (RC) moment frames is to install a stiff shear wall, which limits drift and ensures that the mainframe remains elastic, but imposes large floor accelerations. This implies extensive non-structural damage, as building contents and nonstructural components are unlikely to be detailed for seismic resistance in Thailand. An alternative retrofit solution is to employ energy dissipation devices to control both drift and accelerations while protecting the existing structure.

Supplementary energy-dissipating devices have been reported to be an effective seismic retrofit solution for RC frame buildings and have been applied in practice. For example, Takeuchi et al. (2009) integrated buckling-restrained braces (BRBs) into a new facade of a 6- story RC university building in Tokyo, Japan. Hussain et al. (2013) proposed installing chevron braced frame with viscous fluid dampers (VFDs) into high-end retail store building in Southern California, United States. Sarno et al. (2012) and Khampanit (2014) tested low-rise RC frames retrofitted with BRB. Other applications and methods of connecting the BRBs to the RC frame have

been proposed by Oviedo et al. (2010), Qu et al. (2012), and Mahrenholtz et al. (2014). Sutcu et al. (2014) proposed a retrofit design method for RC frame structures where the BRBs are installed in parallel with a supplementary elastic steel frame and designed using the equivalent linearization (EQ) method proposed by Takeuchi et al. (2002), which is based on a proportional damping distribution. Kasai and Ito (2005) and Pu and Kasai (2005) introduced a design method for passively controlled systems that minimizes the peak story drift, while Fujishita et al. (2015) applied an improved version of this method to an RC frame retrofitted with BRBs and an elastic steel frame.

The challenge in Thailand is that the seismic hazard is relatively small, with response control retrofits requiring smaller dampers installed at fewer stories than in a typical Japanese or Turkish application. While still a potentially effective retrofit solution, the low demands introduce unique challenges in determining an efficient number, size and distribution of dampers, as the optimal damper type, distribution and design approach may be different from those countries. This study investigates the performance of existing response control design methods for elasto-plastic (EP) dampers and introduces a new method that permits dampers to be omitted from some stories while controlling the vertical irregularity. These are referred to as the constant stiffness method. All three The method is then used to design a response control retrofit of the 2-story building as shown in Figure 1 and the designs are verified through time history analysis.



Figure 1. School buildings : Observed damage on buildings in Thailand by Mae Lao earthquake

2. RESPONSE CONTROL METHOD

The inelastic story force-displacement response of the bare RC frame is first obtained through pushover analysis. While the example structure Figure 1 was subjected to large drift and strength degradation due to column bending failure in Mae Lao 2014 earthquake, only the response up to the target story drift is needed for this analysis, set as $\theta_{tar} = 1/150$ (0.67%). A tri-linear degrading Takeda model is adopted to represent the existing RC frame (Takeda et al. 1970) and is calibrated to match the area under the pushover curve at each story i . The post-yield response is assumed perfectly plastic ($\alpha_2 = 0$), the yield story drift θ_{fy} is limited to $1/100 \sim 1/300$ rad, and the crack (δ_{fci}) to yield (δ_{fyi}) displacement ratio initially set as $\mu_c = 0.1$ (Takeda et al. 1970), but permitted up to $\mu_c = 0.2$. The yield shear force Q_{fyi} and displacement δ_{fyi} are then estimated, and the cracking shear force Q_{fci} and displacement δ_{fci} are adjusted to produce the same shear force ratio $N = Q_{fyi} / Q_{fci}$ and cracked stiffness ratio $\alpha_1 = [(Q_{fyi} - Q_{fci}) / (\delta_{fyi} - \delta_{fci})] / K_{fi}$ at all stories, where the initial story stiffness $K_{f0i} = Q_{fci} / \delta_{fci}$. This treatment reduces the multistory frame to a simplified representation, with the same pre-yield stiffness ratio α_1 , crack-to-yield drift ratio μ_c , ductility $\mu_f = \delta_{tar} / \delta_{fyi}$, and secant stiffness $K_f \mu = p K_{f0}$ at each story. The multi-degree of freedom (MDOF) model is then reduced to an equivalent single-degree-of-freedom (SDOF) system using the equivalent height (Heq), mass (Meq), and stiffness (K_f) (Sutcu et al. 2014). The cyclic hysteretic response of the SDOF system is shown in Figure 2 for the cracked and yielding stages.

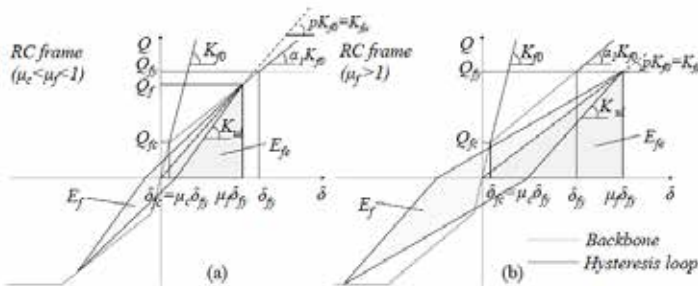


Figure 2. Hysteresis loops for RC frame : (a) Cracked ($\mu_c \mu_f > 1$, $\mu_f < 1$), (b) Yielding ($\mu_f > 1$)

The hysteretic energy dissipated by the RC frame (E_f) depends on the unloading stiffness (K_{ul}), with the unloading stiffness degradation parameter λ assumed as 0.4 (Takeda et al. 1970). The equivalent hysteretic damping for a constant cyclic displacement ($h'f\mu = h'f_0 + E_f / 4\pi E_f e$) is then determined from the hysteretic energy E_f , strain energy E_{fe} and intrinsic damping $h'f_0$ (assumed to be 0.03 for RC structures). As displacement ductility in each cycle varies when subjected to earthquake excitation, the Newmark and Rosenblueth (1971) average damping concept (Equation 1) is employed.

$$h_{f\mu} = h_{f0} + (1 / \mu_{tar}) \cdot \int_1^{\mu_{tar}} (h'_{f\mu} - h_{f0}) d\mu \tag{Equation 1}$$

However, for simplicity, the average equivalent damping ($h_{f\mu}$) (Equation 2) may be estimated from the equivalent damping of the maximum cycle ($h'_{f\mu}$) and a calibrated damping reduction factor ($R_{f\mu}$). The average $h_{f\mu}$ and peak $h'_{f\mu}$ equivalent damping are shown in Figure 3a and the corresponding reduction factors $R_{f\mu}$ is shown in Figure 3b.

$$h_{f\mu} = h_{f0} + R_{f\mu} (h'_{f\mu} - h_{f0}) \tag{Equation 2}$$

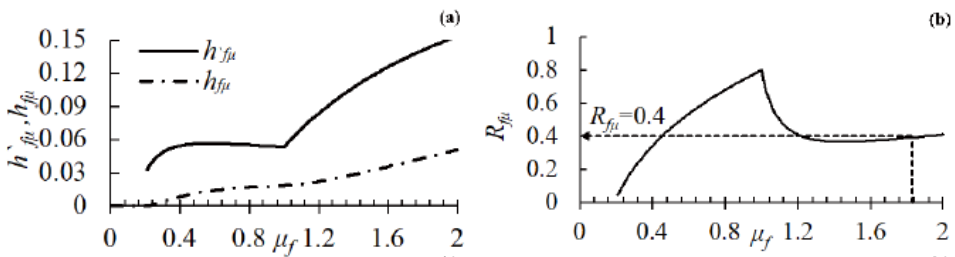


Figure 3. Equivalent damping reduction factor : (a) Equivalent damping and (b) $R_{f\mu}$

The spectral displacement $S_d(T_{f\mu}, h_{f\mu})$ of the bare RC frame is estimated from the design elastic displacement response spectrum at the secant period ($T_{f\mu}$), reduced from the 5% damped spectrum using equivalent damping ($h_{f\mu}$) and reduction factor proposed by Kasai and Ito 2005 (with $a = 25$). The secant period is given by

Equation 3 and uses the secant stiffness ($K_{f\mu}$) of the bare RC frame at the target drift. The roof drift of the bare RC frame ($\theta_{f\mu}$) is estimated from Equation 4 and dampers are required if $\theta_{f\mu}$ exceeds the target story drift θ_{tar} .

$$T_{f\mu} = 2\pi\sqrt{M_{eq} / K_{f\mu}} \tag{Equation 3}$$

$$\theta_{f\mu} = S_d(T_{f\mu}, h_{f\mu}) / H_{eq} \tag{Equation 4}$$

Supplementary dampers are effective in controlling drifts and enhancing the system energy dissipation, but the damper strength and stiffness distribution is important to minimize story drift concentration and to avoid a soft story. In this study, the constant stiffness method, where damper stiffness (K_d) is assigned in proportion to the frame (K_f), is introduced. The method is presented for the RC frame retrofitted with elasto-plastic (EP) dampers, which are placed within a supplemental elastic steel frame (SF). The damper-to-frame stiffness ratio (K_d/K_f) is a key parameter to obtain the damper demand and performance in each of these methods.

The concept of the constant stiffness method is described for the case of EP placed with an additional elastic steel frame to retrofit a yielding RC frame.

A simple elasto-perfectly plastic hysteresis rule is assumed for the EP damper, while the supplemental steel frame is assumed to remain elastic through at least the design drift, as indicated in Figure 4. The combined system response is shown in Figure 5.

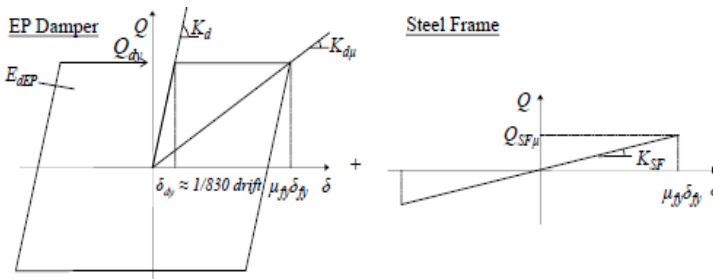


Figure 4. Elasto-plastic damper and elastic steel frame force-displacement models

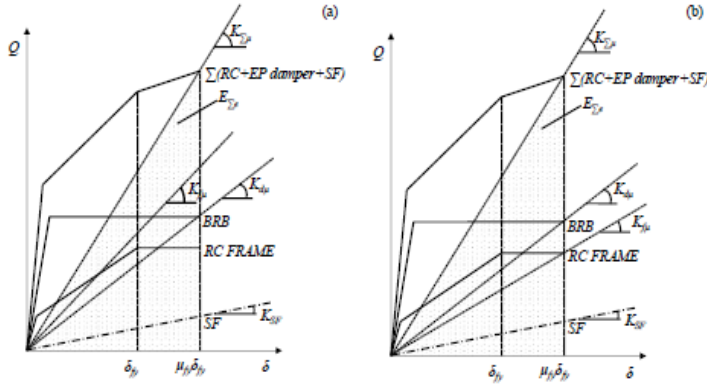


Figure 5. Overall behavior of system model : (a) Cracked ($\mu_c\mu_f > 1$, $\mu_f < 1$), (b) Yielding ($\mu_f > 1$)

The acceleration and displacement responses are affected by the increased equivalent damping (damper ductility) and stiffness (period shift). The damping response reduction factor Dh proposed by Kasai et al. (2005) is adopted, with $a=25$ is used for this study. The period shift effect ($T\Sigma\mu/Tf\mu$) is calculated from the secant stiffness of RC frame ($Kf\mu$) and overall system ($K\Sigma\mu$), based on the following assumptions:

- (a) $Tf\mu$ and $hf\mu$ are assumed constant at all displacement amplitudes.
- (b) The story drift of the bare RC frame $\theta f\mu$ exceeds the target drift θtar and therefore dampers are required
- (c) The story drift of the overall system $\theta\Sigma$ equals the target drift θtar

The required Kd/Kf ratio is denoted as $rdEP$ and is given by Equations 5(a) and 5(b) for the RC frame cracking and yielding stages, with γ_s the elastic steel frame (KSF) to damper stiffness (Kd) ratio.

$$r_{dEP} = \frac{K_d}{K_f} = \frac{p \left(\left(\frac{\theta_{fu}}{\theta_s} \right)^2 - 1 \right) \left(1 + 25 \left(h_{f0} + \frac{1}{\pi} \cdot \frac{\mu_c(1-p)}{p\mu_f + \mu_c} \cdot R_{f\mu} \right) \right)}{(1 + 25h_{f0})(\gamma_s + 1/\mu_d) + (2 \times 25 R_{reqEP} / \pi\mu_d)x(1 - 1/\mu_d)} \quad (\mu_c\mu_f > 1, \mu_f < 1) \quad \text{Equation 5.a}$$

$$r_{dEP} = \frac{K_d}{K_f} = \frac{p \left(\left(\frac{\theta_{fu}}{\theta_s} \right)^2 - 1 \right) \left(1 + 25 \left(h_{f0} + \frac{1}{\pi} \cdot \frac{p\mu_f + \mu_c - p(\mu_f)^k(1 + \mu_c)}{p\mu_f + \mu_c} \cdot R_{f\mu} \right) \right)}{(1 + 25h_{f0})(\gamma_s + 1/\mu_d) + (2 \times 25 R_{reqEP} / \pi\mu_d)x(1 - 1/\mu_d)} \quad (\mu_f > 1) \quad \text{Equation 5.b}$$

The required number of dampers n_i at story i is calculated from the required damper stiffness K_{di} (given the required stiffness ratio $rdEP$ and frame story stiffness K_{fi}), the damper yield story drift δ_{dyi} , and the shear strength Q_{dy1} of one unit, as indicated by Equation 6.

$$n_i = K_{di} \delta_{dyi} / Q_{dy1} \quad \text{Equation 6}$$

3. VALIDATION OF THE DESIGN METHOD

3.1. Design example

This section applies the proposed retrofit design procedure to the 2-story RC school buildings depicted in Figure 1, which requires seismic retrofit. Thailand Seismic Design Code is based on ASCE 7-05 (DPT 1302-52, 2009), and the design level spectral response acceleration parameters for these structures are $SDS = 0.56(g)$ and $SDI = 0.24(g)$ (site class D, Phan, Chiang Rai), approximately half of the seismic demands in Japan and other seismic prone regions.

Pushover curves and calibrated tri-linear Takeda models for the 2-story building are shown in Figure 6 for the first floor and roof, respectively. The story masses of the 2-story building are 266 and 172 ton at the first and roof stories, respectively, and the fundamental period of the bare RC frame is 0.59s in both the longitudinal and transverse directions. Structural properties of the bare SDOF RC structures are summarized in Table 1. The ratio of the area under the pushover curves and tri-linear model ($A_{pushover}/A_{tri}$) are close to 1.0 at each story, indicating a good fit.

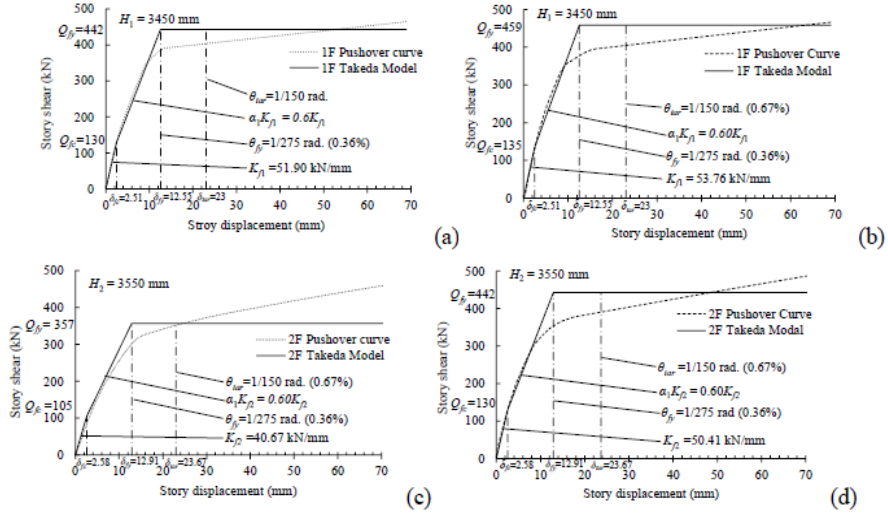


Figure 6. Pushover curve and tri-linear model of 2-story building : (a) Longitudinal direction for first story, (b) Transverse direction for first story, (c) Longitudinal direction for second story, (d) Transverse direction for second story

Table 1. Characteristic of bare RC Frame

Direction	μ_f	K_{f0} kN/mm	H_{eq} mm	M_{eq} t	μ_c	α_1	T_{ft} s	K_{ft} kN/mm	h_{ft}	θ_{ft}
2 story building, $R_{ft} = 0.6$ and $\theta_{tar} = 1/150$										
Longitudinal	1.83	46.6	4510	412	0.20	0.60	0.97	17.3	0.075	1/134
Transverse	1.83	49.4	4469	415	0.20	0.60	0.95	18.3	0.075	1/137

Retrofits applying EP dampers are designed according to the constant stiffness method. The EP damper demands are summarized in Tables 2, where β is an angle of the dampers. The damper stiffness using the constant stiffness method are obtained from Equation 5(b) for 2-story building. The required EP damper strengths are less than 100 kN, which is much smaller than typically used in Japan, and difficult to economically achieve with EP dampers. While the EP dampers retrofit reduce the fundamental period of 2-story building in both directions from

0.59 sec to 0.51 when retrofit the RC building with EP dampers.

Table 2. EP damper distributions for 2-story building model

Direction	Story	K_d/K_f	K_{df}	K_{di}	h_{eq}	Q_{dyi}	n_i	β	SF	
			kN/m	kN					K_{SF}	γ_s
						kN			kN/mm	
Longitudi nal	2	0.20	40.7	8.0	0.098	17.8	2	35.1	0.64	0.058
	1		51.9	10.2		20.8	2	34.1	0.70	0.054
Transverse	2	0.16	50.4	8.3	0.103	35.6	1	26.5	0.67	0.041
	1		53.8	8.8		35.6	1	25.6	0.73	0.044

3.2. Effectiveness of the concept

To validate the retrofit designs, nonlinear time-history was conducted, targeting the design acceleration response spectrum described earlier ($SDS = 0.56(g)$ and $SDI = 0.24(g)$). Two suites of ground motions were used, reflecting common practice in Japan and the US, which the Thai code is based upon. First, a suite of four earthquake ground motions were spectrally matched, consisting of El Centro NS (1940), JMA Kobe NS (1995), TAFT EW (1925), and Hachinohe NS (1968). The duration of four observed waves was 30 s for each wave, and compared to the design spectrum in Figure 7(a). Additionally, a suite of 11 scaled single component records were selected from the PEER NGA2 ground motion database 2 (Figure 7(b)). Scaling was conducted over a target period range of $0.2T1,min$ and $1.5T1,max$ following ASCE 7-16, where $T1,min$ and $T1,max$ are the minimum and maximum fundamental periods from the two models, resulting in a target period range of 0.1 to 2 sec. Records were limited to strike-slip events with magnitudes of $6 \leq Mw \leq 7.5$ within 20km and on soil class D ($180 \leq Vs,30 \leq 360m/s$), consistent with the dominate seismic hazard in the Chiang Rai province and local site conditions. Scale factors varied from 0.5 to 2.0, and the average spectrum matches or exceeds the target spectrum over the range of interest. While the average acceleration response spectra are similar for both suites, the average displacement spectra exceeds the design spectra by a relatively large margin for the scaled suite at periods greater than 1s, as shown in Figure 7.

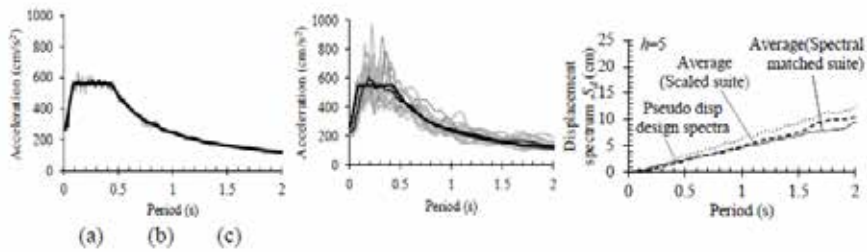


Figure 7.5% damped response spectra : (a) Matched suite, (b) Scaled suite and (c) Displacement spectra

Maximum story drifts of the bare RC frame and the retrofitted models using EP dampers are shown in Figure 8 for the 2-story building. Only the longitudinal direction is shown here as the response is similar in the two orthogonal directions. Drift is concentrated at the first story, exceeding the target story drift angle and matching the observed damage experienced during the Mae Lao earthquake.

Using the spectrally matched suite, adding dampers in proportion to the RC frame stiffness using the constant stiffness method improves the seismic performance of the retrofitted building. The second story drift under all ground motions is 0.2% for design using the constant stiffness method (Figure 8(b)) but increases to 0.67% to 0.78% at the first story.

The scaled ground motions produce a similar average drift distribution for the 2-story building (Figure 8), but exhibit greater record-to-record variability.

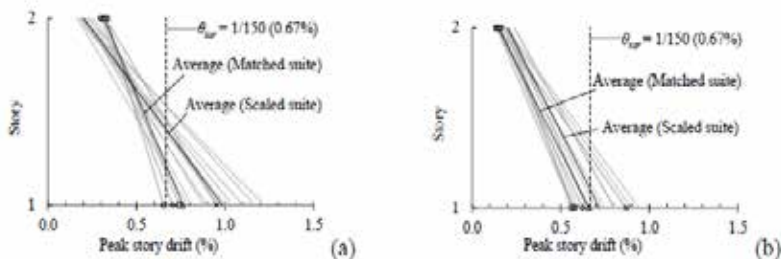


Figure 8. Maximum story drifts in transverse direction: (a) Existing RC frame and (b) Retrofitted building

4. CONCLUSIONS

A response control retrofit based on equivalent linearization was introduced to assign an efficient elasto-plastic damper distribution. The proposed method was compared to existing damper distribution procedures developed for countries with a severe seismic hazard and applied to a 2-story RC school building representative of typical Thai school buildings that were severely damaged in recent earthquakes. The results indicated that assigning damper stiffness in proportion to the bare RC frame stiffness using the introduced response control method improved the seismic performance of the upgrading building and the average maximum story ratio can control within the design target.

RESOURCES

Department of Public Works and Town & Country Planning (DPT), 2009. Thailand Seismic Design Code. (in Thai)

Department of Public Works and Town & Country Planning (DPT), 2014. Strengthening Buildings Recommendation Code. (in Thai)

Fujishita, K., Sutcu, F., Matsui, R., and Takeuchi, T., 2015. Damage distribution based energy- dissipation retrofit method for multi story RC building in Turkey, IABSE Symposium Report 104, 1–8.

Kasai, K., Ito, H., 2005. Passive control design method based on tuning of stiffness, yield strength, and ductility of elasto-plastic damper. *Journal of Structural and Construction Engineering*, AIJ 595, 45-55. (in Japanese)

Khampanit, A., Leelataviwat, A., Kochanin, J., and Warnitchai, P., 2014. Energy-based seismic strengthening design of non-ductile reinforced concrete frames using buckling-restrained braces. *Engineering Structures* 81, 110-122.

Lukkunaprasit, P., Ruangrassamee, A., Boonyatee, T., Chintanapakdee, C., Jankaew, K., Thanasisathit, N., and Chandrangsu, T., 2015. Performance of Structures in the Mw 6.1 Mae Lao Earthquake in Thailand on May 5, 2014 and Implications for Future Construction. *Journal of Earthquake Engineering* 20,219–242

Mahrenholtz, C., Lin, P.C., Wu, A.C., Tsai, K.C., Hwang, S.J., Lin, R.Y. and Bhayusukma, M., 2014. Retrofit of reinforced concrete frames with buckling-restrained braces. *Earthquake Engineering & Structural Dynamics* 44, 59-78.

Newmark, N.M. and Rousenblueth, E., 1971. *Fundamentals of Earthquake Engineering*, Prentice-Hall Inc.

Ornthammarath, T., and Warnitchai, P., 2016. 5 May 2014 MW 6.1 Mae Lao (Northern Thailand) earthquake: interpretations of recorded ground motion and structural damage. *Earthquake Spectra* 32, 1209–1238.

Oviedo A, J., Midorikawa M., and Asari, T., 2010. Earthquake response of ten-story story-drift- controlled reinforced concrete frames with hysteretic dampers. *Engineering Structures* 32, 1735- 1746.

Pu, W., Kasai, K., 2005. Passive control design method for RC building structure added with elasto- plastic damper. *Journal of Structural and Construction Engineering*, AIJ 78, 461–470. (in Japanese)

Qu, Z., Kishiki, S., Sakata, H., Wada, A., and Maida, Y., 2012. Subassemblage cyclic loading test of RC frame with buckling-restrained braces in zigzag configuration. *Earthquake Engineering & Structural Dynamics* 42, 1087-1102.

Sarno, L.D., and Manfredi, G., 2012. Experimental tests on full-scale RC unretrofitted frame and retrofitted with buckling-restrained braces. *Engineering & Structural Dynamics* 41, 315-333.

Sutcu, F., Takeuchi, T., Matsui, R., 2014. Seismic retrofit design method for RC buildings using buckling-restrained braces and steel frames, *Journal of Constructional Steel Research* 101, 304-313.

Takeda T., Sozen M.A., Nielsen N.N., 1970. Reinforced concrete response to simulated earthquakes.

Journal of Structural Division, *Journal of structural Engineering*, ASCE 96(12), 2557-73.

Takeuchi, T., Kasai, K., Oohara, K., Kimura, Y., Nakashima, H., 2002. Performance evaluation and design of passively controlled building using equivalent linearization. *Structural Engineering World Congress*, October 9-12, 2002, Yokohama, Japan.

Takeuchi, T., Yasuda, K., and Iwata, M., 2009. Seismic retrofitting using energy dissipation facade. *ATC-SEI09 Conference on Improving the Seismic Performance of Buildings and Other Structures*, December 9-11, 2009, San Francisco.

URBAN TRANSFORMATION APPLICATIONS IN LOW-RISE REINFORCED CONCRETE BUILDINGS

Abdullah Nigdeliöglu¹, Ouiame Chakkor², Mehmet Fatih Altan³

¹*Istanbul Aydin University, Civil Engineering, abdullahnigdeliöglu@aydin.edu.tr*

²*Istanbul Aydin University, Anadolu BIL Vocational School, ouiamechakkor@aydin.edu.tr*

³*Istanbul Aydin University, Civil Engineering, mehmetaltan@aydin.edu.tr*

*Responsible author: abdullahnigdeliöglu@aydin.edu.tr

ABSTRACT

Istanbul is Turkey's largest metropolis and is one of the region's leading cities in terms of economy and culture. Due to the expected great Istanbul earthquake, the urban transformation application remains popular in Turkey and its popularity is increasing day by day. It is important for Turkey, which is a developing country, to rapidly transform and renew its old building stocks. In this study, a case analysis of a building considered to be risky are conducted. An earthquake risk analysis of the building was carried out within the scope of the law on the transformation of areas under disaster risk numbered 6306. In earthquake calculations, response spectrum analysis has been used. The concrete and steel classes used in the building has been examined. The material properties of the structural building components has been investigated by using destructive and non-destructive methods. The average concrete compressive strengths, steel reinforcement types, stirrup spacing, and corrosion rates of the building has been examined. The principles in the RYTEIE-2019 regulation, which are used to determine the buildings considered as risky, are examined. The performance analysis results of the building has been evaluated according to TBEC-2018 and RYTEIE-2019. In the study, the average existing concrete strength of the building is found 9.42 MPa according to experiments. It has been determined that plain rebar S220 steel, which is not allowed to be used today, was used in the construction of the building. As a result of the analysis, it has been concluded that the performance of the building is insufficient under lateral and vertical loads and it has been observed that all floors of the building are risky.

KEYWORDS: Urban transformation, case study, earthquake, reinforced concrete buildings, RYTEIE-2019, TBEC-2018.

1. INTRODUCTION

The population in cities is increasing day by day. The economic conditions created by the cities allowed people to migrate from the rural to the cities. Urban transformation refers to the efforts carried out to revive the urban texture that has lost its purpose. Urban transformation initiatives are becoming increasingly important in Istanbul as the city's population grows. One of the main aims of urban transformation is to eliminate risky buildings and reconstruct them with earthquake-resistant structures. Urban transformation projects are important not only for earthquakes but also for all natural disasters that may occur. Urban transformation is a necessity for Istanbul, not only to prevent the destruction caused by the earthquake, but also to increase the quality of life of people and to ensure both social and physical sustainability [1]. For this reason, it is necessary to identify risky buildings and to transform these risky buildings to construct safer buildings. Urban transformation is carried out to solve problems such as the need for renewal of the city, inadequate infrastructure in areas that have lost their function [2].

Earthquakes cause loss of life and injuries by damaging people's living spaces. Thousands of people die today due to the damage caused by the earthquake. Urban transformation projects play an important role in the development of cities. Although there is a 15% margin of error according to the Istanbul earthquake master plan prepared in 2003, it has been stated that an earthquake of 7.0 or greater will be seen in Istanbul with a probability of 62% in thirty years [3]. Since the earthquake risk cannot be completely eliminated, the risk should be minimized [4]. In order to minimize the risk, the demolition and rebuilding of the buildings within the scope of urban transformation or strengthening will reduce the loss of life and injuries in the expected great Istanbul earthquake. It is aimed to ensure the active and continuity of production-marketing and trade zones with urban transformation projects [5]. With the urban transformation projects, the problems of the depressed areas are eliminated and the welfare of the city life is increased [6].

Istanbul acts as a bridge connecting Europe and Asia (Fig. 1). The city, which has hosted many civilizations over the years, has the distinction of being the largest economic city in the region due to its location. The population of Istanbul in 2021 is

15 840,900 according to the data [7]. If Istanbul suffers great damage in the expected great Istanbul earthquake, it will cause difficulties for the country and the region (Fig. 2). The expected great Istanbul earthquake poses a great threat to Istanbul. Especially, it is necessary to examine the buildings built before 2000 and to control them against earthquakes. Turkey has been exposed to many great earthquakes in the past years. Some of the recent great earthquakes in Turkey are given in table 1.

Earthquake	M_w
Caldıran Earthquake (1976)	7.5
Golcuk Earthquake (1999)	7.4
Duzce Earthquake (1999)	7.2
Bingol Earthquake (2003)	6.4
Van Earthquake (2011)	7.2
Elazig Earthquake (2020)	6.8
Izmir (Seferihisar) Earthquake (2020)	6.6



Figure 1. Istanbul Map [8]

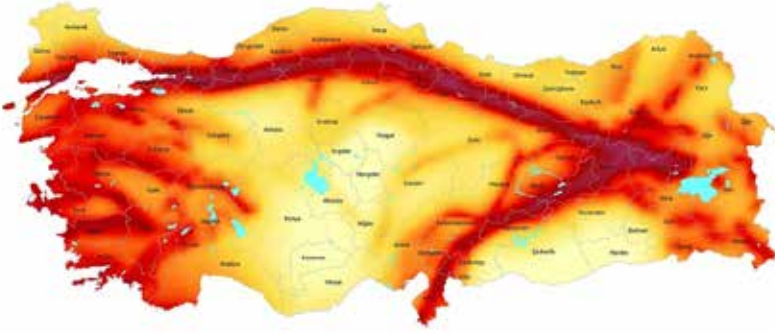


Figure 2. Turkey Earthquake Risk Map [9]

2. BUILDING INFORMATION

The building under investigation is located in the province of Istanbul. The building was built before 2000. As stated in RYTEIE-2019, buildings with a height of up to 30 meters including the basement floor or structures with less than 10 floors are considered as low-rise [10]. The low-rise reinforced concrete building, which has a total of seven floors, has frame structural system. The floor type of the building is beam and slab floor. The ground floor was chosen as the examination floor for the samples to be taken from the building. The reason for selecting the ground floor of the examination floor is that it is the lowest building floor with all its facades exposed throughout the floor height. There are 48 vertical structural members on the examination floor. Although the building has structural system projects, the knowledge level of the building has been chosen as minimum according to RYTEIE-2019 since the production of the building is not the same as the projects. The other structural system information of the building and the information of the ground floor are given in table 2.

Table 2. Building structural system information

Total building area (m ²)	3448,63
Building size (m)	30,2 x 13,6
Building total height (m)	19,6
Average floor height (m)	2,8
Column size (cm)	30 x 60
Beam size (cm)	15 x 50
Slab thickness (cm)	10

The ground class of the building was determined by ground survey as ZD according to TBEC-2018 [11]. Concrete samples taken from the ground floor columns, which are the examination floor, were taken as 85% of the average found after the correction, and the concrete strength of the building was found as 9.42 MPa and the elasticity modulus of the concrete was calculated as 15344 MPa. It has been determined that plain rebar (S220) is used in the longitudinal and transverse reinforcements used in the building. Corrosion was observed in the column reinforcements. Rebar diameters decreased due to corrosion. The average corrosion rate of the four columns in the examination floor is found to be 4.46%(Table 3). In Equation 1, the equation used to calculate the corrosion rate is given.

$$\text{Corrosion Rate} = 1 - \left[\frac{\text{Measured Rebar Diameter}}{\text{Rebar Diameter In The Project}} \right] \quad (1)$$

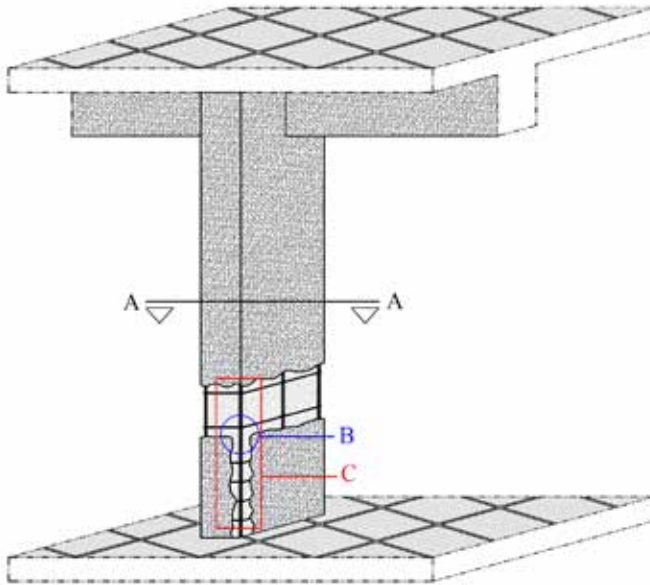
Table 3. Corrosion rates

Column number	Corrosive rebar diameter (mm)	Corrosion-free rebar diameter (mm)	Rebar diameter reduction amount	Corrosion rate (%)	Average corrosion rate (%)
Column-1	13.86	14	0.14	1.00	4.46
Column-2	12.79	14	1.21	8.64	
Column-3	12.89	14	1.11	7.93	
Column-4	13.96	14	0.04	0.29	

In Figure 3, the schematic of the process called destructive stripping from the column of a building where a risky structure has been detected is shown. The average reinforcement ratio is calculated as 0.00630 for the columns in which reinforcement is determined in the examination floor. It has been observed that Ø12 and Ø14 are used in the longitudinal reinforcement of the columns. In Table 4, the reinforcement calculation for the columns in which the reinforcement was determined by destructive and non-destructive methods is given in the examination floor. It has been observed that Ø8 rebar is used in transverse reinforcement and it is manufactured at 25 cm intervals. It has been observed that there are no hooks on transverse reinforcement in the columns.

Table 4. Rebar ratio calculation in columns

Detection method	Column number	Column size	Number of equipment	Rebar diameter (mm)	Rebar class	Rebar Ratio	Average reinforcement ratio
Destructive	Column-1	30 x 60	10	14	S220	0.00855	0.00630
Destructive	Column-2	30 x 60	8	14	S220	0.00684	
Destructive	Column-3	30 x 60	8	14	S220	0.00684	
Destructive	Column-4	30 x 60	8	14	S220	0.00684	
Non-destructive	Column-5	30 x 60	8	12	S220	0.00503	
Non-destructive	Column-6	30 x 60	8	12	S220	0.00503	
Non-destructive	Column-7	30 x 60	8	12	S220	0.00503	
Non-destructive	Column-8	30 x 60	10	12	S220	0.00628	



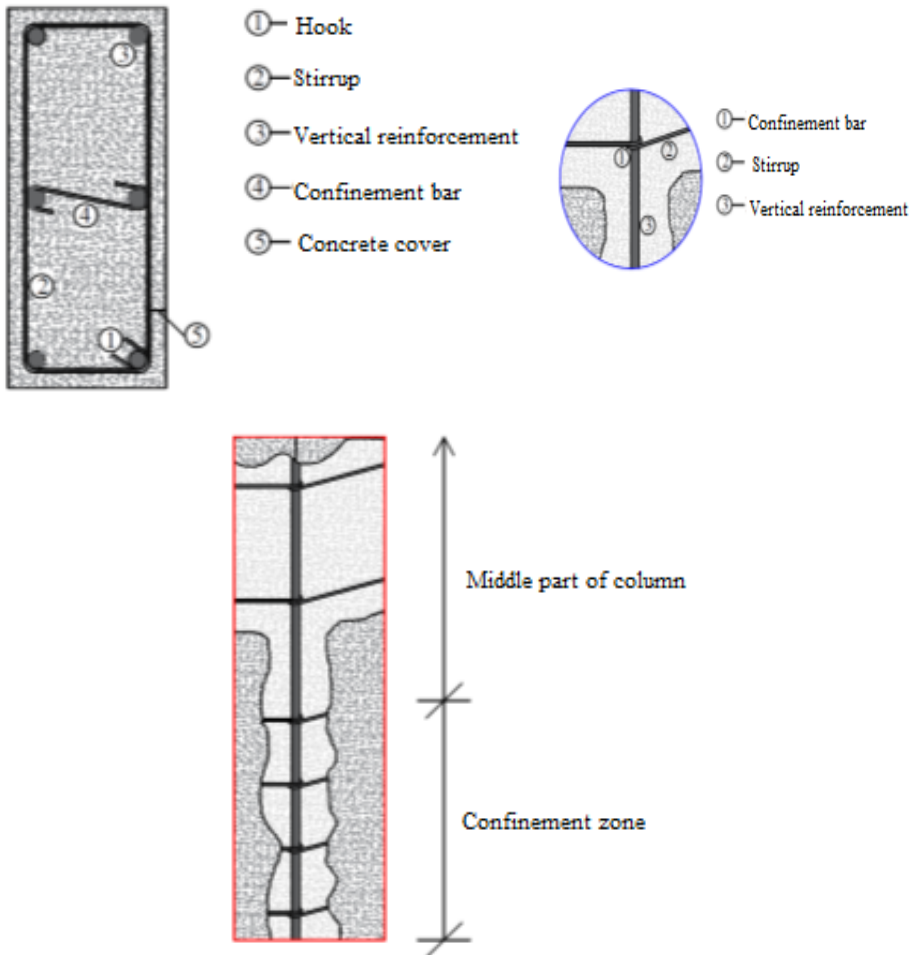


Figure 3. Longitudinal and transverse reinforcement determinations by stripping method in columns (RYTEIE-2019)

3. FINITE ELEMENT ANALYSIS OF BUILDING

The analysis of the building has been carried out with the three-dimensional analysis program STA4Cad V.14.1 [12]. In the analysis phase, the DD-2 earthquake ground motion level is used. Dynamic analysis is performed using spectral acceleration method in earthquake calculation. TS500(2000) is used in the reinforced concrete

calculation method [13]. The soil bearing coefficient is found to be 11000 kN/m^3 and the soil safety stress is 90 kN/m^2 . The beam reinforcement calculation was found under the vertical loads ($1.4G+1.6Q$) specified in TS500. Beam lower support reinforcement is taken into account by taking $1/3$ of the upper support reinforcement. Table 5 shows the parameters used in the analysis of the building. According to RYTEIE-2019, no additional eccentricity was applied in the modelling of the building. Beams and columns are modelled as frame elements. Controlled damage performance level was determined as the performance limit in the analysis. In the modal analysis, 21 modes were included in the analysis and the mode participation rate was 99% in the x and y directions. These ratios calculated for the analysed building meet the 95% dynamic mass ratio stated by TBEC-2018.

Table 5. Parameters used in the analysis of the building

Response reduction factor (R)	4,0
Overstrength factor (D)	2,5
Live load participation (n)	0,3
Knowledge level coefficient	0,9
Importance factor (I)	1
S_s	1,261
S_1	0,340
Seismic design class (DTS)	1
Permitted height categories (BYS)	5
Building use categories (BKS)	3

As a result of the analysis, the building dominant period is found to be 1.7405 seconds. After the analysis, the total mass of the building is calculated as 3726.59 tons. No vertical irregularities are detected in the building.

4. CONCLUSIONS

Samples were taken from the examination floor of the low-rise reinforced concrete building, and the structural element properties of the building were determined. After the examinations and analyses of the building, it has been stated that the building will be risky if any floor is risky according to the principles regarding the detection of risky structures in RYTEIE-2019. As a result of the analysis, all floors of the building were determined as risky. The building has insufficient performance against earthquakes in its current form. The building needs demolition or strengthening. Corrosion rate was found as 4.46% in the four columns on the examination floor and it was concluded that the concrete cover in the examined columns is insufficient. The plain rebar (S220) used in the building should no longer be used today according to the current TBEC-2018. The concrete strength of the building was found to be 9.42 MPa. This value found is well below the minimum C25/30 strength required by the Turkish building earthquake code. Against the expected great Istanbul earthquake, many old buildings in Istanbul are not still earthquake resistant and the building stock is not at a sufficient level. It can be concluded that many buildings in Istanbul built before the year 2000 are not earthquake resistant as the building analyzed in this study. Urban transformation projects should be accelerated for the province of Istanbul and measures should be taken for the great Istanbul earthquake, which will affect at least 1 million people.

ACKNOWLEDGEMENT

We would like to thank the Istanbul Ministry of Environment, Urbanization and Climate Change and Directorate General for Infrastructure and Urban Transformation Services and their staff, who provided data support for this study.

REFERENCES

- [1] Okumuş, D.E., Eyuboglu, E.E., (2017), Healthy environments or high prices? Residents'perspective to the urban regeneration projects in Ataşehir, İstanbul, Current Urban Studies, 5(4).
- [2] Genç, F.N., (2008), Urban transormation in Turkey: General view of legislation and practices, 15(1).
- [3] IBB: İstanbul için Deprem Master Planı, (2003), İstanbul Büyükşehir Belediyesi Planlama ve İmar Dairesi Zemin ve Deprem İnceleme Müdürlüğü, İstanbul.
- [4] Köktürk, E., Köktürk, E., (2007), Relations between earthquake and urban transformation, Journal of geodesy and geoinformation, 97.
- [5] Boyraz, Z., Hoş, B.Y., (2014), Urban renewal samples in terms of city geography in Turkey, Journal of World of Turks, 6(3).
- [6] Şahin, M., (2020), The project of urban regeneration, determination and evaluation of risky buildings: Alanya's Specimen, İstanbul Aydın University.
- [7] <https://www.nufusune.com/istanbul-nufusu>
- [8] <https://www.arcgis.com/home/webmap/viewer.html?layers=b165c3df453e4be6b5ac4fdb241effbe>
- [9] AFAD, (2018), Turkey Seismic Hazard Map.
- [10] MoEU, (2019), Riskli Yapıların Tespit Edilmesine İlişkin Esaslar, Çevre ve Şehircilik Bakanlığı Altyapı ve Kentsel Dönüşüm Hizmetleri Genel Müdürlüğü, Ankara.
- [11] TBEC, (2019), Turkey Building Earthquake Code, T.C. Resmi Gazete, Ankara.
- [12] STA4Cad V.14.1, (2019) STA Bilgisayar Mühendislik Müşavirlik Limited Şirketi, İstanbul.
- [13] TS500, (2000), Betonarme Binaların Tasarım ve Yapım Kuralları, Ankara.

INVESTIGATION OF THE EFFECT OF MATERIAL MODELS ON BEHAVIOR OF REINFORCED CONCRETE COLUMNS BY ANALYTICAL MODELS

Selim AYKUTLU¹, Sinan CANSIZ²

¹*Istanbul Aydin University, Besyol Kucukcekmece/Istanbul,
selimaykutlu@aydin.edu.tr*

²*Istanbul Aydin University, Besyol Kucukcekmece/Istanbul,
sinancansiz@aydin.edu.tr*

*Responsible author: *selimaykutlu@aydin.edu.tr*

ABSTRACT

Reinforced concrete carrier systems may show different behavior types due to the fact that are composite materials due to their structure. There are many studies on the behavior of reinforced concrete structural systems. Experimental studies for this purpose have limited number of experimental samples. The reason for that requires cost and high workforce. In addition, these studies are usually carried out on one or more parameters that affect the behavior of reinforced concrete carrier systems. However, thanks to the analytically correct modeling of the studies, the effect of multiple parameters on the behavior can be verified over a large number of samples. For this purpose, analytical modeling of a reinforced concrete column, which has been experimentally investigated, has been made within the scope of this study. In this context, it has investigated to find the model closest to the experimental result by using the Seismo-Struct program. In addition, the effect of the material models that most accurately reflect the experimental behavior has investigated. The most suitable binary combinations in the concrete and steel models examined at the end of the study are explained in the results section. Thanks to this study, it is planned to allow the limited number of experimental samples to be reproduced and examined under different parameters.

KEYWORDS: Analytic model, Seismo-Struct, Experimental study.

1. INTRODUCTION

The behavior of reinforced concrete systems varies according to the physical properties of the material used. In order to analyze the behavior of reinforced concrete systems, it is necessary to know the mechanical properties of the main materials used in them. Therefore, the behavior of concrete and steel used in reinforced concrete systems guides us. For many years, researchers have been trying to understand the behavior of reinforced concrete systems by doing different studies. With the increase in the use of computers and the development of software, these software have started to be used in the analysis of reinforced concrete systems.

In this study, a previously experimental model was compared with the analytical models created with the seismo-struct program.

2. MATERIAL PROPERTIES

2.1. Experimental Study

In the experimental study conducted by Soesianawati, the test sample with the dimensions (400 mm. * 400 mm) whose properties are given in Table-1 was taken as basis. For a correct comparison, it is modeled in the Seismo-Struct program with the same material properties and the same dimensions.

Table 1. Material Properties of Experimental Study

<i>Material Properties</i>	<i>Grade</i>	<i>Yield Stres</i>	<i>Strength</i>
Concrete			40 Mpa
Longitudinal Steel	380	446 Mpa	702 Mpa
Transverse Steel	275	255 Mpa	402 Mpa

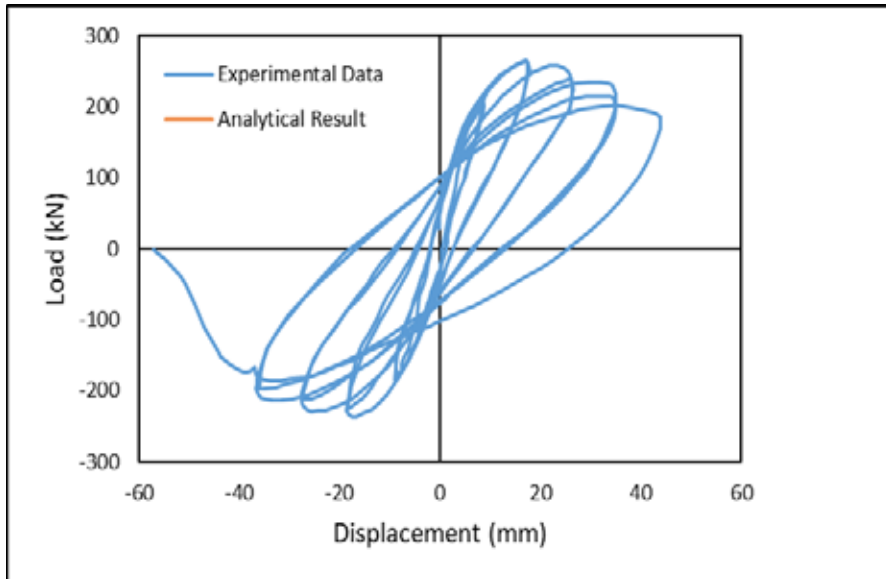


Figure 1. Soesianawati Experimental Study (Soesianawati et al. 1986, No. 4).

2.2. Material Models

Material models designed in the Seismo-Struct program, which we will use for the analytical models of the experimentally studied system, are listed as items.

- Mander Concrete Model
- Trilinear Concrete Model
- Chang and Mander Concrete Model
- Kappos and Konstantinidis Concrete Model
- Bilinear Reinforcement Model
- Menegetto-Pinto Reinforcement Model
- Ramberg-Osgood Reinforcement Model

Table 2. Material Properties of Analytic Models

Model Name	Concrete Model	Steel Model
M01	Mander	Menegotto Pinto
M02	Mander	Bilinear
M03	Mander	Ramberg Osgood
M04	Trilinear	Menegotto Pinto
M05	Trilinear	Bilinear
M06	Trilinear	Ramberg Osgood
M07	Chang And Mander	Menegotto Pinto
M08	Chang And Mander	Bilinear
M09	Chang And Mander	Ramberg Osgood
M10	Kappos and Konstantinidis Nonlinear	Menegotto Pinto
M11	Kappos and Konstantinidis Nonlinear	Bilinear
M12	Kappos and Konstantinidis Nonlinear	Ramberg Osgood

3. ANALYTICAL RESULTS

The load-displacement relationship of the models used in this study is shown in Figure 2-13.

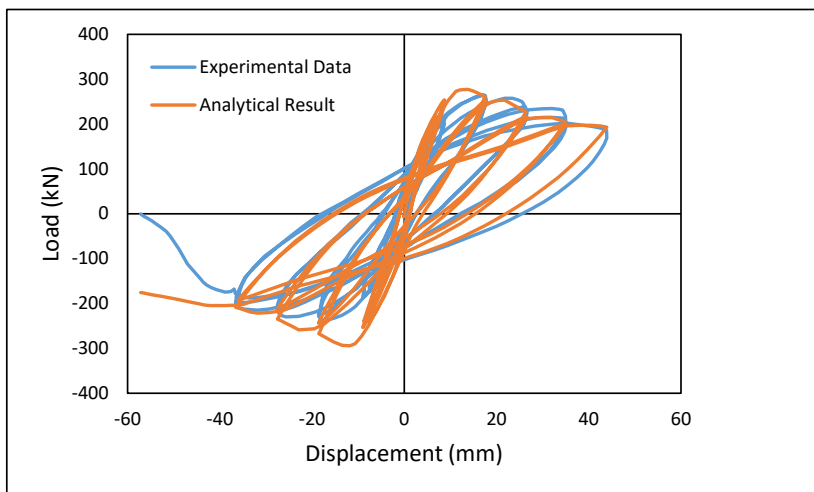


Figure 2. Mander Concrete -Menegotto Pinto Steel Model – M01

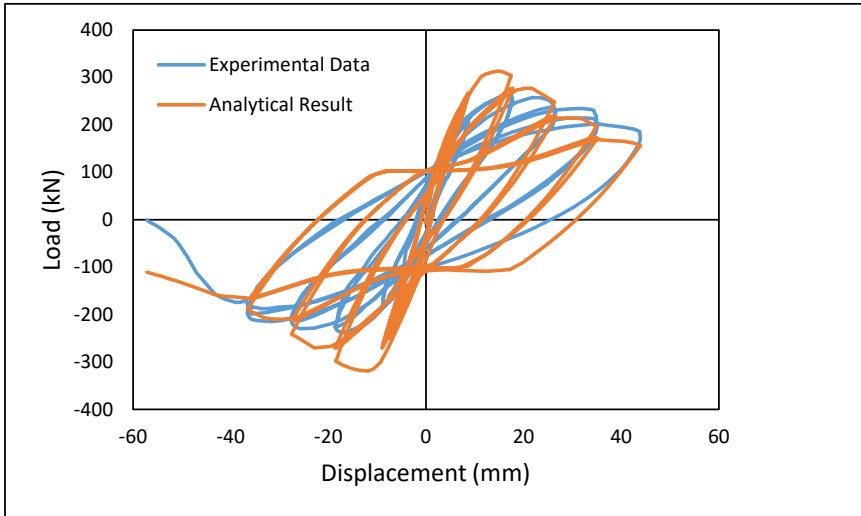


Figure 3. Mander Concrete -Bilinear Steel Model – M02

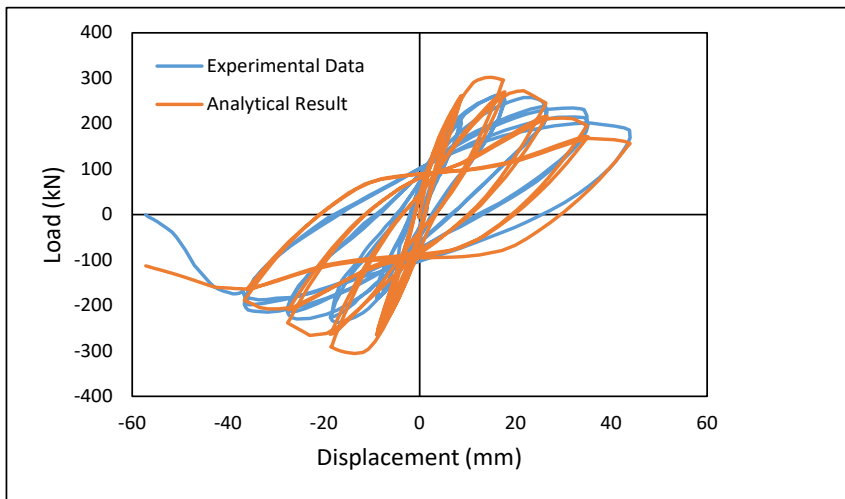


Figure 4. Mander Concrete -Ramberg Osgood Steel Model – M03

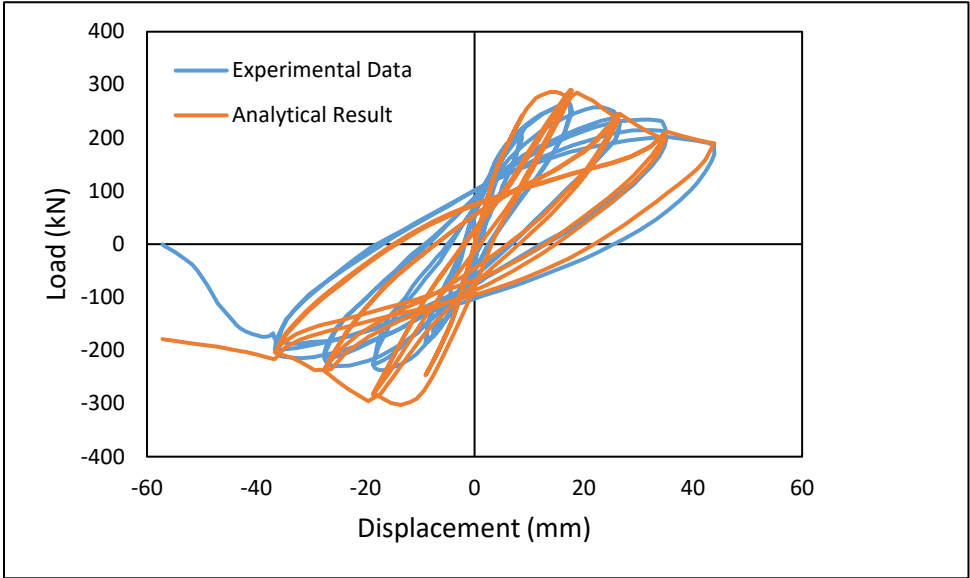


Figure 5. Trilinear Concrete -Menegotto Pinto Steel Model – M04

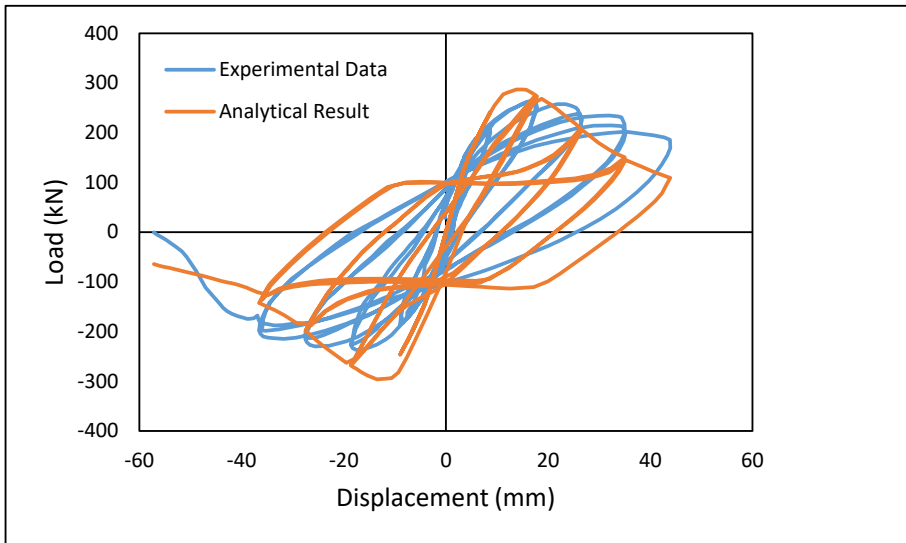


Figure 6. Trilinear Concrete - Bilinear Steel Model – M05

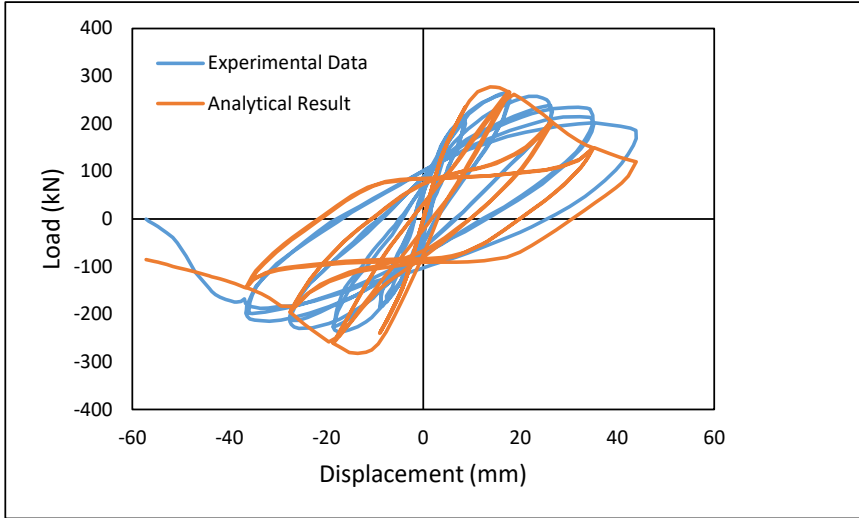


Figure 7. Trilinear Concrete – Ramberg Osgood Steel Model – M06

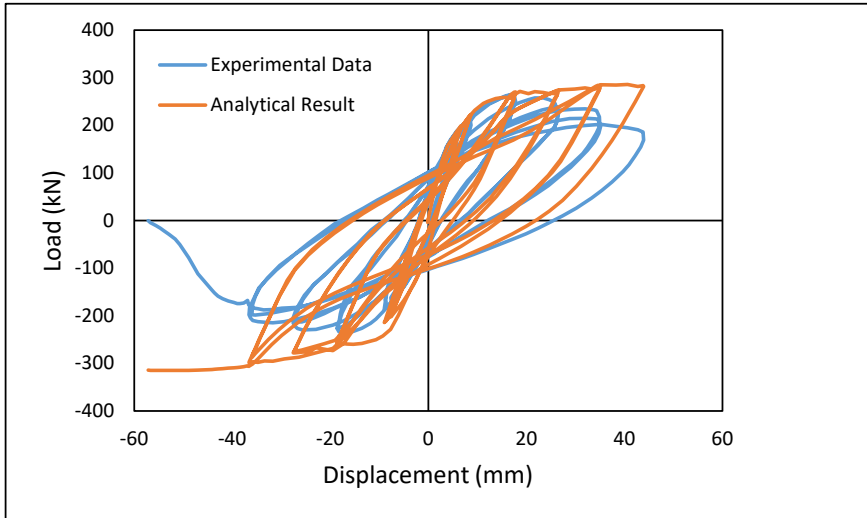


Figure 8. Chang and Mander Concrete -Menegotto Pinto Steel Model – M07

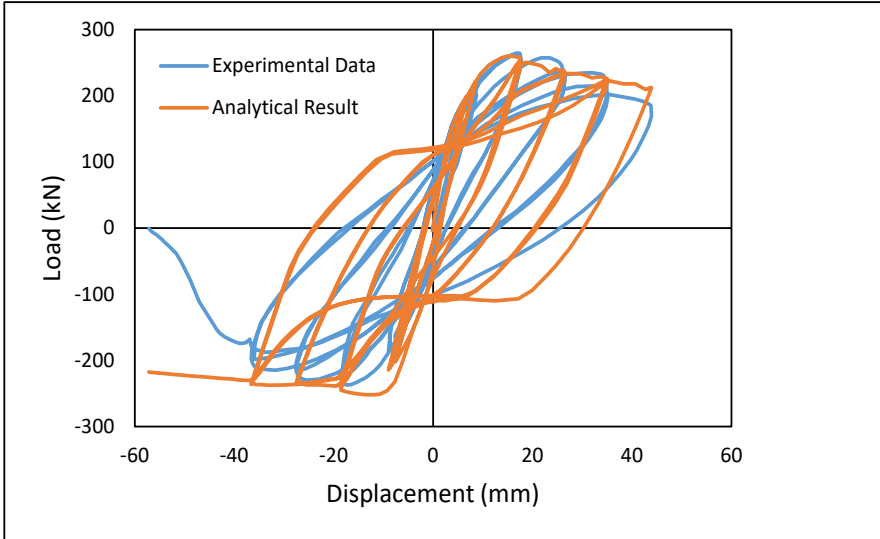


Figure 9. Chang and Mander Concrete - Bilinear Steel Model – M08

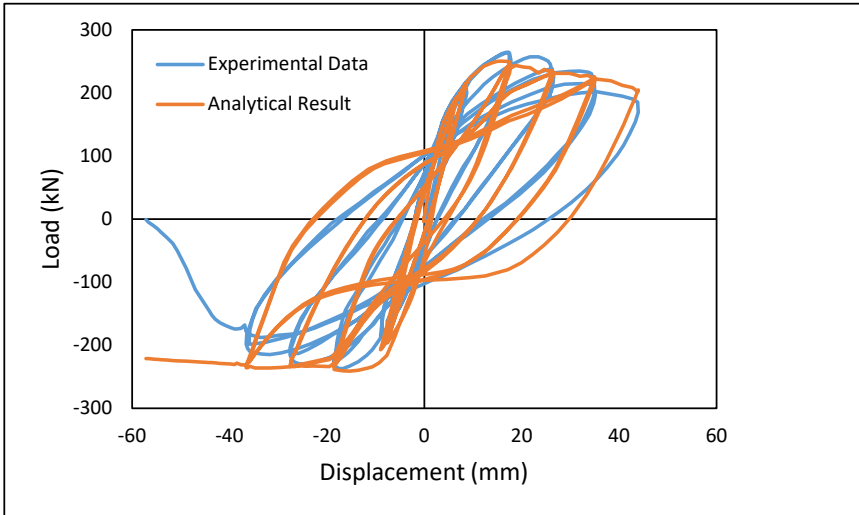


Figure 10. Chang and Mander Concrete – Ramberg Osgood Steel Model M09

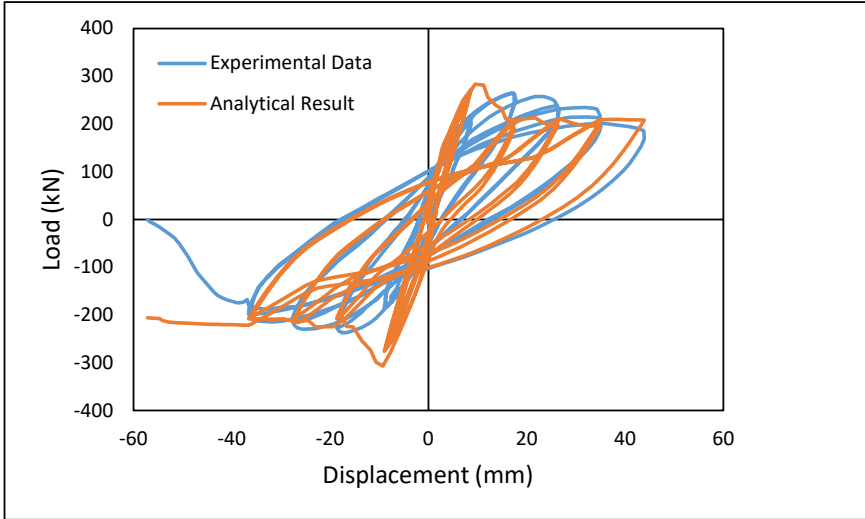


Figure 11. Kappos ve Konstantinidis Concrete -Menegotto Pinto Steel Model -M10

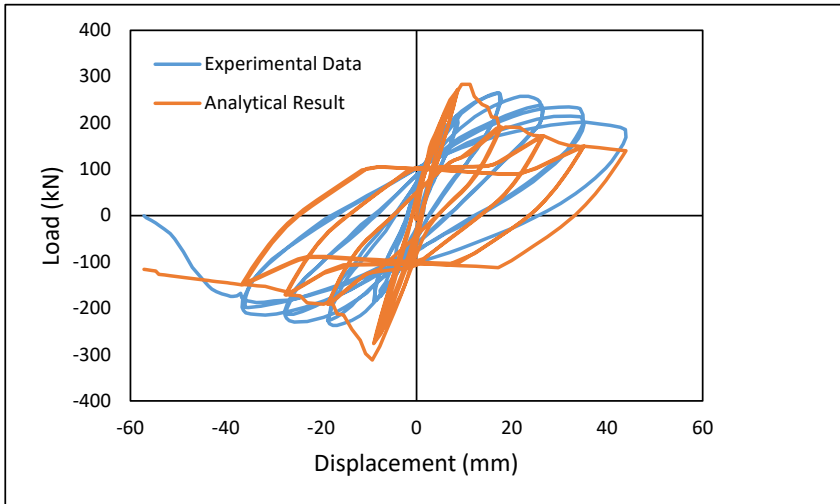


Figure 12. Kappos ve Konstantinidis Concrete - Bilinear Steel Model - M11

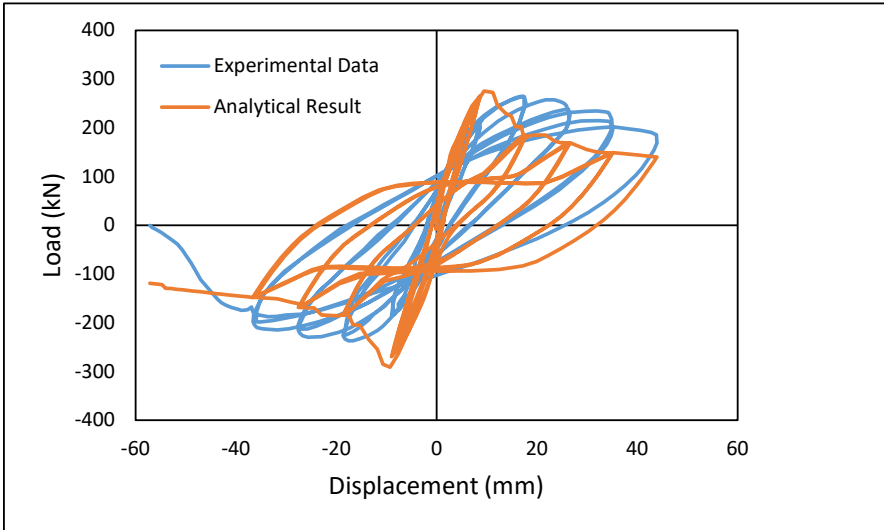


Figure 13. Kappos ve Konstantinidis Concrete – Ramberg Osgood Steel Model – M12

4. CONCLUSION

When we compared the material pairs used with the experimental sample, the M01 model gave the closest result to the experimental study. The M07, M12, M13 models are far from the result. Kappos and Konstantinidis converge with the concrete model Menegotto-Pinto. Among the Trilinear concrete models, it gives approximate results only with the Menegotto-Pinto steel model. Chang and mander moved away from the result with the concrete model Menegotto-Pinto. Therefore, the Mander concrete model and the Menegotto-Pinto steel model are the closest material models. However, considering that the Chang and Mander concrete model is not compatible with the Menegotto-Pinto steel model, it would be best to choose the material models we will use as pairs that are compatible with each other.

As a result, it is possible to obtain results close to the experimental results by coherent modeling of Seismo-Strcut models.

RESOURCES

Mander J.B., Priestley M.J.N., Park R. [1988] "Theoretical stress-strain model for confined concrete," *Journal of Structural Engineering*, Vol. 114, No. 8, pp. 1804-1826.

Menegotto M., Pinto P.E. [1973] "Method of analysis for cyclically loaded R.C. plane frames including changes in geometry and non-elastic behaviour of elements under combined normal force and bending," *Symposium on the Resistance and Ultimate Deformability of Structures*

Acted on by Well Defined Repeated Loads, International Association for Bridge and Structural Engineering, Zurich, Switzerland, pp. 15-22.

Ramberg W., Osgood W.R. [1943] *Description of Stress-Strain Curves by Three Parameters*, National Advisory Committee on Aeronautics, Technical Note 902.

Kent D.C., Park R. [1971] "Flexural members with confined concrete.", *Journal of the Structural Division, Proceedings of the American Society of Civil Engineers*, Vol. 97, Issue 7, pp. 1969-1990

Kappos A., Konstantinidis D. [1999] "Statistical analysis of confined high strength concrete," *Materials and Structures*, Vol. 32, pp. 734-748.

Soesianawati, M.T.; Park, R; and Priestley, M.J.N., "Limited Ductility Design of Reinforced Concrete Columns," Report 86-10, Department of Civil Engineering, University of Canterbury, Christchurch, New Zealand, March 1986, 208 pages.

A STUDY ON BEAM DISCONTINUITY AND RECESSED BALCONY

Halil Nohutcu^{1*}, Adem Solak², Taner Kılıç³

¹*Manisa Celal Bayar University, Şehit Prof. Dr. İlhan Varank Yerleşkesi 45140 - Yunusemre–Manisa–Türkiye, halil.nohutcu@cbu.edu.tr.*

²*Burdur Mehmet Akif Ersoy University, Architecture faculty/ Faculty of Engineering and Architecture, Türkiye, asolak@mehmetakif.edu.tr.*

³*Serbest Araştırmacı, Didim/AYDIN, Türkiye, tanerr_kilic@hotmail.com*

*Responsible author: *halil.nohutcu@cbu.edu.tr*

ABSTRACT

As an engineer, we create these structural elements in the most appropriate way to ensure adequate load and force transfer in the design of the carrier system. Depending on various factors, although we need to connect the end points of the beam elements to the columns and shear walls, we may ignore this situation and connect the beams together or go through without making beams. In this case, discontinuities and irregularities may occur in the load and force transfer in the structure. If there are frames that cannot provide continuity at a sufficient level, this transfer to columns and walls should be carried out by floors instead of beams. However, floors, due to their structural features, cannot perform this load transfer. Due to the magnitude of the horizontal forces, conditions such as buckling, and shrinkage occur in the floors.

Due to the discontinuity of the structural system, various rules have been introduced to the designers in order to prevent such discontinuities in various public codes. In this study, it was stated with some studies that beam discontinuities should be included in the Code, therefore it was discussed that various methods determined in other Codes could be used. It has been pointed out that various coefficients can be calculated for the classification of structures with beam discontinuities.

In this study, the reliability of the structural systems in line with these coefficients and the reactions occurring in the elements were investigated in accordance with the coefficients calculated depending on the beam discontinuity in the structures under consideration. It has been observed that the coefficients work proportionally with the

change of beam discontinuities in the structure. In addition to this approach, it has been shown by examining the shear forces in the columns that the effect of discontinuity can be reduced by adding shear walls to the structure.

As a result, it has been observed that due to the discontinuities of the beams in the structural system, much higher loads are placed on the columns and damage occurs as a result of these loads. It has been noted that these damages can be prevented by using shear walls.

KEYWORDS: Beams columns disconnections, Earthquake, Collapse.

1. INTRODUCTION

There are various reasons why columns are not connected with beams. Mostly, beams are not desired in building corridors and halls, due to architectural concerns, in order not to create a drooping appearance. In this case, a long flooring system is formed in the corridor running in one direction. Depending on the slab opening, slab vertical moments also take small values. Since the horizontal load effects are not taken into account in the slab static reinforced concrete calculations, the slab thickness can be calculated as a small value. However, slabs can form a unity plane with the beams and can transmit earthquake loads to the columns.

Disadvantages of not connecting columns with beams:

- Horizontal load (earthquake/wind) transfer becomes difficult.
- The floor cannot act rigidly enough, the distribution of the horizontal force on the columns and shear walls becomes uneven.
- Under the influence of horizontal force, the floor may buckling.
- Shrinkage effects become evident.
- Since it does not form a frame, the column is forced excessively.

Meral, E., within the scope of her study, investigated the effects of recessed balcony type sections in reinforced concrete buildings on the earthquake behavior of structures. He analyzed the structures with non-linear time history analysis method, classified them according to the type of irregularity, number of floors, and made analyzes and compared the parameters of the structures such as base shear force,

vertex displacements and maximum relative story drifts. As a result, it has been determined that the base shear forces are low and the displacement demands are higher in the beamless recessed balcony buildings compared to the other analyzed buildings.

In the study of Mert, N., Kasap, H. et al., the effect of beam discontinuities in structures on structural performance was investigated and earthquake behavior was investigated. Analyzes were made by considering the reference model without beam discontinuities and the model with different discontinuities. They compared the period, base shear, relative story drifts and A1 torsional irregularities of the structures.

Seven, S., and Keleşoğlu, Ö., in their study, investigated the effective relative storey drifts in structures with beam discontinuities and, accordingly, the second-order effects. They analyzed and compared buildings with different storeys according to different types of discontinuity and irregularity. In the light of the data obtained as a result of the study, they have seen that the effective relative storey drift and second order effects of the structures with beam discontinuity are high numerically and approach the limit values.

Due to the lack of space in terms of architecture, space is gained by constructing structures that come out as cantilevers outside the vertical bearing systems of the building, which are known as recessed balcony in our country and in almost all countries of the world. In building designs where all the effects of earthquakes are met with reinforced concrete frames with high ductility level, it is tried to transfer the horizontal earthquake loads by taking into account architectural concerns, with beams formed on the outer contour of the building, apart from the column axes. Can this design provide sufficient earthquake loads to be transmitted?

Is it possible to provide the transmission of earthquake loads with a fictitious beam that will remain in the floor in structures with recessed balcony?

In systems designed as non-beam slabs, can the horizontal earthquake loads be transferred with slabs in the sections with recessed balcony by connecting the columns to each other with beams?

What can be done to avoid this situation.

Columns should be connected to each other with beams and discontinuities in beam axles should be eliminated.

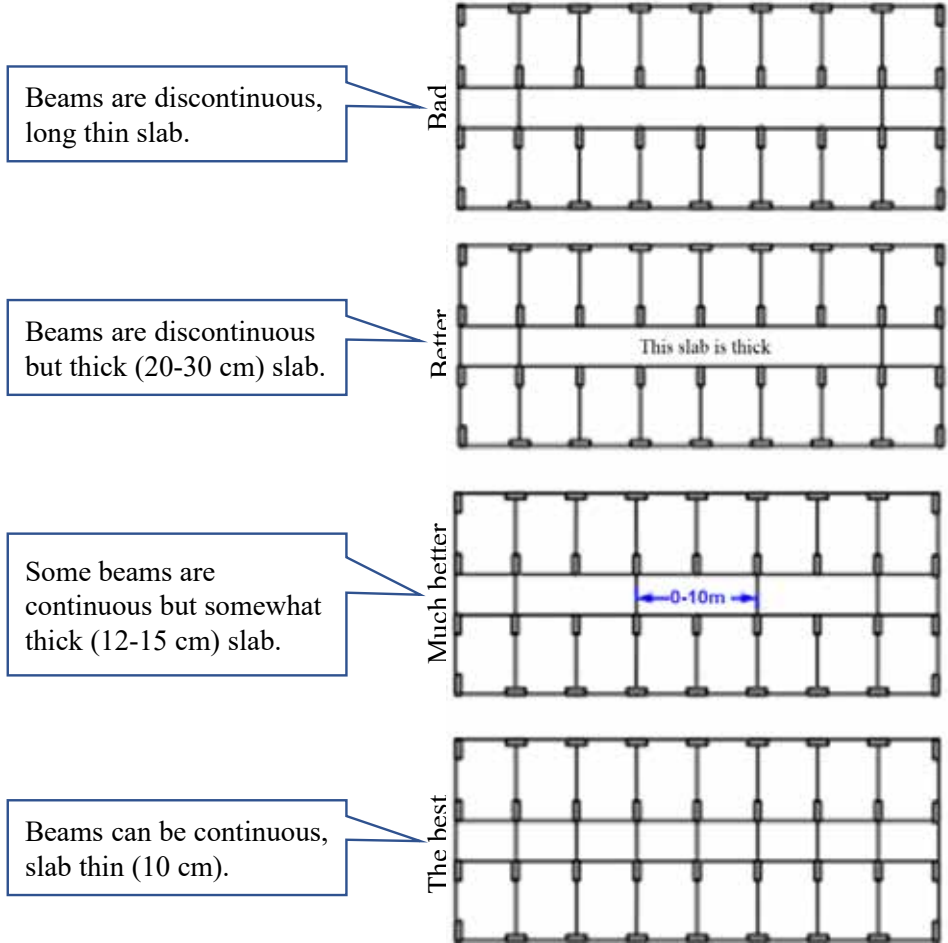


Figure 2. Continuity Recommendations in Beam [1]

Discontinuities in beams cause more strain on the columns. This causes more damage to the columns. As can be seen in Figure 2, the columns were heavily damaged due to discontinuities in the beams.



Figure 3. Columns damaged by the effect of discontinuous beams [1]

One of the factors that allows the discontinuities in the beams to be tolerated is the presence of sufficient amount of shear wall in the structure. When the studies on reinforced concrete shear walls are examined, it is recommended that the total building area should contain 1.5 per thousand of the wall [2], [3], [4]. Recommended *Shear Wall Ratios* in the Building as follows [2], [3], [4].

$$A_{\text{Shearwall}} \geq 0.0015nA_{\text{Building}} \left\{ \begin{array}{l} n: \text{Number of floors of the building} \\ A_{\text{Building}}: \text{The area of the building in the plan of a floor} \\ A_{\text{Shearwall}}: \text{The total area of the shear wall resisting a horizontal force in one direction} \end{array} \right.$$

$$\frac{A_{\text{Shearwall}}}{A_{\text{Building}}} \geq 0.008$$

There should be columns at the connection point of the beams. In this case, the cross-sectional effects of the beam are transferred to the columns in the shortest way. In the absence of columns at the connection point of the beams, stud beam irregularity occurs. One of the beams carries the other. Loads cannot be transferred directly to the beam, they are transferred from beam to beam. Which beam carries the other depends on beam stiffnesses, and is not always clear-cut. It is not always possible to prevent this disorder. When a column is placed at each beam-beam junction, very

close columns and beams with very small spans are formed. For this reason, some beams have to be studded. However, stud beams should be avoided as much as possible. The worst and worst thing to do is to get a studded beam into another beam.

Drawbacks and precaution:

- Beam load is transferred from beam to beam indirectly, not to columns in the shortest way.
- The reaction of the transported beam acts as a singular force on the carrying beam.
- Moment and shear force of bearing beam is high.
- Large deflection occurs in the carrying beam.
- Torsional moment occurs in the bearing beam.
- Obvious shear and tension cracks occur in the bearing beam.
- Transmission of horizontal force from column to column becomes difficult.
- The carried beam must be attached to the carrying beam with special precautions (suspended rods).
- Beam with studs should be wrapped with tight stirrups [1].

In Özmen's study, beam discontinuities were examined and the optimum discontinuity coefficient was proposed [5]. A circular of Kadıköy Municipality Directorate of Zoning Affairs, referring to the regulation, shows that beams should be made continuously.

In Bal and Özdemir's study, it was emphasized that beam discontinuities should also be considered within the scope of earthquake code. It is stated in the regulation that it is necessary to give a method that obliges the control of column-slab joints as well. It has been suggested that a similar application exists and can be implemented in ACI 350.

In Mustafa Erkan's study, an α beam discontinuity coefficient has been defined for beam discontinuities, and it has been found that structures with an alpha value greater than 70 percent are undamaged and this coefficient criterion used is appropriate.

Suggested equation

$$\alpha_{x(y)} = \frac{\text{Number of columns connected by beams}}{\text{Total number of columns}} \geq 0.70$$

It will be applied separately in both directions.

Figure 4. Recommended Alpha Beam Coefficient Calculation

Ozmen also determined 3 building types in his study. In the first two of these building types, values less than 70% were obtained. In Building Type 3, it achieved values greater than 70% and emphasized that the building was sufficient in terms of performance at values greater than 70%. He determined the earthquake shear force in the columns for building types 1, 2 and 3, and accordingly, it showed that the columns connected by beams received greater earthquake force. It has been shown that this causes problems with an α value of less than 70 percent. It is stated that the alpha coefficient criterion in the solved examples is a recommended reliable method.

2. EXAMPLE STUDY

Producing solutions to all kinds of problems is seen as a necessity of engineering in a way. Due to various reasons, discontinuities that occur during the structural system arrangements and which should be considered in general use should be well examined and calculations should be made carefully. With these calculations, it should be examined how acceptable the existing discontinuities are.

In the following case study, a building is studied as systems with different beam discontinuities. The reliability and usability of the alpha coefficient stated in the previous issues were evaluated.

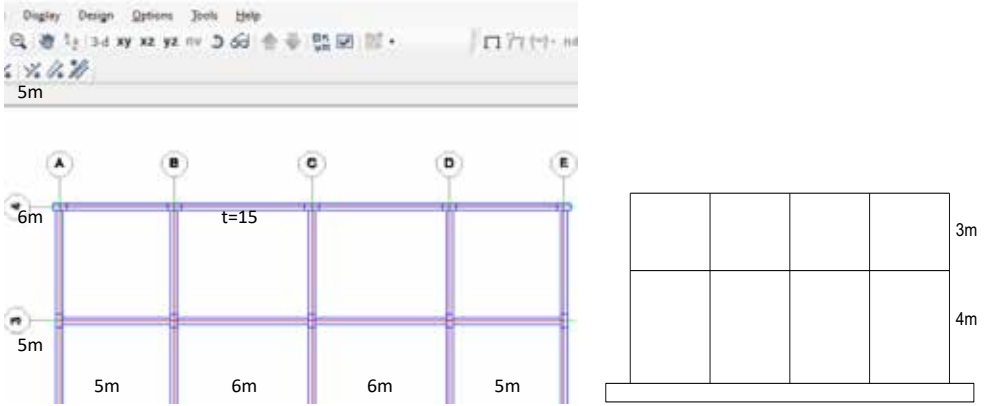
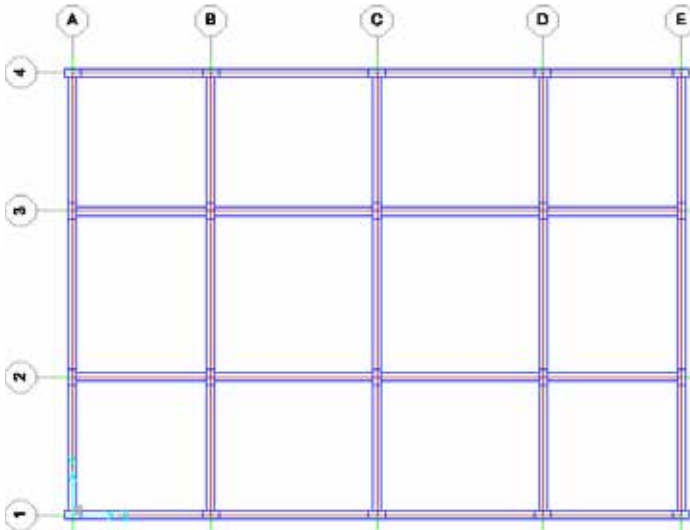


Figure 5. Example Construction Plan

All columns in the building are 30x60 cm, beams are 30x60 cm, the earthquake load reduction coefficient of the building is $R=8$ and it is a residential type building located in the 1st degree earthquake zone.

2.1. Continuous Beam Solution



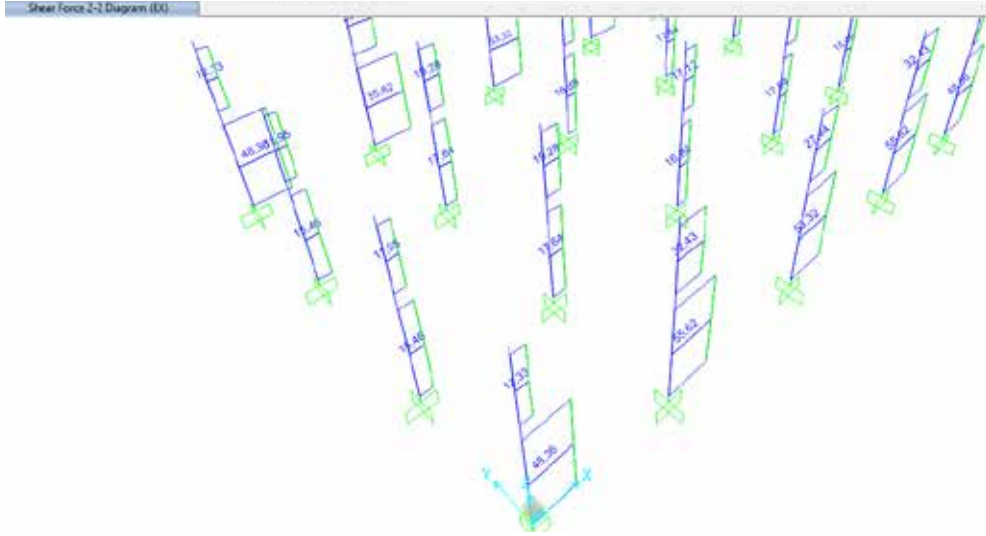


Figure 6. Continuous System Column Shear Forces

Earthquake analyzes were made in the structure whose carrier system plan is shown in **Hata! Başvuru kaynağı bulunamadı.** and the column shear forces shown in Figure 6 were obtained.

2.2. Discontinuous Beam Solution with Alpha 0.5

2 m cantilever beams were formed to create a discontinuity in the y direction. Here Alpha is 0.5 in the x direction. With the construction of stud beams, the shear force of the idle columns suddenly decreased and the other columns received the shear force. The columns of the 1st floor received more shear forces than the ground floor. Columns cannot carry such shear forces in the weak direction. It is seen that it is not safe to take a discontinuity coefficient below 70%.

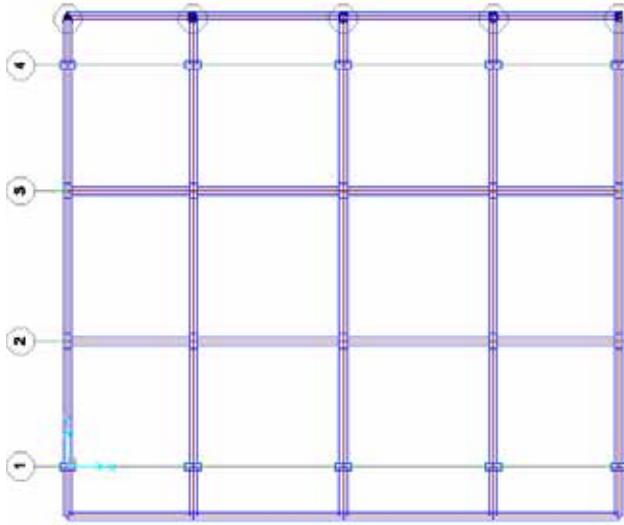


Figure 7. Floor Plan with Alpha Value of 0.5

When we create a discontinuity in the x direction, with an alpha of 0.5, the shear forces on the columns are as follows. When we compare the building with continuous beams and the building with Alpha 0.5, while the moment increases in the columns with discontinuity in the ground floor, the moment decreases in the first floor. At the same time, very large shear forces come to the y-direction middle columns on the first floor. These columns bear the shear forces of the discontinuous beam columns of the 1st floor. This creates an insecure structure.

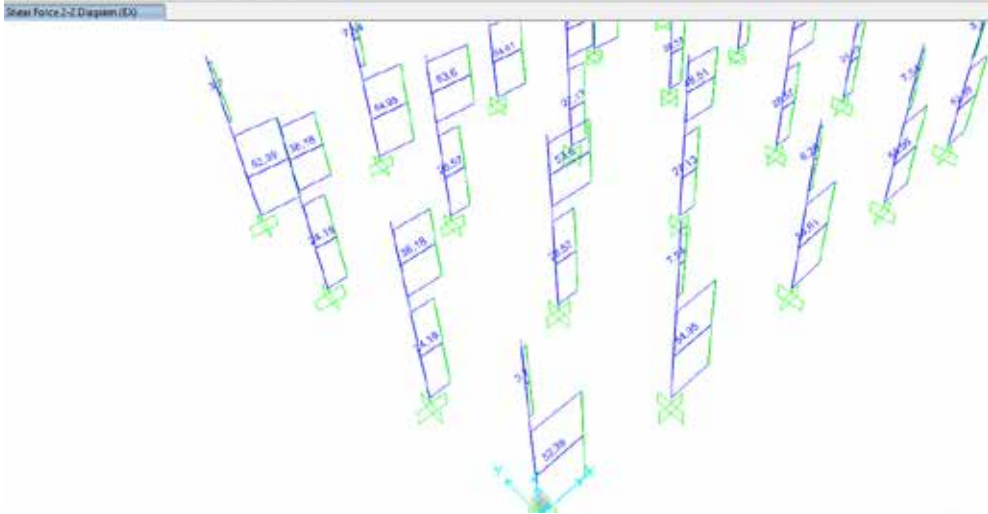


Figure 8. System Column Shear Forces with Alpha Value of 0.5

2.3. Discontinuous Beam Solution with Alpha 0.73

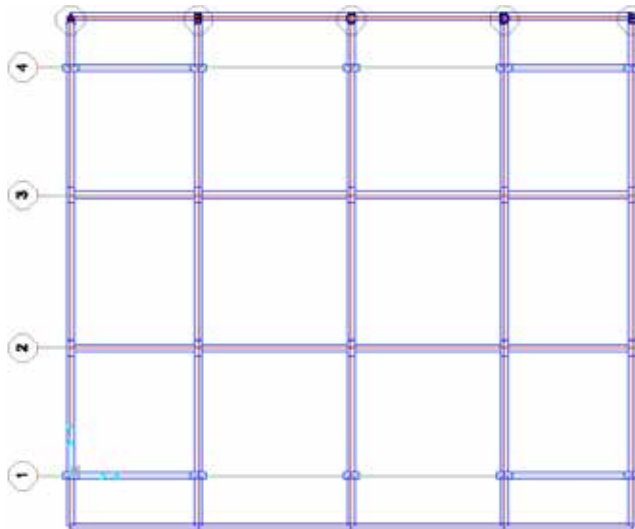


Figure 9. Floor Plan with Alpha Value of 0.73

2.4. Solution Implemented by Using Shear Walls in the Building

It has been observed that the shear force in the columns has decreased excessively with the use of shear wall at the building. This eliminates the disadvantage of discontinuous beams. The amount of shear wall used at the building;

$$A_{shearwall} = 3m^2 > 0.0015nA_{building} = 0.0015 \times 2 \times 22 \times 20 = 1.32m^2$$

$$\%A_{shearwall} = A_{shearwall}/A_{building}=3/(22*20)=0.007$$

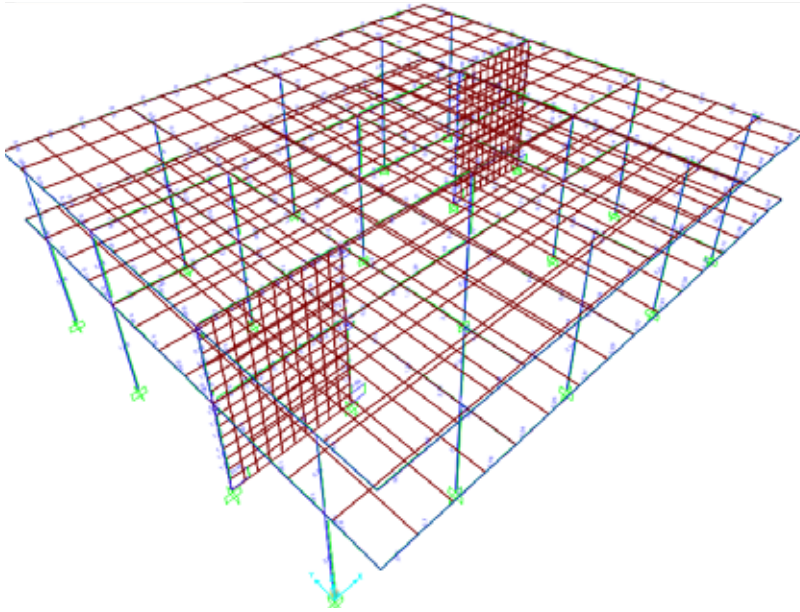


Figure 11. The shear forces formed in the structure by placing a shear wall have decreased excessively.

3. RESULTS

It has also been seen in recent earthquakes how dangerous designs that create discontinuity in building frames can be. In the investigations we made during the latest İzmir earthquake of 2020, it was observed that some of its structures collapsed due to the discontinuity created in the beams. In order to prevent this, although some relevant administrative units impose sanctions, it has been thought to determine this with structural analysis and to make suggestions. As a suggestion, it is suggested to keep the discontinuity level at a minimum or to apply a shear wall and solutions in this regard are shown.

In this study, first the beams were modeled to form a continuous frame and the structures were examined under earthquake forces. Then the discontinuous beam system was created. It was observed how much the column shear forces increased on the ground floors and a very large amount of fall occurred on the 1st floor, with a 50% alpha value at the beam discontinuity, with a 2 meter recessed balcony. When the alpha value was increased to 70%, it was observed that there was a great decrease in the column shear forces with discontinuity. When the alpha value was increased to 73%, the growing shear forces of the middle columns decreased and became safe. In our study, it has been determined that an Alpha value of over 70 percent will not cause a disadvantage in beam discontinuity in our structures, and discontinuities below seventy percent may cause problems in our structures. The first suggestion of importance is to minimize the effect of discontinuity as a result of using shear wall in buildings. Secondly, the amount of discontinuous frame beams should be minimized and the alpha value should be greater than 70 percent.

RESOURCES

- [1]. Topçu, A., “Dün-Bugün. İyi-Kötü. Doğrular-Yanlışlar-Hasarlar”, http://www.imo.org.tr/resimler/dosya_ekler/5e70853596044de_ek.pdf?tipi=79&turu=X&sube=7
- [2]. Ersoy, U., “13 Mart 1992 Erzincan Depremi Mühendislik Raporu”, İMO, Ankara 1992.

- [3]. Atımtay, E., “Açıklamalar ve Örneklerle Afet Bölgelerinde Yapılacak Yapılar Hakkında Yönetmelik”, Ankara, 2000. (Turkish)
- [4]. Gülkan, P., Deniz, U., “Okul Binalarının güvenliği için Minimum dizayn kriterleri”, Turkey Engineering News, 425, s.13-22, Ankara, 2003. (Turkish)
- [5]. Özmen, G., “Çok Katlı Yapılarda Yatay ve Düşey Düzensizlikler”, http://imoistanbul.org/imoarsiv/seminer2010-not/gunay_ozmen.pdf. (Turkish)
- [6]. Bal, İ.B., Özdemir, Z., “Çevre Çerçeve Kirişi Süreksizliğinin Yapı Deprem Davranışı Üzerindeki Etkileri, IMO Istanbul Bulletin, Issue 87, 2006. (Turkish)
- [7]. Özmen, G., “Çok katlı yapılarda yatay süreksizlikler” IMO Istanbul Bulletin, Issue 119, 2012. (Turkish)
- [8]. Meral, E., “Kapalı Çıkmalı Betonarme Binaların Deprem Davranışının Değerlendirilmesi” Fırat University Journal of Engineering Science, 2019, 31(2), 309-318. (Turkish)
- [9]. Mert, N., Kasap, H., Özyurt, M.Z., Khurram, M.K., “Betonarme Yapılarda Kiriş Süreksizliğinin Yapısal Performansa Etkisi” 2018, 2ND International Symposium on Natural Hazards and Disaster Management. (Turkish)
- [10]. Seven, S., Keleşoğlu, Ö., “Betonarme Perde Çerçeveli Yapılardaki Kiriş Süreksizliğinin Etkin Görelî Kat Ötelemeleri ve İkinci Mertebe Etkileri Bakımından İrdelenmesi” 2018, Mus Alparslan University Journal of Science, 6(2) 571-580. (Turkish)
- [11]. Kasap, H., Başkaya, E., Başar, İ., Mert, N., “Bina Taşıyıcı Sistemlerinde Çerçeve Düzensizliklerinin Yatay Ötelemeye Etkisi” 2017, 5th International Symposium on Innovative Technologies in Engineering and Science. (Turkish)

INVESTIGATION OF SOCIAL AWARENESS AND AWARENESS REGARDING THE CONCEPT OF RISKY BUILDING IN THE CONTEXT OF THE POTENTIAL ISTANBUL EARTHQUAKE

Yunus ORHAN^{1*}, İsmail Cengiz YILMAZ²

¹*Istanbul Arel University, Turkey. y.orhan1903@hotmail.com,*

² *Assoc. Prof. Dr., Istanbul Arel University, Turkey, Istanbul, cengizyilmaz@arel.edu.tr.*

*Responsible author: *y.orhan1903@hotmail.com*

ABSTRACT

The unconsciousness of the use of risky buildings, combined with the earthquake, caused loss of life and property. Efforts to minimize these causes and to make the public sufficiently conscious about this issue should be supported by education. In this study, a survey was conducted with 429 people residing in Istanbul. It is aimed to develop social awareness and consciousness level for a possible Istanbul earthquake and to develop solutions for these questions. SPSS 22 analysis program was used to obtain the data in the survey study conducted for this purpose. As a result of the study, it was seen that this awareness and consciousness were not at a sufficient level.

KEYWORDS : Risky structure, earthquake, earthquake awareness.

1. IMPORTANCE AND AIM OF THE RESEARCH

In this study, it is aimed to reveal the concept of risky building and public awareness about the earthquake phenomenon. In this context, a survey study was conducted to examine the participants' knowledge of the legislation and the adequacy of using information technology related to earthquakes. It is aimed to give direction to the survey questions under three main headings as earthquake preparedness awareness, risky building concept and information technology usage awareness. According to the results of the answers given by the participants, discussions were made and various solution suggestions were made.

2. METHOD OF THE RESEARCH

In the study, face-to-face survey technique, which is a method of obtaining information directly from human resources, was used and the survey form was designed as a single section and 25 questions. The scale used was designed as a 5-point Likert type (1=Very Insignificant and 5=Very Important).

3. MODEL and HYPOTHESIS OF THE RESEARCH

Quantitative studies are studies that allow statistical conclusions to be drawn, numerical interpretation and generalization. The survey method is the most used method in primary data collection. It is a research method that is done by directing the question paper designed to get the opinions of the respondents about a problem to be researched. It is the best method for collecting data on people's views/perceptions. In this framework, the hypotheses developed and considered suitable for the purpose of the research are presented in Table 1;

Table 1. Research Hypothesis

H₁: The views of tenants and property owners differ according to their gender.
H₂: The opinions of the tenants and property owners differ according to their age.
H₃: The opinions of the tenants and property owners differ according to their education level.
H₄: Opinions of tenants and property owners differ according to different duration of residence.
H₅: Opinions about the risk status of property differ according to demographics.
H₆: The level of knowledge about Risky Building Detection of the Ministry of Environment and Urbanization in e-government varies according to demographic characteristics.
H₇: Risky buildings legislation The information status about the "registered buildings" legislation, which is determined as "risky construction" within the scope of the law numbered 6306, differs according to demographic characteristics.
H₈: Consciousness about the demolition legislation after the risky structure determination of the property differs according to the demographic characteristics.

H₉: In case the projects are not delivered within the maximum period determined by the legislation, the awareness of the citizens about the sanctions differs according to the demographic characteristics.
H₁₀: Knowledge and adequacy of risky buildings on municipal zoning laws differ according to demographic characteristics.
H₁₁: The level of awareness about your entitlement in valuation and application varies according to demographic characteristics.
H₁₂: The state of awareness about the desire to demolish and build your structure at twice the cost instead of strengthening it differs according to demographic characteristics.
H₁₃: The state of awareness about the previous use of the questioning of the emergency assembly area from the state, where you live, differs according to demographic characteristics.
H₁₄: The state of awareness about the suitability and adequacy of the emergency assembly area for your location varies according to demographic characteristics.
H₁₅: Awareness of the emergency assembly area in case of a possible disaster differs according to demographic characteristics.
H₁₆: The level of awareness about the awareness of the earthquake hazard map of Turkey in the e-government system differs according to demographic characteristics.
H₁₇: The awareness of the earthquake hazard of the region you live in varies according to demographic characteristics.
H₁₈: The level of awareness about the existence of an earthquake bag, despite a possible earthquake hazard, differs according to demographic characteristics.
H₁₉: The level of awareness about the location of the earthquake kit and the importance of keeping it in a place that can be taken for emergency exits varies according to demographic characteristics.
H₂₀: The state of consciousness about the awareness of what should be in the earthquake kit differs according to demographic characteristics.
H₂₁: Awareness of the amount to be received from Earthquake Insurance in the event of a possible disaster differs according to demographic characteristics.
H₂₂: The awareness of the ground class of the place you live in varies according to demographic characteristics.
H₂₃: The state of awareness about how old and in what year your building was built differs according to demographic characteristics.
H₂₄: The state of awareness about looking at the ground survey and earthquake map while purchasing a property differs according to demographic characteristics.
H₂₅: The state of awareness about attending any training seminar on risky structures differs according to demographic characteristics.

H₂₆: The state of awareness about attending any earthquake-related training seminar differs according to demographic characteristics.
H₂₇: The state of consciousness about the thought that your building will be damaged after an earthquake varies according to demographic characteristics.
H₂₈: The state of awareness about the analysis studies of the "detection principles of risky structures" of reinforced concrete structures determined by rapid observation techniques differs according to demographic characteristics.
H₂₉: The results of the performance analysis or if there was a crack or breakage that you can see, the awareness about the desire to move varies according to the demographic characteristics.
H₃₀: The opinions of the tenants and property owners differ according to their different working status and the level of awareness about demographic characteristics.
H₃₁: The opinions of tenants and property owners differ according to different years of residence, and the level of awareness about them differs according to demographic characteristics.

4. UNIVERSE and SAMPLE

Making estimations for the whole population from the results obtained by examining a part of the whole population is called sampling. According to Şimşek (2012), he explains this situation quite clearly with the example of the pool and the sea. While a glass of water taken from a small pool has the ability to represent all the water in the pool that makes up the universe, a glass of water to be taken from the sea will not be able to represent the whole sea, which is the universe, since it can show different characteristics such as color, pollution, density and clarity in different regions. Then, depending on the size of the universe, it will be necessary to increase the size of the samples, and to create more samples with more water taken from different regions, not with a glass of water. As the sample size increases, the sample distribution approaches normal. This is also called the "central limit theorem (Şimşek, 2012).

5. LITERATURE REVIEW

Ozcan (2019) emphasized that risky structures should be identified in order to minimize the loss of life and property caused by earthquakes and earthquakes in Turkey. For this purpose, within the scope of the Law on the Transformation of Areas Under Disaster Risk, enacted by the Ministry of Environment and Urbanization, General Directorate of Infrastructure and Urban Transformation Services, the risk detection rates of the buildings in the existing building stock were determined and a risk assessment was made by looking at these determined rates. As a result of the determinations made, it was decided to strengthen the existing structures by looking at the risk ratio values or to demolish them and apply new projects in their place. Mustafa (2016), from selected buildings to critical buildings, were strengthened and inspected according to the regulation 2007 (DBYBHY2007) on buildings to be built in earthquake zones using the sta4cad program. Halil (2018) evaluated the regulations and conflicts regarding the detection and demolition of the risky building and the process of making a decision about the risky building, and by making use of the studies on this issue, solutions were offered to the problems encountered in practice. Kazım (2015) evaluated the existing buildings with the FEMA 154 method without making a static calculation using the visual inspection technique. Ertuğrul (2018), Risky Building Detection Principles (RBTE), which came into force in 2013 and made the risky building transformation process faster and more practical, were examined. Yakup (2018), reconstruction costs of selected risky structures, quantity lists, work items, specification of the work to be done; It has been prepared within the scope of architectural, construction, mechanical and electrical projects. Gökhan (2015), on the other hand, left the consumer's awareness in a durable structure at a superficial level and almost completely ignored. In this article, opinions and suggestions have been made on how to create a more conscious consumer mass, how to improve the concept of earthquake resistant buildings with needed new structures, and how to establish the concept of trust. Halil Burak (2018) evaluated the regulations and conflicts regarding the detection and demolition of the risky building and the process of making a decision about the risky building, and by making use of the studies on this issue, solutions were offered to the problems encountered in practice. Hamide Tekeli (2003), the cost of the housing type reinforced concrete building carrier system; The changes depending on the number of floors, earthquake zone and local soil classes were examined. A two-flat residential reinforced concrete building; Four, six and eight layers were modeled and

solved with the help of Probing Orion 2000 analysis program. In the study of Demirci and Yıldırım (2015), a questionnaire was prepared to measure the knowledge, attitudes and behaviors of students about earthquakes, and the questionnaire was applied to 836 11th and 12th grade students in 11 high schools located in four different districts of Istanbul.

Menassa (2011) presents a quantitative approach to assessing the value of investment in sustainable improvements for existing buildings, taking into account different uncertainties regarding life-cycle costs and the perceived benefits of the investment.

6. ANALYSIS OF RESEARCH DATA

The data obtained from the people in Buyukcekmece district of Istanbul province were analyzed using the SPSS 22 statistical package program. In order for the data obtained in quantitative studies to be accepted as scientifically correct or to be credible, reliability was measured with Cronbach's Alpha in the SPSS 22 program.

Table 2. Findings Regarding Reliability Analysis

Scales	Number of questions	Coefficient of Confidence(α)
Legislation and Technical Subject Awareness	12	0,834
Information Technology Use Sufficiency	3	0,723
A Potential Earthquake Preparedness Awareness	10	0,788

According to the reliability analysis results in Table 2; The answers of the people of Istanbul, who constitute the research sample, about the awareness of the legislation and technical subject awareness ($\alpha = 0.834$), the adequacy of information technology use ($\alpha = 0.723$), and the awareness of preparedness for a possible earthquake ($\alpha = 0.788$), are acceptable at a reliable level. according to Cronbach's Alpha.

In this context, it should be checked whether the data are equal and show a normal distribution. It is stated that if the P values are greater than 0.05 in the said tests, there is no significant difference as a result of the comparison. Therefore, if P values are found to be $P < 0.05$ in the analysis, it means that there is a significant difference as a result of the comparison.

The demographic characteristics of the analysis and the level of participation in the statements in the scale were determined. In the evaluation of the expressions in the scale; Value ranges of “absolutely no for 1.00-1.80, no for 1.81-2.60, partially yes for 2.61-3.40, yes for 3.41-4.20 and absolutely yes for 4.21- 5.00” were taken into account.

The t-Test (independent sample t-test) was used to determine whether there was a significant difference between two independent groups, and the One-Way ANOVA test was used to determine the significant difference between more than two independent variables.

7. FINDINGS OF THE RESEARCH

7.1. Findings Regarding Descriptive Information

Within the framework of identifying information; Data on gender, age, education and employment status, residence time and property status of people residing in Istanbul and participating in the research were examined (Table 3).

Table 3. Findings Regarding Descriptive Information

Gender	n	%	Educational Status	n	%
Male	241	56	Secondary education	32	8
Woman	188	44	High school	128	29
Age	n	%	Bachelor	256	59
18-34	176	41	Graduate	13	4
35-49	182	42	Working Status	n	%
50-64	58	14	Working	288	67
65 and Above	13	3	Not working	125	29
Year of Residence in the Residence	n	%	Retired	16	4
Less than 1 year	22	5	Ownership of the Residence	n	%
1-2 Year	90	21	Rent	173	40
3-4 Year	118	28	Property owner	256	60
4 Years and Above	199	46	TOTAL	429	100

56% of the respondents were male and 44% were female. Among female and male participants, 8% are secondary school graduates, 29% high school graduates, 59% undergraduate and 4% postgraduate degrees. It is seen that 4% of the participants are retired, 29% are not working and 67% are working. 5% of the participants have been residing for less than 1 year, 21% for less than 2 years, and 74% for more than 3 years in their current situation. In terms of residential property, 60% of the participants declared that they stayed on their own property and 40% as tenants. 41% of the participants are 18-34 years old, 42% are 35-49 years old, 14% are 50-64 years old, 3% are 65 and over.

In this part of the research, the questions asked to the participants in their basic views on "Examination of Social Consciousness Regarding the Concept of Risky Building in the Context of a Possible Istanbul Earthquake" were divided into three separate scales, and these scales were respectively "Legislation and technical subject awareness, Information Technology Usage Adequacy and Preparedness for a Possible Earthquake". The average of the answers given by the participants to the survey questions according to the "Consciousness" was examined. In this context, the level of participation of the participants in the views on the legislation and technical subject awareness is presented in Table 4.

Table 4. Findings Regarding Legislation and Technical Subject Awareness

Question s		Definitely No	No	Partially	Yes	Definitely yes	Total	\bar{x}	S.D
		n							
S1	n	0	203	142	76	8	429	2,541	0,812
	%	0	47,3	33,1	17,7	1,9	100		
S2	n	1	309	93	26	0	429	2,336	0,591
	%	0,2	72	21,7	6,1	0	100		
S3	n	145	217	47	5	15	429	1,900	0,895
	%	33,8	50,6	11	1,2	3,5	100		

S4	n	158	182	70	6	13	429	1,914	0,925
	%	36,8	42,4	16,3	1,4	3	100		
S5	n	125	203	72	22	7	429	2,028	0,901
	%	29,1	47,3	16,8	5,1	1,6	100		
S6	n	104	208	94	16	7	429	2,1	0,866
	%	24,2	48,5	21,9	3,7	1,6	100		
S7	n	111	167	109	41	1	429	2,193	0,939
	%	25,9	38,9	25,4	9,6	0,2	100		
S8	n	14	191	126	97	1	429	2,720	0,857
	%	3,3	44,5	29,4	22,6	0,2	100		
S9	n	0	388	15	26	0	429	2,156	0,504
	%	0	90,4	3,5	6,1	0	100		
S10	n	1	364	43	16	5	429	2,207	0,561
	%	0,3	84,8	10	3,7	1,2	100		
S11	n	0	3	125	104	197	429	4,154	0,87
	%	0	0,7	29,1	24,3	45,9	100		
S12	n	153	204	58	13	1	429	1,846	0,782
	%	35,7	47,6	13,5	3	0,2	100		
S1. Do you have information about the risk status of your property?									

S2. Risky buildings legislation Do you have any information about the "registered buildings" legislation, which is determined as "risky buildings" within the scope of the law numbered 6306?
S3. Do you have any information about the demolition legislation after the risky structure determination of your property?
S4. Do you have any information about the sanctions of the citizens if the projects are not delivered within the maximum period determined by the legislation?
S5. Do you have any information about the knowledge and adequacy of risky buildings on municipal zoning laws?
S6. How much do you know about your entitlement in the field of valuation and enforcement?
S7. Do you know the soil class where you live?
S8. Do you know how old your building is and in what year it was built?
S9. Have you attended any training seminars on risky structures?
S10. Do you have any information about the "detection principles of risky structures" regulation and analysis studies of reinforced concrete structures determined by rapid observation techniques?
S11. Would you want to move if there was a crack or breakage that you can see with the results of the performance analysis?
S12. If your building was an old one, how many times the cost of reinforcement would you demolish and build?

The averages of the answers given to the questions about the adequacy of using information technology are given in Table 5.

Table 5. Findings Regarding Awareness of Information Technology Use Adequacy

Questions		Definitely No	No	Partially	Yes	Definitely Yes	Total	\bar{x}	S.D
S13	n	0	365	6	58	0	429	2,284	0,689
	%	0	85,1	1,4	13,5	0	100		
S14	n	3	254	27	145	0	429	2,732	0,943
	%	0,7	59,2	6,3	33,8	0	100		
S15	n	121	206	84	15	3	429	2,005	0,826
	%	28,2	48	19,6	3,5	0,7	100		
S13. Do you have any information about risky structure detection in e-government?									
S14. Have you used the e-government emergency assembly area questioning of where you live before?									
S15. Do you know the earthquake hazard map of Turkey in the e-state system?									

The averages of the answers given to the questions regarding the awareness of preparedness for a possible earthquake are given in Table 6.

Table 6. Findings Regarding the Awareness of Preparedness for a Possible Earthquake

Questions		Definitely No	No	Partially	Yes	Definitely yes	Total	\bar{x}	S.D
S16	n	156	26	231	6	10	429	2,273	1,047
	%	36,4	6,1	53,8	1,4	2,3	100		
S17	n	5	334	16	69	5	429	2,382	0,808
	%	1,1	77,9	3,7	16,1	1,2	100		
S18	n	109	175	108	29	8	429	2,189	0,954
	%	25,4	40,8	25,2	6,7	1,9	100		
S19	n	3	196	32	165	33	429	3,069	1,084
	%	0,7	45,7	7,4	38,5	7,7	100		
S20	n	11	86	82	63	187	429	3,768	1,269
	%	2,6	20	19,1	14,7	43,6	100		
S21	n	2	90	29	302	6	429	3,513	0,853
	%	0,5	21	6,7	70,4	1,4	100		
S22	n	14	317	54	42	2	429	2,303	0,708
	%	3,2	73,9	12,6	9,8	0,5	100		
S23	n	0	220	173	36	0	429	2,571	

	%	0	51,3	40,3	8,4	0	100		0,64 3
S24	n	0	387	19	23	0	429	2,152	0,48 7
	%	0	90,2	4,4	5,4	0	100		
S25	n	1	130	249	49	0	429	2,807	0,62 5
	%	0,2	30,3	58,1	11,4	0	100		
S16. What do you think about the suitability and adequacy of the emergency assembly area for your location?									
S17. Do you know the emergency assembly area in case of a possible disaster?									
S18. Do you know the earthquake risk of the area you live in?									
S19. Do you have an earthquake bag in case of a possible earthquake?									
S20. Do you care that the earthquake bag is in a place where it can be taken for emergency exits?									
S21. Do you know what should be in the earthquake bag?									
S22. Do you know the amount of support you will receive from earthquake insurance in the event of a disaster?									
S23. Do you look at the ground survey and earthquake map when purchasing a property?									
S24. Have you received any training seminars on earthquakes?									
S25. Do you think your building will be damaged after the earthquake?									

8. CONCLUSION AND RECOMMENDATIONS

In the examination, which was conducted by dividing the questions asked to the participants into 3 separate scales, the averages of the answers given by the participants to the survey questions were examined according to "Legislation and technical subject awareness,

Information Technology Usage Sufficiency and Awareness of Preparedness for a Possible Earthquake", respectively.

1. There are 12 questions in the Questionnaire on Findings Regarding Legislation and Technical Subject Awareness. It is seen that the participants did not take into account the risk situation in the structure, which is related to the risky structures, legislation and technical issues. Therefore, it has been determined that the participants do not have sufficient awareness about the risky structures legislation, demolition legislation, risky building determination legislation.
2. Comparison of Information Technology Usage Adequacy by Demographic Characteristics; There are 3 questions in the questionnaire and the result of the answer given to them is that it is not at a sufficient level. Considering the results of the participants' opinions about the adequacy of information technology use, it can be said that the risky structure detection in the e-state extension, the citizen's not using the e-state extension, and the questioning of the emergency assembly area in case of a possible risk in the e-state extension are partially used by the citizens and they are not conscious enough about the earthquake hazard map.
3. Comparison of Possible Earthquake Awareness by Demographic Characteristics; There are 10 questions in the questionnaire and the result of the answer given to them is that it is not at a sufficient level. It has been revealed that the suitability of the emergency assembly areas of the participants in the research is not sufficient according to their location, and that the emergency assembly areas are not known by the participants in case of a possible disaster. In this study, it is seen that the awareness of the citizens of the region they live in is insufficient despite the earthquake hazard, and as this danger results in destruction, they should know the earthquake insurance support cost, but they do not have enough awareness.

In this study, it was seen that the answers of the participants in the studies conducted in Istanbul, where the risk status evaluated as 1st degree is high, were mostly due to lack of awareness and the degree of caring for the risk situation was low. As a suggestion, it is necessary to organize training seminars on these subjects in schools, starting from the young age of the citizen, and to provide training not only to students but also to parents. In order to increase awareness about legislation and technical issues, the use of technological structure and a possible earthquake, public institutions, social organizations and ministries should arrange advertisements on televisions related to earthquake bags and what should be in earthquake bags. It is necessary for the muhtars to inform the people living in the area they are responsible for, and in case of a possible risk, the citizens of the parks and assembly areas, which are the gathering areas, by text message to the phones. It is expected that this study can be carried out in other cities of Turkey and new researches will be paved by developing different scales.

REFERENCES

Şimşek, A. (2012). Evren ve örneklem. A. Şimşek. (Ed.). Sosyal bilimlerde araştırma yöntemleri (sayfa. 108-133). Eskişehir: Anadolu Üniversitesi AÖF yayınları.

Özcan Kınaş, 2019; Riskli yapılar ve kentsel dönüşüm çalışmaları, Tunceli örneği, T.C. Süleyman Demirel Üniversitesi Fen Bilimleri Enstitüsü

Mustafa Olbak 2016; Kentsel Dönüşümün Deneysel Verileri Işığında Doğrusal Olmayan Analiz Yöntemleri ile Riskli Yapıların Yeniden Kullanılabilirliği ve Yararları, T.C. İstanbul Aydın Üniversitesi Fen Bilimleri Enstitüsü 142

Halil Burak Çakır 2018; Kentsel Dönüşüm Kapsamında Riskli Yapıların Yıkılması ve Yeniden Değerlendirilmesi Sürecinde Meydana Gelen Uyuşmazlıklar, T.C. İstanbul Ticaret Üniversitesi Sosyal Bilimler Enstitüsü Özel Hukuk Yüksek Lisans Programı

Kazım Yeşilkaya 2015; Hızlı Gözlem Teknikleri ile Belirlenmiş Betonarme Yapıların “Riskli Yapıların Tespit Esasları 2013” Yönetmeliği ile Analizi, T.C. On dokuz Mayıs Üniversitesi Fen Bilimleri Enstitüsü

Ertuğrul Ekinci 2018; Türkiye’de Riskli Yapı Stokuna Yönelik Kentsel Dönüşüm Çalışmaları ve Maliyet Analizi: Bir Vaka Çalışması, Gazi Üniversitesi Fen Bilimleri Enstitüsü

Yakup Timur Demirel 2018; Kentsel Dönüşümde Riskli Yapı Bileşenlerinin Yapı Değerlemesine Etkisi, TC Ondokuz Mayıs Üniversitesi Fen Bilimleri Enstitüsü

Gökhan Tunç 2015; Depreme Dayanıklı Bina, Bilinçli Tüketici Ve Güven Kavramları Üzerine İnceleme Ve Öneriler, 3. Türkiye Deprem Mühendisliği ve Sismoloji Konferansı

Halil Burak 2018; Kentsel Dönüşüm Kapsamında Riskli Yapıların Yıkılması ve Yeniden Değerlendirilmesi Sürecinde Meydana Gelen Uyuşmazlıklar.

Hamide Tekeli 2003; Isparta Deprem Bölgesi ve Yerel Zemin Sınıflarının Bina Maliyetine Etkileri.

Demirci ve Yıldırım 2015; İstanbul’da Orta Öğretim Öğrencilerinin Deprem Bilincinin Değerlendirilmesi Ali Demirci- Salih Yıldırım 2015 Meb Yayını Süreli Yayınlar Eğitim ve Sosyal Bilimler Dergisi Milli Eğitim/207/Yaz/2015.

Menassa Carol C. 2011; Evaluating sustainable retrofits in existing buildings under uncertainty, Energy and Buildings

THE EFFECT OF LABOR CHARACTERISTICS ON WORKER TRAINING IN THE CONSTRUCTION SECTOR

Melek Ceylan¹, Sinan Cansız²

¹*Istanbul Aydin University, Quality Management, melekceylan@aydin.edu.tr*

²*Istanbul Aydin University, Civil Engineering, sinancansiz@aydin.edu.tr*

*Responsible author: *melekceylan@aydin.edu.tr*

ABSTRACT

The Vocational Qualification Authority, which was established as an institution that inspects exams in technical and professional fields by accepting national and international standards as a reference, acts as a control mechanism in vocational exams. Vocational exams are held under the control of the Vocational Qualifications Authority within the framework of national qualifications in many fields in our country. Vocational Qualifications Certificate is required as a prerequisite for recruitment, especially since the construction sector is a risky area in terms of occupational safety and health. These exams are held in two stages: theoretical and performance. Personal characteristics come to the fore in the success of the candidates who take the exams. Within the scope of this study, the parameters that have an impact on the success graphics of the candidates who are examined in the construction sector are examined.

KEYWORDS: Vocational Qualification Authority, Graduate Conditions, Candidate Profiles.

1. INTRODUCTION

The employee working in the construction sector are generally unskilled. In countries with rapidly developing economies due to socio-economic conditions. In addition, according to studies, occupational accidents are deadlier and more numerous in developing and non-developing countries. Most of the occupational accidents has occurred in the construction industry in Turkey. Due to the nature of

the construction sector, it stands out as the sector that is frequently audited in our country due to the dispersed working environment, heavy labor requirement, dangerous machines working together with the workers, and the presence of a dangerous environment. The distribution of fatal occupational accidents in Turkey by sectors is presented in Table 1.

Table 1. Distribution of occupational accidents by sectors

Year	Construction	Agriculture/Forest	Logistics	Mine
2013	%24	%16	%11	%7
2014	%23	%17	%7	%21
2015	%25	%23	%14	%4
2016	%22	%20	%13	%4
2017	%23	%19	%13	%5
2018	%23	%24	%12	%3
2019	%24	%13	%14	%3

When Table 1 is examined, the construction sector is constantly at the forefront in the rate of fatal occupational accidents in Turkey by years. In this context, the construction sector is considered to be the riskiest area in the occupational health inspections in Turkey. The Vocational Qualifications Authority, which was established with the law passed in 2006, is responsible for measuring and supervising the professional levels of employees in Turkey.

With the certification activity started in 2009, it has reached 2 million documents by 2022. Among the documents given, the rate of employees working in very dangerous and dangerous areas is at the level of 95%. Since VQA certification is mandatory in risky areas for work in Turkey, certification activities are mostly concentrated in risky areas. According to TUIK data, there are approximately 2 million direct employees in the construction sector, which is one of the riskiest and most intense areas of work in the manufacturing sector. According to the data obtained from the certification companies in the sector, the certificate rate of the employees in the construction sector could not reach the desired level and it seems difficult to reach

this figure with the current number of certification companies and employees. According to the data received from the certification bodies, it is seen that approximately 400,000 certifications have been made in the construction sector in Turkey. Approximately 15% of the employees in the construction sector, which is one of the riskiest sectors, work by obtaining a VQA certificate.

Being a risky area, studies have been carried out by many researchers to prevent occupational accidents (Kale and Yanık 2018, Temel et al. 2013, Yanık 2017, Çolak et al. 2004, Bayram 2018, İpek and Döger 2017, Canbey 2019). Akboğa and Baradan, one of the previous studies, evaluated fatal occupational accidents in İzmir and found that primary school graduates (66%) were exposed to the highest death rates. It has stated that the lowest rate is among the personnel who received VQA (2%). In addition, while the mortality rate is 15% in certified candidates, this rate has determined as 70% in non-certified candidates.

An employee who has been certified in accordance with the VQA law must renew her certificate after an average of 5 years in the construction industry. Due to the number of certification firms accredited by VQA, labor force and workload, the surveillance of the candidates whose certificate surveillance period has come, and the certificate renewal requests of the candidates whose certificate period has expired may cause disruption in the system. When VQA's working structure is examined, there is a similar validity period and similar surveillance number for all candidates. When similar applications in the world are examined, it is seen that very successful candidates and limited successful candidates do not have the same validity period and are subject to different applications.

Within the scope of this study, the exams of the accredited certification body in the construction sector were analyzed by VQA, which has its headquarters in Istanbul, and suggestions were made for the certificate renewal periods and the number of surveillances.

2. MATERIAL AND METHOD

The construction industry stands out as the area where people with different qualifications work in many fields due to its structure. Construction provides the

opportunity to work for workers with dozens of different professional qualification certificates, from the building's license to the settlement and use. Strict monitoring and continuous control of the construction industry, which is in the field of the riskiest occupations, is important. Exam activities are carried out by institutions accredited by the Vocational Qualifications Authority operating in this field in Turkey. In this context, it is obligatory for those working in the construction sector to obtain a VQA certificate, and it has been observed that they have a certificate of approximately 15%. In order to reduce the workload in the sector, it is important to revise the document renewal and surveillance periods according to the status of the candidates. In order to verify this situation, the exams of 144 candidates in the construction sector by the certification body headquartered in Istanbul have analyzed.

2.1. Candidate Profiles

According to the data received from the certification body, the marital status of the candidates is shown in Table 2.

Table 2. Marital status of candidate

Parameter	Marital Status	
	Married	Single
Number of Candidate	70	74

Candidates' graduation status, respectively; primary school, secondary school, general high school, vocational high school and university. According to these data, the number of candidates is shown in Table 3.

Table 3. Graduation status of candidate

Graduation status	Number of Candidate
Primary school	31
Secondary school	27
General high school	16
Vocational high school	14
University	56

Similarly, the age range of the candidates is shown in Table 4.

Table 4. Graduation status of candidate

Birth date	Number of Candidate
1979 and earlier	24
1980-1989	27
1990-1999	78
2000 and later	15

2.2. Results of Exam

Candidates' exams within the scope of VQA consist of 2 main stages: theoretical and performance. In addition, it can be found in sub-branches in every examination branch that the candidates enter. After the theoretical exams, the candidates take the exam in the fields of occupational health and safety. In this direction, the analysis of the exam results accepted in accordance with the VQA rules according to the marital status of the candidates is presented in Table 5.

Table 5. The average of the exam results out of 100 point according to the marital status of the candidates

Marital Status	Theoretical	Performance
Married	64.78	78.12
Single	74.95	84.18

It is seen that the candidates whose marital status is married are successful in both stages of the exams. For this situation, it shows that the professional awareness of married candidates is higher. Similarly, the effect of candidates' graduation status on their success is shown in Table 6.

Table 6. The average of the exam results out of 100 point according to the graduation status of the candidates

Graduation status	Theoretical	Performance
Primary school	63.25	80.26
Secondary school	65.10	82.15
General high school	71.91	84.59
Vocational high school	75.22	93.10
University	88.41	94.15

The effect of the candidates' graduation status on their success is summarized in Table 7, and it is seen that especially vocational high school graduates and college graduates are more successful in both theoretical and performance exams. In addition, it has observed that primary school graduates have unsuccessful especially in theoretical exams. Looking at the results of the performance exams, it is seen that the effect of graduation seems to be limited. The effect of the age range of the candidates on the exam results is shown in Table 7.

Table 7. The average of the exam results out of 100 point according to the age range status of the candidates

Birth date	Theoretical	Performance
1979 and earlier	70.68	85.22
1980-1989	69.08	87.24
1990-1999	70.92	86.15
2000 and later	68.47	80.44

When the exam results of the candidates are examined according to the age profile of the candidates, the minority of those born in 1979 and before come to the fore. In

addition, when the results are evaluated, it seems that the age profile has little effect on the exam result.

3. CONCLUSIONS AND SUGGESTIONS

The results of the vocational exams conducted on candidates from different regions in Turkey, made according to the rules of the Vocational Qualifications Authority, of the candidates with different age groups, different graduations and different marital status are summarized.

When the candidates have evaluated according to their marital status, it has seen that the married candidates have more successful than the single candidates.

Considering the effect of the graduation status of the candidates, it was seen that the graduates of the college were the most successful in the theoretical exams. In addition, it has been determined that vocational high school graduates and college graduates are the most successful groups in the performance exam. On the other hand, it has observed that the graduation status of the candidates is more evident in the theoretical exams and less pronounced in the performance exams.

When the exam results of the candidates are evaluated according to their age profiles, it is seen that the candidates born in 2000 and later are the most unsuccessful group, and it has been determined that the age effect is very limited.

The recommendations made as a result of this study are summarized below.

- The same document usage period is adopted for all candidates who are successful in the vocational qualification exams. On the other hand, it should be longer than other graduation conditions in terms of preventing the intensity that may be experienced in the system, since graduates of college and vocational high schools are more successful. In this direction, these periods can be revised with a study with wider participation.
- According to VQA legislation, candidates holding VQA certificate are subject to surveillance throughout the validity period of the certificate. In successful groups, this number of surveillances can be reduced.

- The conclusions and recommendations made according to the study conducted on a limited number of candidates will shed light on more comprehensive studies.

RESOURCES

Akboğa, Ö., & Baradan, S. (2015). İnşaat sektöründeki ölümlü iş kazalarının karakteristiklerinin incelenmesi: İzmir alan çalışması, 5. İşçi Sağlığı ve İş Güvenliği Sempozyumu, İzmir, 215-224.

Bayram, S. (2018). Şantiyelerde Yaşanan Güncel İş Kazaları, Çalışan Farkındalıkları ve Eğitim Seviyeleri Arasındaki İlişki. Çukurova Üniversitesi Mühendislik ve Mimarlık Fakültesi Dergisi, 33(1), 241-252.

Canbey-Özgüler, V. (2019). Türkiye’de Mesleki Yeterlilikler Sistemi Ve Sendikalar-Vocational Qualifications System And Trade Unions In Turkey. Mehmet Akif Ersoy Üniversitesi Sosyal Bilimler Enstitüsü Dergisi, 9(22), 15-43.

Colak, B., Etiler, N., & Bicer, U. (2004). Fatal occupational injuries in the construction sector in Kocaeli, Turkey, 1990-2001. Industrial health, 42(4), 424-430.

Kale, Ö. A., & Yanık, S. (2018). İnşaat sektörü çalışanlarının işçi sağlığı ve iş güvenliği eğitimleri konusundaki bilinç düzeylerini ölçmeye yönelik bir sektörel araştırma. Sakarya University Journal of Science, 22(2), 637-649.

MYK (2006). “Mesleki Yeterlilik Kurumu”. Ankara.

Mümtaz, İ., & Döğner, S. TS EN ISO/IEC 17024 Personel Belgelendirme Standardına Göre Uygunluk Değerlendirme Kuruluşlarının Akreditasyonu Uygulaması: Sakarya Üniversitesi Sürekli Eğitim, Uygulama Ve Araştırma Merkezi Sınav Ve Belgelendirme Faaliyetleri. Sakarya İktisat Dergisi, 6(3), 63-73.

Occupational Safety & Health Administration, 2015, OSHA Data, Statistics <https://www.osha.gov/oshstats/commonstats.html>.

Resmi Gazete, 2013. Çalışanların İş Sağlığı ve Güvenliği Eğitimlerinin Usul ve Esasları Hakkında Yönetmelik, Başbakanlık Basımevi, 28648.

Sosyal Güvenlik Kurumu (SGK); http://www.sgk.gov.tr/wps/portal/sgk/tr/kurumsal/istatistik/sgk_istatistik_yilliklari

Temel, B. A., Başağa, H. B., & Atasoy, M. “İnşaat Sektöründe Çalışan İşçilerin Profilleri ile İş Sağlığı ve Güvenliği Hakkındaki Bilgi Düzeyleri; “Trabzon Ölçeğinde.

TÜİK. (2018). “Türkiye İstatistik Kurumu” Ankara.

Yanık, S. (2017). İnşaat sektöründe çalışan işçilerin profilleri ile iş sağlığı ve güvenliği eğitimlerinin belirlenmesi (Master's thesis).

THE EFFECT OF VOCATIONAL QUALIFICATION CERTIFICATE ON OCCUPATIONAL ACCIDENTS OCCURRING IN THE CONSTRUCTION SECTOR

Melek Ceylan¹, Sinan Cansız²

¹*Istanbul Aydin University, Quality Management, melekceylan@aydin.edu.tr*

²*Istanbul Aydin University, Civil Engineering, sinancansiz@aydin.edu.tr*

*Responsible author: *melekceylan@aydin.edu.tr*

ABSTRACT

Economic and social losses occur as a result of work accidents in the construction sector in Turkey. The contribution of vocational training to reduce these accidents is accepted by all authorities. The most important contribution to vocational education has been made by the Vocational Qualification Certificates issued by the Vocational Qualifications Authority in recent years. Vocational Qualification certificate, which has been actively given since 2015, has mostly been given to workers working in hazardous areas. Due to the fact that the construction sector is at the forefront of the accident statistics analyzed by years, the importance and impact of the vocational qualification certificate has increased continuously. With the increasing number of documents in recent years, it has been observed that approximately 30% of the employees in the construction sector have vocational qualification certificates. However, fatal accident statistics, especially in private construction activities, have decreased significantly, along with the percentage of VQA certified employees. Within the scope of this study, the change of accident statistics in the construction sector depending on the number of VQA certificates was investigated.

KEYWORDS: Vocational Qualification Authority, Fatal Accidents, Construction Sector.

1. INTRODUCTION

With the developing economy in Turkey, continuous infrastructure and construction investments continue to increase. In addition, the renovation works of the old building stock continue in the regions where there is a dense population living in the active earthquake zone. Under the influence of such reasons, the construction industry constitutes approximately 10% of the total number of SGK employees in Turkey. When the occupational accident statistics are examined, the construction sector is at the forefront. Due to the nature of the construction industry, there are always work accidents in the form of material and loss of life due to dangerous jobs. Occurring occupational accidents usually cause serious economic and social losses due to loss of life or irreversible disability. For this reason, studies have been carried out by many researchers to reduce occupational accidents in the construction industry (Çolak et al. (2004), Güvel and Oral (2018), Güllüoğlu and Güllüoğlu (2019), Kale and Yanık (2018), Kale (2018)). As a result of these studies, it has been seen that vocational training and awareness significantly reduce occupational accidents. According to the data of Vocational Qualifications Authority, it has been observed that the probability of occupational accident in employees with VQA certificate is 25% lower than other employees. In this context, many incentives are provided by public institutions to enable employers and employees to turn to VQA certification. According to the data obtained from the Social Security Institution, there are approximately 2 million workers in the construction sector. When the data of the last 5 years are examined, this number of employees is constantly at this level. The change in the number of employees in the construction sector by years is presented in Table 1.

Table 1. The number of Employee in the construction sector

Year	The number of Employee in the construction sector
2016	1.887.099
2017	2.083.438
2018	1.601.184
2019	1.294.788
2020	1.587.666

When the occupational accident statistics are examined, it is seen that the most occupational accidents occur in the construction sector. The distribution of occupational accidents occurring by years according to sectors is presented in Table 2.

Table 2. Distribution of occupational accidents by sectors

Year	Construction	Agriculture/Forest	Logistics	Mine
2013	%24	%16	%11	%7
2014	%23	%17	%7	%21
2015	%25	%23	%14	%4
2016	%22	%20	%13	%4
2017	%23	%19	%13	%5
2018	%23	%24	%12	%3
2019	%24	%13	%14	%3

When the fatal occupational accidents are examined, the change over the years for the construction sector is shown in Table 3.

Table 3. Distribution of occupational accidents by sectors

Field	Year				
	2016	2017	2018	2019	2020
Building construction	239	340	360	207	199
Except of the building construction	130	158	162	105	98
Private construction works	127	89	69	56	50
Total	496	587	591	368	347

2. MATERIAL AND METHOD

Vocational Qualifications Authority, which is one of the most important actors of vocational education and supervision, was established in 2006. Responsible for certification of personnel working in Turkey. In this context, it undertakes the supervision of the certification bodies it has authorized. Vocational Qualifications certificate is the document that determines the professional competencies of the employees and is given according to the results of the theoretical and performance exams. Candidates who want to have a certificate have to prove their theoretical and practical proficiency in the field of occupational health and safety. For this reason, it is seen that certified employees are more competent in occupational safety. The number of certificates issued by years in all sectors in Turkey is summarized in Table 4.

Table 4. Number of certificate issued by year

Year	The number of certificate	Cumulative The number of certificate	The number of total employee
2016	80.000	80.000	21.131.000
2017	170.000	250.000	22.280.000
2018	210.000	460.000	22.072.000
2019	470.000	930.000	22.000.000
2020	400.000	1.330.000	23.344.000

When the number of certificates given until 2020 are examined, it is seen that it remains at the level of 10% among all employees. According to the data received from the Vocational Qualifications Authority, the change in the number of certificates issued for the construction sector by years are shown in Table 5.

Table 5. Number of certificate issued by year in the construction sector

Year	Cumulative The number of certificate	The number of employee in the construction sector	Percentage of VQA Certified Employees (%)
2016	29.000	1.887.099	1.54
2017	91.000	2.083.438	4.37
2018	165.000	1.601.184	10.47
2019	340.000	1.294.788	26.17
2020	485.000	1.587.666	30.52

When the results are examined, the percentage of employees with VQA certificate in the construction sector is constantly increasing. This shows that employees have become more conscious. However, it shows that most of the employees work without a certificate, since the employees in the construction sector are obliged to have a VQA certificate. With the increasing number of VQA certificates, the number of fatal accidents occurring in the construction sector is constantly decreasing. This situation is illustrated in Figure 1.

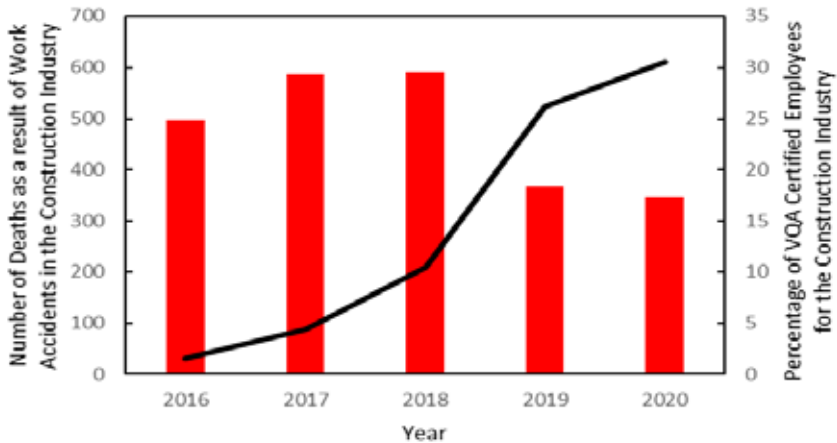


Fig. 1. Variation of fatal work accidents according to the percentage of employees with VQA certificate in the construction sector

As can be seen in Figure 1, with the significant increase in the number of employees with VQA certificate in the construction sector, there is a decrease in fatal occupational accidents. Similarly, when we divide the construction industry into subgroups, the number of fatal occupational accidents are shown in Figure 2-4.

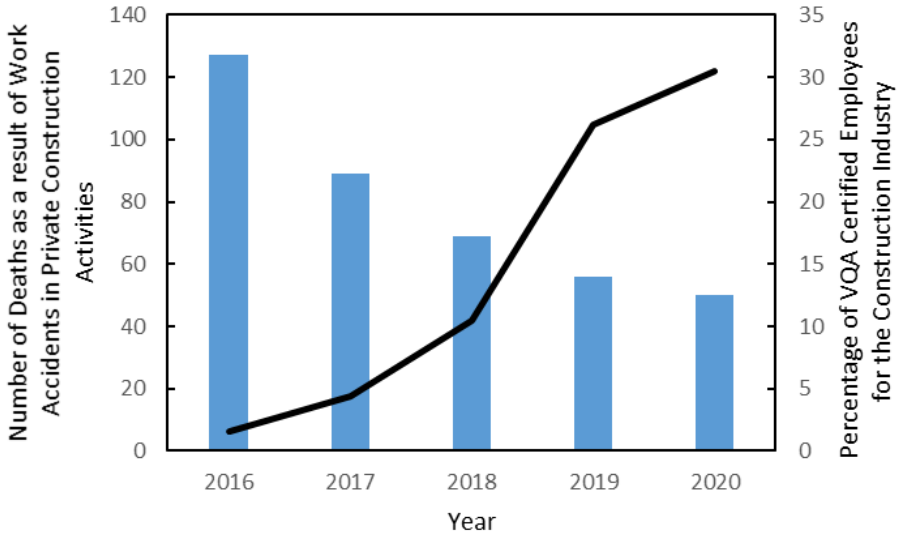


Fig. 2. Variation of fatal work accidents according to the percentage of employees with VQA certificate in the private construction activities

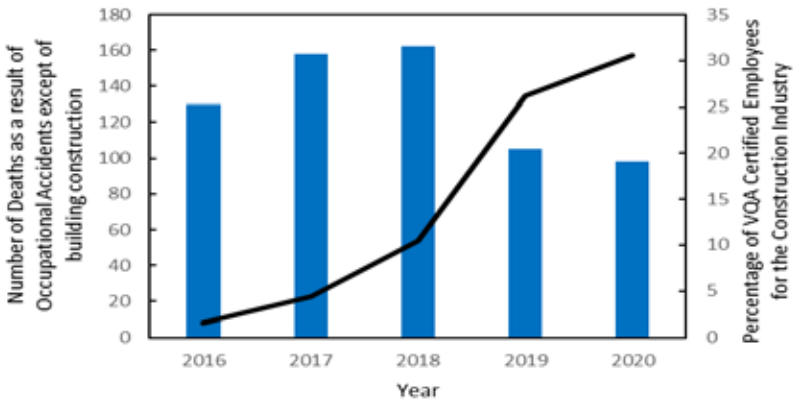


Fig. 3. Variation of fatal work accidents according to the percentage of employees with VQA certificate except of the building construction

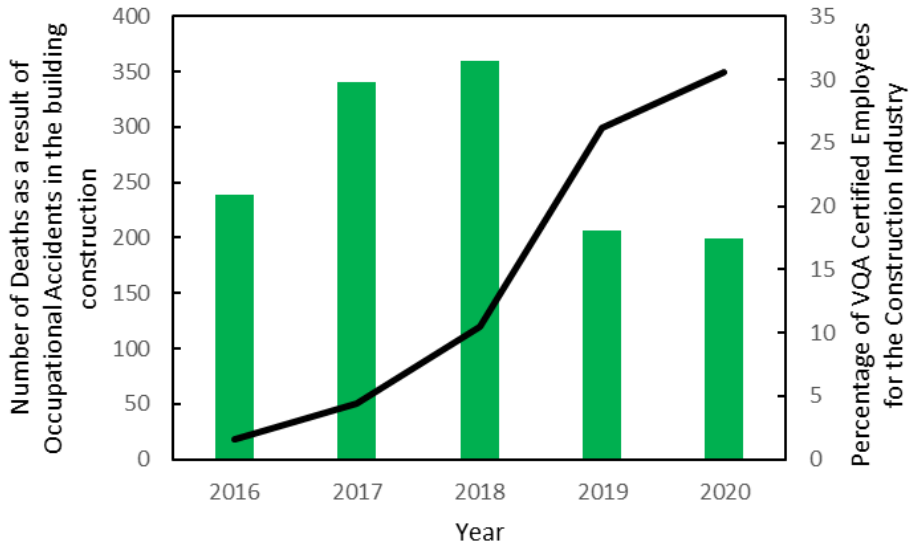


Fig. 4. Variation of fatal work accidents according to the percentage of employees with VQA certificate in the building construction

When the construction sector is examined in sub-branches, the following business lines emerge according to the statistics of the Social Security Institution.

Building Construction: It covers the construction of all buildings that are not intended for residence or residence.

Construction of non-building structures: Construction of highways and highways, construction of railways and subways (railway tunnel and underground construction), Construction of bridges and tunnels, Construction of water projects, Construction of other non-building structures not classified elsewhere.

Private Construction Activities: Demolition, Site preparation, Test drilling and drilling, Electrical installation, Plastering works, Joinery installation, Floor and wall covering, Paint and glass works, Roofing works.

When the results are evaluated, the most significant decrease is seen in the number of fatal work accidents with the increasing number of certificates, since private construction activities are jobs that require direct professional knowledge.

3. CONCLUSIONS AND SUGGESTIONS

Within the scope of this study, the effect of vocational qualification certificate on accident statistics in the construction sector has investigated. The results obtained in this context are listed as items.

- Although the vocational qualification certificate started to be issued in 2015, its effects on the sector have started to be seen since 2018.
- The average number of employees in the construction sector is 1.5 million, and the number of documents has reached 600.000 as of 2021. In addition, the number of fatal occupational accidents decreased by about 40%, although there was no significant decrease in the number of employees.
- Special construction activities; Due to the fact that there are business lines that require full professional knowledge such as plaster, paint and plaster, there has been a continuous decrease in fatal work accidents with the increasing number of documents.

RESOURCES

Colak, B., Etiler, N., & Bicer, U. (2004). Fatal occupational injuries in the construction sector in Kocaeli, Turkey, 1990-2001. *Industrial health*, 42(4), 424-430.

Güvel, Ş. T., & Oral, E. L. (2018). İş sağlığı ve güvenliği yasal mevzuatının Türkiye inşaat sektöründe uygulanma düzeyi. *Çukurova Üniversitesi Mühendislik-Mimarlık Fakültesi Dergisi*, 33(1), 189-198.

Güllüoğlu, E.N., & Güllüoğlu, A.N. (2019). Türkiye inşaat sektöründe istihdam ve iş kazalarının analizi. *Karaelmas İş Sağlığı ve Güvenliği Dergisi*, 3(2), 65-81.

Kale, Ö. A., & Yanık, S. (2018). İnşaat sektörü çalışanlarının işçi sağlığı ve iş güvenliği eğitimleri konusundaki bilinç düzeylerini ölçmeye yönelik bir sektörel araştırma. *Sakarya University Journal of Science*, 22(2), 637-649.

Kale, Ö. A. (2018). İnşaat sektöründe iş kazaları ve alandaki iyileşmeleri etkileyen faktörlerin analizi. Dicle Üniversitesi Mühendislik Fakültesi Mühendislik Dergisi, 9(2), 895-906.

MYK (2006). “Mesleki Yeterlilik Kurumu”. Ankara.

Sosyal Güvenlik Kurumu (SGK);
http://www.sgk.gov.tr/wps/portal/sgk/tr/kurumsal/istatistik/sgk_istatistik_yilliklari

TÜİK. (2018). „Türkiye İstatistik Kurumu” Ankara.

EARTHQUAKE REINFORCEMENT OF HISTORICAL MASONRY BUILDINGS OF TOPKAPI PALACE INCILI MANSION

Hafez Keypour¹, Ali Tarmigh², Cevdet Şentürk³, Zeyneb Kilic⁴

¹*Assis. Prof. Dr., Dept. of Civil Engineering, IAU, Turkey.
hafezkeypour@gmail.com.*

^{2,3}*İndis Engineering, İstanbul, Turkey.*

⁴*Assis. Prof. Dr., Dept. of Civil Engineering, IAU, Turkey.
zeynebkilic@aydin.edu.tr*

*Responsible author: *hafezkeypour@gmail.com*

ABSTRACT

Masonry structures are complicated systems that necessitate in-depth understanding and information about their behaviour when subjected to seismic loading. A reliable earthquake resistant design or assessment requires accurate modelling of masonry structures. Modelling a real structure to a reliable numerical (mathematical) representation, on the other hand, is a difficult, time-consuming, and computationally intensive operation. In this study, the results of the analysis of the historical structure of the İncili Mansion under the influence of different earthquake loads and reinforcement suggestions are presented.

KEYWORDS: Earthquake, Finite element analysis, Historical structures, Masonry building.

BEHAVIOR OF HIGHLY DUCTILE PVC-CONFINED TUBULAR STUB COLUMNS

Ahmet Emin Kurtoglu¹

¹*Igdir University, Faculty of Engineering Sehit Bulent Yurtseven Campus, Igdir, Turkey, aemin.kurtoglu@igdir.edu.tr*

*Responsible author: aemin.kurtoglu@igdir.edu.tr

ABSTRACT

Reinforced concrete (RC), a common and popular building material, plays an important role in civil engineering. With the development of modern engineering structures towards wide-span, complex, high-rise and heavy load, ordinary reinforced concrete structures cannot fully meet the bearing capacity requirements, especially against earthquake forces. One of the approaches to overcome these problems is the use of composite structural elements. Confining concrete with steel, FRP or PVC tubes is an effective way to increase its load carrying capacity and ductility. In this study, an emerging research concept of highly ductile PVC tube-confined concrete (PTCC) stub columns is briefly reviewed. Current studies on axial compressive and flexural behaviour of PTCC are analysed. Additionally, the advantages and drawbacks of PTCC columns are discussed. Increased level of ductility and energy dissipation capacity of PTCC columns verify that PVC can be utilized as an alternative confining material.

KEYWORDS: Confined concrete, composite, PVC, ductility

PROBABILISTIC ASSESSMENT OF THE GROUND VIBRATION INDUCED BY ROCK EXPLOSION

Mahdi Shadabfar¹, Nemat Hassani², Hadi Kordestani³

¹Center for Infrastructure Sustainability and Resilience Research, Department of Civil Engineering, Sharif University of Technology, Tehran 145888-9694, Iran. Email: mahdi.shadabfar@sharif.edu

²Faculty of Civil, Water and Environmental Engineering, Shahid Beheshti University, Tehran, Iran. Email: n_hassani@sbu.ac.ir

³School of civil engineering, Shandong Jianzhu University, Jinan, China. Email: hadikordestani@zju.edu.cn

ABSTRACT

Following the underground explosions, severe shock waves are released into the surrounding rock environment causing damage to adjacent structures. Peak particle velocity (PPV) is typically used to assess the effects of explosion-induced vibration on the surrounding environment. However, the uncertainty involved in PPV estimation caused these approaches to accompany with a margin of error. Thus, a probabilistic approach is utilized in this paper to assess the ground vibration induced by rock explosion. For this mean, the Monte Carlo sampling method was utilized to calculate the exceedance probability of various values of PPV. The results showed that an increase in the PPV value reduced the exceedance probability so sharply that PPV values greater than 9 mm/s had the occurrence probability of less than 5%. Besides, the reliability sensitivity analysis showed that the maximum charge per delay (W) exerted the highest effect on the small range of PPV values, between 0.5 and 4 mm/s, while the monitoring distance (R) mostly affected the medium range of PPV values, between 1.5 to 6.5 mm/s. It was also demonstrated that the burden effect (B) on probability was less than 2%, which was exerted on a small range of PPV values (smaller than 2.5 mm/s); therefore, it could be disregarded in the main model.

Keywords: Performance-based design; uncertainty modelling; probabilistic fragility curves; resilience measures; recovery models

**THE APPLICATION OF NORMALIZED DISTRIBUTED ENERGY
DIRECTLY CALCULATED FROM STRUCTURAL ACCELERATION
RESPONSE AS A SENSITIVE DAMAGE INDEX FOR STRUCTURAL
DAMAGE IDENTIFICATION**

Hadi Kordestani^{1*}, Zhang Chunwei², Mahdi Shadabfar³

1- School of Civil Engineering, Shandong Jianzhu University, Jinan, China

*2- Structural Vibration Control Group, Qingdao University of Technology,
Qingdao, China*

*3- Center for Infrastructure Sustainability and Resilience Research,
Department of Civil Engineering, Sharif University of Technology, Tehran,
Iran*

*Responsible author: hadikordestani@zju.du.cn

Abstract

Signal processing-based structural health monitoring approaches usually define a damage index from one or more features of the structural vibration response. Therefore, these approaches are typically two-steps approaches in which the signal's features are determined in the first step and the damage index is calculated in the second step. The use of normalized energy along the structure as a damage index can omit the first step since it does not need to determine the signal's features anymore. Therefore, it will be possible to identify a structural damage with, for example, no need of determining the modal parameters. The authors proposed normalized energy-based damage index in 2018 for the first time and successfully applied it to different numerical and experimental health monitoring cases. Since there are few papers available about this damage index, this paper is going to illustrate how a damage can be identified using the normalized energy of bridge seismic acceleration response with no need of determining the modal parameters. A numerical example of an arch-tied bridge subjected to different seismic loads is used in this conference paper.

Keywords: Bridge health monitoring, Seismic assessment, Acceleration response, Normalized energy, Arch-tied bridge.

SIMPLIFIED SEISMIC RETROFIT COUNTERMEASURES FOR URBAN GAS RISERS

Nemat Hassani¹, Saeed Beheshti¹, Mohammad Safi¹, Shiro Takada², Yasuo Ogawa³, Junichi Ueno⁴, Hossein Mohammadsaleh⁵, Kaveh Zanganeh⁵, Masoud Samadian⁵

1- School of Civil, water and Environ. Eng., Shahid Beheshti Univ. (SBU), Tehran, Iran

2- School of Civil Eng., Kobe Univ., Kobe, Japan

3- Osaka Gas Eng. Co., Osaka, Japan

4- RILE Co., Osaka, Japan

5- Tehran Province Gas Company, Tehran, Iran

Responsible author: n_hassani@sbu.ac.ir

ABSTRACT

The effect of earthquake on the components of the gas system has always been a major disastrous concern in big cities. The extensive and comprehensive studies of the Tehran gas system showed that the gas riser from meter-stop valve to house regulator, with 60 Psi pressure and screw joints and Insulation Unit (IU rubber ring), is the most vulnerable component of the system. Although the riser itself is not vulnerable to seismic vibration, however possibility of damage to the neighboring walls and roofs of the buildings and their collapse on riser can cause severe gas leakage following with fire or explosion. During last two decades, a variety of countermeasures proposed for riser seismic countermeasures. However, most of them were not practical, safe and/or economic. In this paper, in addition to the behavior of risers and failure modes in past earthquakes, various parameters including repair limitations, area seismicity and urban texture, buildings lateral load bearing system and age, support wall condition (with or without roof) are considered. There are three types (plans) of simplified retrofit countermeasures based on the risers' conditions. Two plans are for existing risers and one for new ones. A guideline manual also is provided for Iran National Gas Company (NIOC) for riser vulnerability assessment and suitable countermeasures by their own staffs. Changing the location of IU from Meter-Stop Valve to the top of house regulator, clamp reinforcement of Meter-Stop Valve, using flexible nipple pipe and adding cast-casing protection for screw parts are the main innovations in developed countermeasures.

Keywords: Gas Riser, Earthquake, Seismic Retrofit.



PROCEEDINGS OF INTERNATIONAL CONFERENCE ON ISTANBUL AND EARTHQUAKE 2022

Organized by IAU Disaster Training Application and Research Center (AFAM)



İSTANBUL AYDIN ÜNİVERSİTESİ
YAYINLARI

ISBN 978-625-7783-48-4



9 786257 783484